1975

Bit penetration into rock - A finite element study

Jaw-Kuang Wang

Department: Mechanical and Aerospace Engineering

BIT PENETRATION INTO ROCK - A FINITE ELEMENT STUDY

by

JAW-KUANG WANG, 1943-

A DISSERTATION

Presented to the Faculty of the Graduate School of the

UNIVERSITY OF MISSOURI - ROLLA

In Partial Fulfillment of the Requirements for the Degree

DOCTOR OF PHILOSOPHY

in

MECHANICAL ENGINEERING

1975

Jerry F. Lehnhoff
Advisor

Robert L. Davis

ABSTRACT

A finite element approach has been developed to simulate bit penetration from bit-rock interaction to chip formation. A mathematical rock failure model, based on a review of the existing literature on rock tests, has been proposed to represent post-failure rock behavior and applied in the penetration simulations. The finite element program has been developed for two dimensional plane strain problems with non-linear material properties, geometrical non-linearities and fracture. An anisotropic element as well as variable stiffness and stress release methods have been used. An iteration method, using an incremental approach, has been applied for continuous penetration and modifications of material properties and displacements. Quantitative information on stress, displacement and material failure in the entire penetration process can be obtained through computer simulation. Blunt point, wedge and cylindrical bits are used in the penetration simulations. Blunt point bit penetration, with two different post-failure rock strengths, has been simulated and compared with experimental results.

ACKNOWLEDGEMENTS

The author wishes to express his sincere appreciation to Dr. Terry F. Lehnhoff for direction, assistance and encouragement throughout the course of graduate study. Gratitude is also extended to the Ph. D. advisory committee, Drs. R. L. Davis, C. R. Barker, G. B. Clark and A. J. Penico.

The author is grateful to Dr. G. B. Clark for financial assistance in the form of a research assistantship in the Rock Mechanics and Explosives Research Center.

Special thanks are extended to Dr. H. D. Keith for correcting this dissertation, and to Mr. and Mrs. W. R. Heincker for reading the manuscript.

Finally the author wishes to thank his parents Mr. and Mrs. C. P. Wang for their unending encouragement during his years of educational pursuit, and his wife, Shu-Huei, for typing this dissertation.

TABLE OF CONTENTS

Page

LIST OF ILLUSTRATIONS

Figure Page

NOMENCLATURE

x,y	-global coordinates
N	-normal load
S	-shear load
σ	-normal stress
τ	-shear stress
ε	-strain
u,v	-displacement components in x, y coordinates
E	-Young's modulus
ν	-Poisson's ratio
p	-pressure
V	-volume
f	-coefficient of friction
μ	-slope of Mohr envelope
θ	-angle of Mohr envelope
c	-slope constant
P	-ratio of strength
β	-compressibility
Λ	-increment
$[T]$	-coordinate transformation matrix
$[D]$	-elasticity matrix
$[D']$	-local elasticity matrix
$[K]$	-stiffness matrix
$\{\delta\}$	-nodal displacements
$\{R\}$	-nodal forces
$\{\sigma\}$	-stress matrix

$\{f\}$	-displacement function
$[N]$	-shape function
$[B]$	-strain displacement coefficient matrix

Superscripts and Subscripts:

e	-element
T	-transpose of a matrix
o	-initial
i	-instantaneous
max	-maximum
r	-residual
c	-compression
t	-tension
1,2,3	-principal
n	-number of iterations

I. INTRODUCTION

Although many novel rock disintegration techniques have been introduced in recent years, only a few have shown promise for practical applications. The most common and practically important method, which has been used to drill millions of feet of rock every year, is still the mechanical action of drilling machines. In spite of the importance of the method, however, the basic bit penetration mechanisms involved are still not well known. Advances in basic studies could result in better designs and faster penetration rates.

The bit penetration mechanisms are essentially a sequence of rock failures. Unfortunately, knowledge of the post-failure behavior of rock is very limited. Only a few investigators in the past have extended their studies in this area, and the information at hand is far from being sufficient. On the other hand, the constitutive theories, which we generally apply for describing rock behavior in the elastic state, become inadequate for the fractured rock. The complexity of the post-failure character of rock makes our task for a general constitutive law and its solution practically impossible at present.

Because of these difficulties, much of the past success in bit penetration studies has been achieved through experimentation, and some empirical formulae developed from these studies have been introduced[1*]. They generally provided guidelines in particular circumstances and could rarely be generalized or used to predict

---

*Numbers refer to references listed in the Bibliography.

different and untried conditions. With regard to analytical methods, progress has been made only in the prediction of the initial crack of an elastic brittle rock under the penetration of a rigid wedge and in the calculation of the stress field beneath indentors using the slip-line theory of plasticity[2,3].

Sikarskie and Cheatham, in their recent review of the present art of penetration problems in rock mechanics, made the following suggestions for further study[4].

1. An improvement in the description of fracture growth--how the stress field changes due to the fracture region and the stability of the fracture growth.

2. A better description of the crushing phase.

3. Possible extensions: a) extension to other geometries and tool conditions, b) extension to other constitutive behavior.

The purpose of this study is primarily to develop a general mathematical model to simulate the sequences of failure mechanisms and provide a better description of the aforesaid penetration phases --initial cracking, crushing and chipping. Furthermore, a satisfactory model of this nature (non-linear material properties, geometrically non-linearities and fracture) will also serve the common interest of a broad area of rock mechanics.

The finite element method, which has been applied to numerous rock mechanics problems, will be used for this study. Its special suitability lies in the fact that the complexity of rock behavior can be handled, and arbitrary geometrical configurations and boundary conditions can be applied without difficulty.

II. REVIEW OF LITERATURE

A. Experimental Studies

Experimental studies on bit penetration have been conducted extensively by many means. Among them, quasistatic tests and drop tests, with strain gage measurement and high speed photography were used most often. Although different methods have been used and the quantitative results have varied over a wide range, the penetration phenomena observed have been similar, i.e., sequences of radial cracking, crushing and chipping. The Drilling Research Institute has conducted a series of studies on rock failure and crater formation under the impact of a blunt wedge bit. The events were recorded using high speed photography and strain gage measurements and can be summarized by the following (Fig. 1)[5]:

1. Crushing of surface irregularities as bit first makes contact with rock.

2. Elastic deformation of rock from continued application of load by bit. Surface cracks radiate out from lines of stress concentration at boundary of cutting edges.

3. Crushing of central wedge of rock into fine fragments.

4. Chipping out of large fragments along curved trajectory to surface adjacent to crushed zone.

5. Crumbling away of crushed zone and displacement by bit as it continues to penetrate. Entire sequence may be repeated if blow energy is sufficient.

These observations have been generally confirmed by later investigators in both static and dynamic experiments[1,4-10].

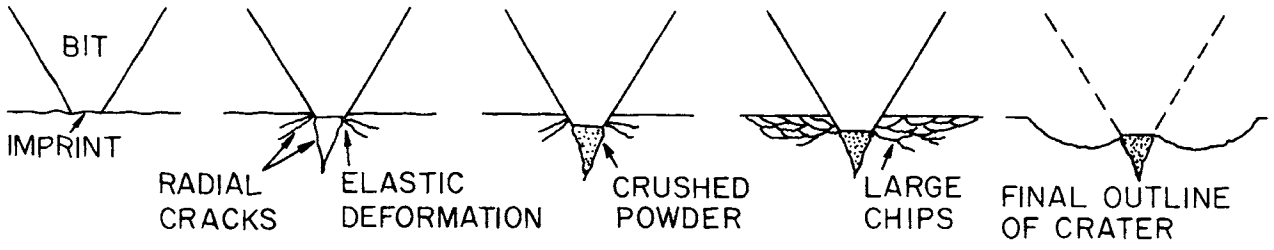

Figure 1. Sequence of Rock Failure and Crater Formation (After Hartman[5])

Reichmuth and others investigated the depth of penetration after cutting the indented specimen perpendicular to the wedge[6,7]. The sectioned surfaces showed that the damaged depths were greater than those observed after removing the crushed material, and tensile cracks were initiated a short distance away from the bit-rock interface. These fractures started in directions radiating out from the bit. The vertical cracks ran deep into the rock while others tended to curve toward the free surface as shown in Fig. 2.

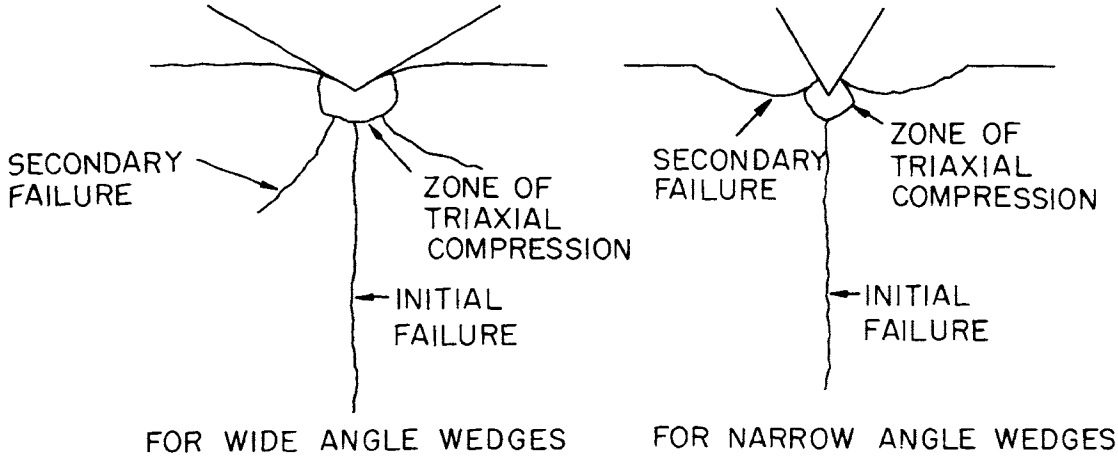

Figure 2. Fracture Patterns for Wedges (After Reichmuth[6])

Porosity is an important material property in bit penetration. Ladanyi, using a flat-ended cylindrical punch in his study, concluded that in the case of a dense rock of low porosity indentation failure initiated at the edge of the punch with a tensile crack forming a truncated cone beneath the punch[8]. As the applied load increased, the cracks continued stable growth up to a certain load level. Finally, the cone crushed and the cracks propagated to the free surfaces in an unstable manner (Fig. 3a). In the case of a porous brittle rock, the punch could be pushed to a certain depth with little damage to the surrounding material. With increasing load, the crushed and compressed rock beneath the punch led to radial cracking in a way similar to the case of a dense rock (Fig. 3b).

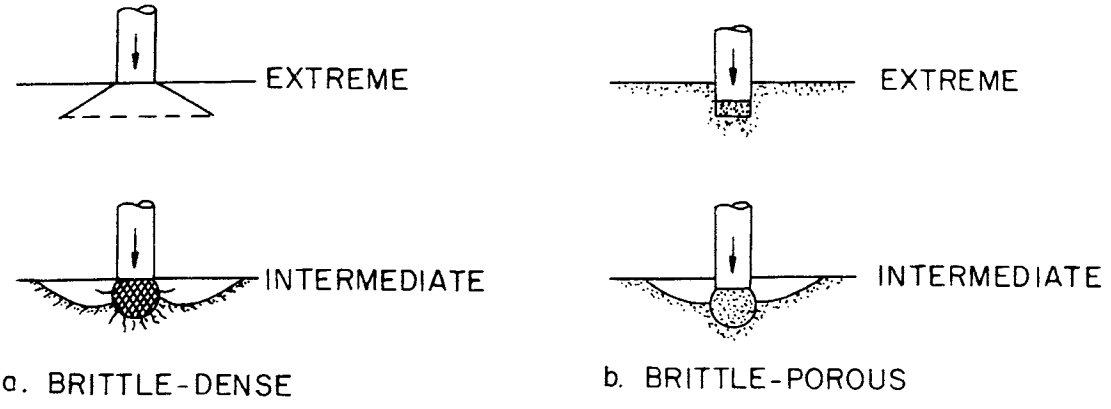

Figure 3. Assumed Indentation Failure Modes for Extreme and Intermediate Cases of Brittle-Dense and Brittle-Porus Rocks (After Ladanyi[8])

One of the most consistent results in experimental penetration studies has been the force-penetration (F-P) characteristics[7-12]. Reichmuth recorded F-P curves during the process of penetration using a load cell and a displacement transducer[7]. As shown in Fig. 4a, the

oscillating curve represents cyclic material failure while the penetration process alternates phases of crushing and chipping. Figure 4b shows a typical F-P curve in Indiana Limestone due to impact of a blunt point bit[9]. A crushed zone formed along AB and a chip was formed at B. Along BC the chip flow from the crater resulted in collapse of the zone of crushed rock beneath the tooth with a decrease in the force. The process was repeated with different degrees of chipping at D and E. F-P curves are functions of loading rates, rock properties and tooth profiles.

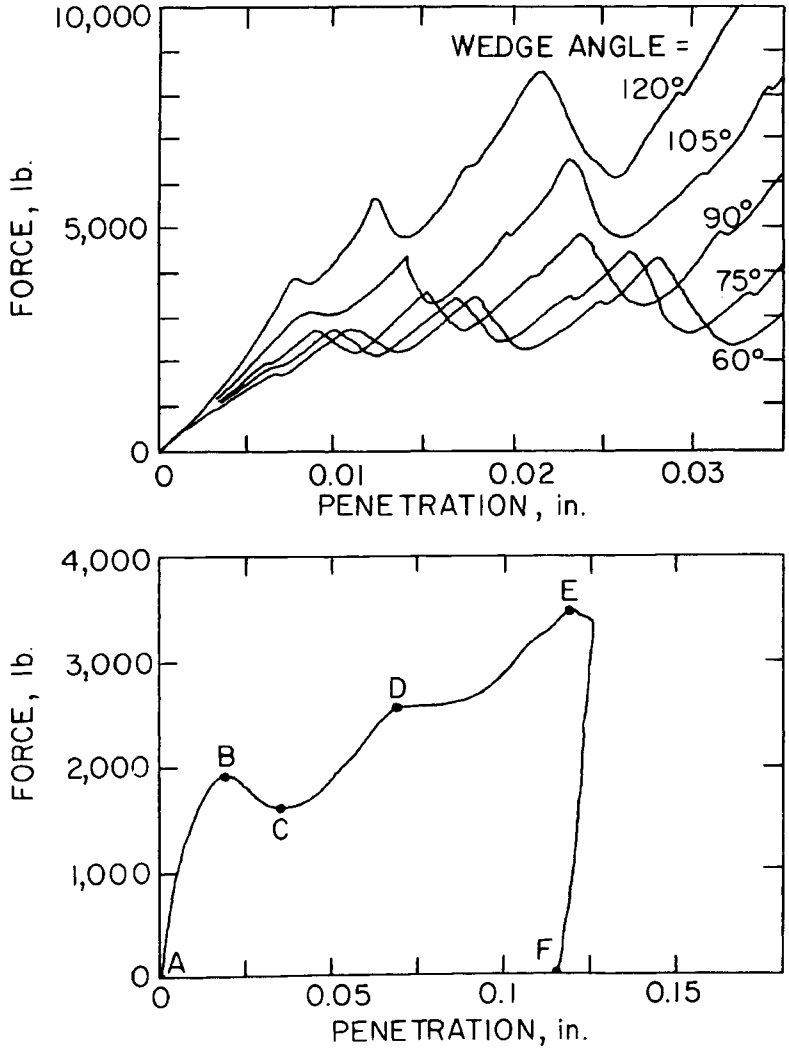

Figure 4. Typical Force-Penetration Curves (After Reichmuth[6] & Mourer[9])

B. Analytical Studies

The slip-line theory of plasticity has been applied in the study of stress field indentation problems[12-17]. The theory, which was originally developed to analyze the deformation of a rigid perfectly-plastic solid under conditions of plane strain, has been mainly employed for investigating industrial processes such as rolling, extrusion and forging. Hill extended the theory to the case of a plastic material using a yield condition based on the Coulomb-Mohr criteria[12]. He showed that two families of characteristics exist which are inclined at an angle of $\pm$ ($\pi/4-\phi/2$), where ϕ is defined as the angle of internal friction. The Coulomb-Mohr criteria was used to represent rock behavior because of its good first approximation with experimental results and also for mathematical simplicity.

Cheatham used this theory to study maximum and minimum forces necessary to penetrate a rock with a wedge-type tooth[14]. These forces corresponded to the limiting cases of rough and smooth tooth-rock interfaces. The influences of tool profile and confining pressure on the required forces were also briefly discussed. Parieau and Fairhurst extended the work on a wedge tooth to smooth, frictional and rough interface conditions[15]. Clark et al. extended the study to blunt point, round point and cylindrical indentors using the same interface conditions[17].

While the slip-line theory gives a good first approximation of the stress field under an indentor, especially at the high confining pressure condition where rock behaves as a ductile material, the theory with its idealized material properties is, however, unable to

interpret the brittle penetration failure mechanism. Some simplified wedge penetration models for brittle rock have been proposed. Paul and Silarskie introduced a model for brittle crater formation in rock[2]. They assumed that fractures occurred along a plane extending from the wedge tip to the free surface at an unknown angle ψ, and the Coulomb-Mohr criteria is satisfied simultaneously along the entire chip surface. According to the theory, the peaks on the F-P curve should lie on one straight line (Fig. 5). Dutta suggested similar models based on experimental observations and obtained a linear F-P relationship for wedges, and a parabolic one for cones[11]. These models covered some important events in the failure sequence; however, they could not describe the detail of the crater formation and gave no quantitative evaluation of the stress and displacement fields during the penetration process. The simplified models also neglected the effects of some important material properties such as porosity, brittleness, etc.

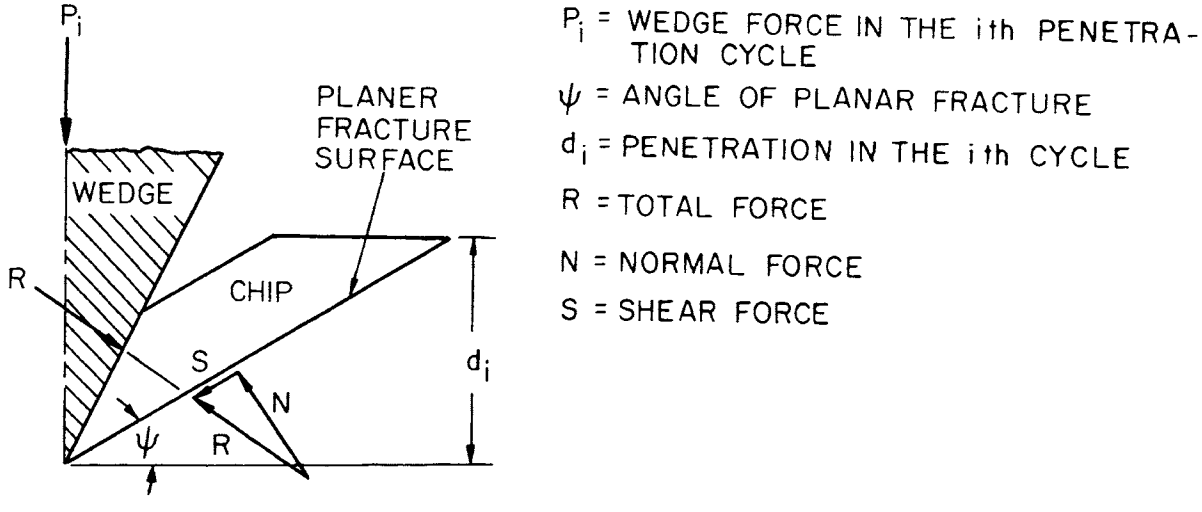

Figure 5. Idealized Model of Incipient Chipping (After Paul & Sikarskie[2])

Sikarskie and Altiero, using an integral method, have succeeded in predicting incipient fracture from the penetration of a wedged-shaped tool without considering the compressive failure of the material and the change of stress field[3].

III. MECHANICAL PROPERTIES AND FAILURE THEORIES OF ROCK

In almost every engineering problem, equations are used to obtain quantitative information for the selections and decisions of design. Some material properties and constitutive equations must be inserted into the equations to yield data. The validity of the solution obtained is no greater than the validity of the material properties and constitutive law applied. Therefore, understanding rock behavior is of primary importance in the study of rock mechanics problems and is an essential element in a better engineering design of bits and drilling equipment. In this chapter, mechanical properties and failure theories of rock, which are related to the penetration study, will be discussed.

A. Tensile Strength

Rock is weak in tension. For an igneous rock, the compressive strength could reach 20 times greater than the tensile strength[18]. Zienkiewicz et al. considered rock as a 'no tension' material in their study of the structure of a rock mass[19]. Fissured rocks and joints are often considered incapable of sustaining tensile load[20].

In the axial tension test, rock failure is instantaneous and always clear cut, disposed normally to the axis of the cylinder. The primary difficulty in this test is the lack of a satisfactory means to grip a specimen without introducing bending stress. Improving methods such as glueing the metal end caps to the sample or widening the cylindrical diameter at the ends of the specimen have been tested with some success. Many investigators prefer the indirect methods, such as bending or Brazilian tests. The dispersion of results from

tensile tests is usually large. A number of results are required to obtain acceptable average values.

B. Uniaxial Compression

The behavior of intact rock in uniaxial compression has been investigated by Bieniawski on Quartzite[21]. He found that the stress-strain curve can be divided into four regions. At the beginning of the compression, preexisting microcracks in the specimen are closed over a small increment of stress. During the crack closing, an increase in modulus of elasticity takes place resulting in a non-linear region of the stress-strain curve as shown in Fig. 6. In region II, the stress-strain curve is essentially linear. Initial cracks may start at the end of this stage. Region III represents stable fracture propagation as the stress level increases. Before the applied stress reaches its peak, an unstable fracture propagation takes place resulting in progressive flattening of the stress-strain curve in region IV. Meanwhile, experimental results in uniaxial compression tests indicate that microfractures in a specimen tend to propagate in the axial direction. These tensile cracks in the axial planes result in a fast increase in lateral strain and a reversal in volumetric change as shown in Fig. 6.

Most uniaxial compression tests have been terminated after the ultimate strength has been reached. Little is known of the post-failure behavior of rock, which is important to many engineering and geological problems in drilling, excavation and bearing. In conventional testing machines, when the maximum carrying ability of the specimen is exceeded, the sudden release of the stored energy in the

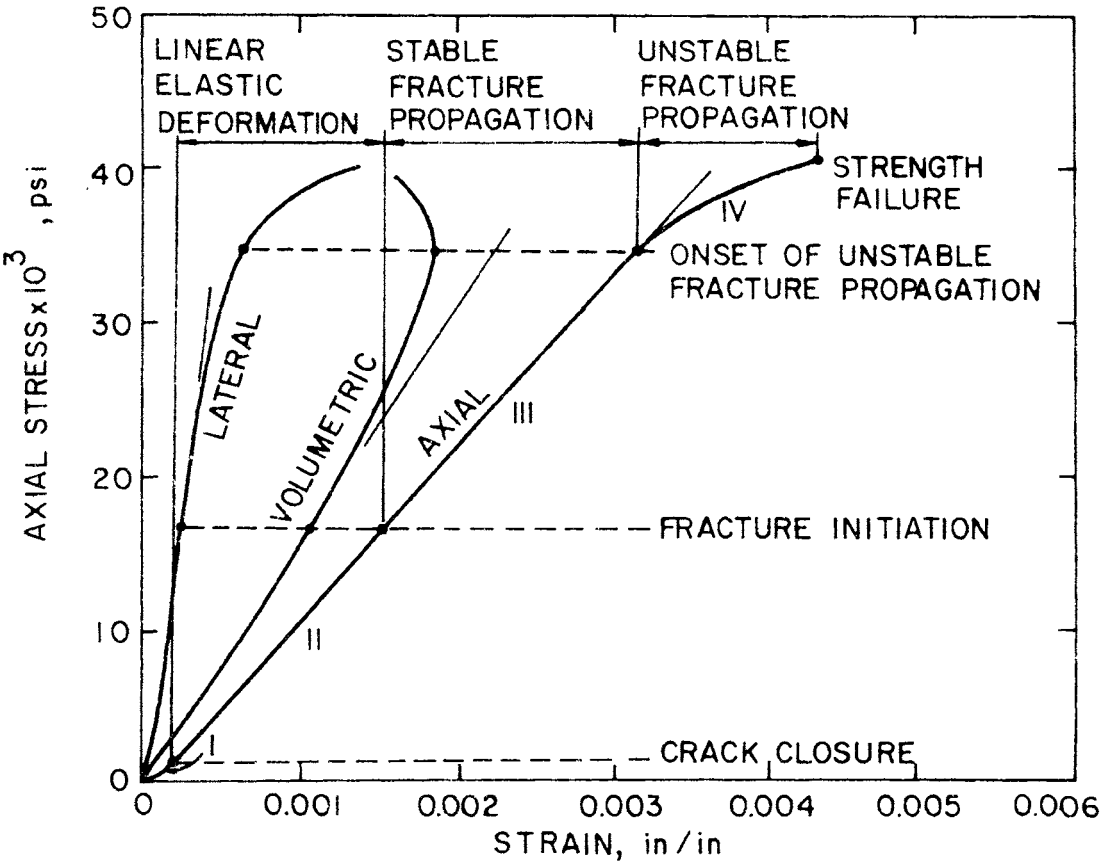

Figure 6. Brittle Fracture Processes for Quartzite in Uniaxial Compression (After Bieniawski[21])

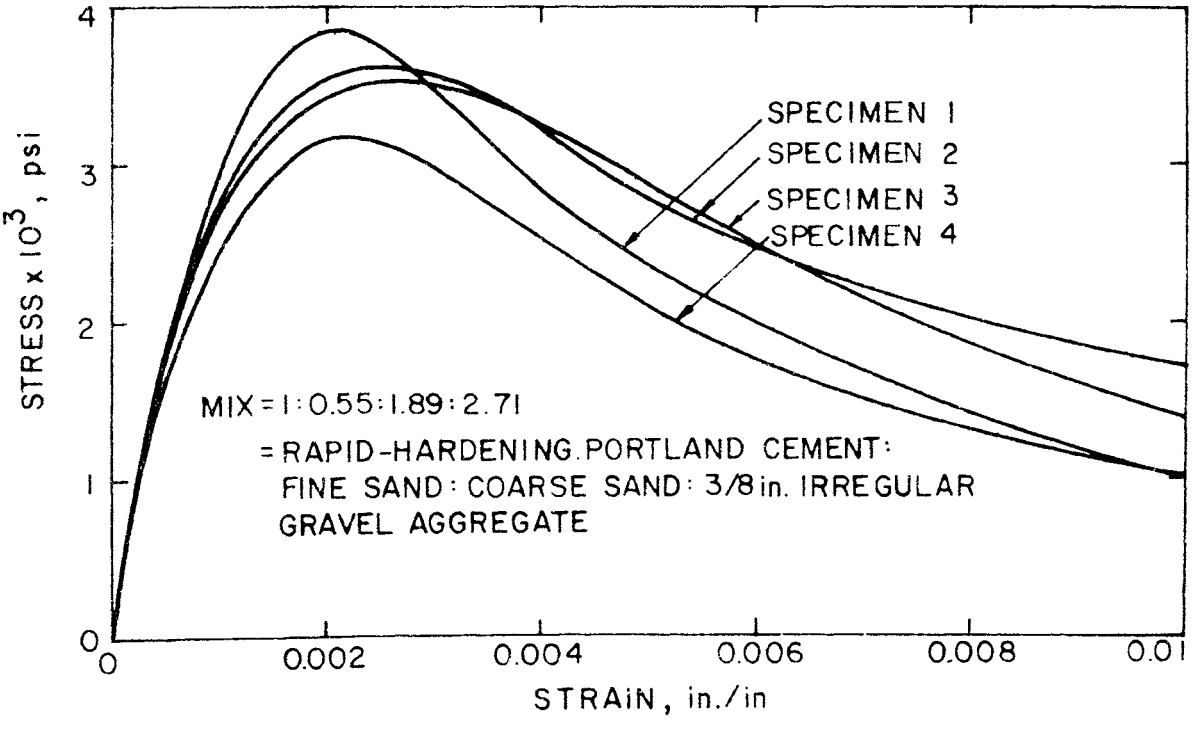

Figure 7. Complete Stress-Strain Curves for Concrete (After Barnard[22])

machine drives the sample to a rapid, uncontrolled collapse. Only in recent years, have attempts been made to control brittle fractures in compression tests by increasing the stiffness of testing machines[22-24].

Barnard developed a very stiff compressive machine and successfully obtained complete stress-strain curves for concrete[22]. The results demonstrated the ability of concrete to undergo a very large displacement without ceasing to carry load (Fig. 7). He also suggested that reduced cross section specimens give more consistent results over prisms due to the fact that reduced cross section specimens yield a more consistent failure position and a more homogeneous gage reading.

C. Shear Strength

Figure 8a illustrates shear strength versus displacement of an intact rock sheared in a direct shear device[25]. In this process, shear strength reaches a maximum at some small value of displacement where fracture occurs along the potential discontinuity. With continuing displacement, shear resistance gradually decreases until it finally approaches a minimum value corresponding to the residual failure stress. If a series of identical tests are conducted with various normal loads N, then the maximum and residual failure strengths associated with their normal loads can be drawn to form two extreme failure envelopes as shown in Fig. 8b. The vertical distance between the two envelopes indicates the reduction in shear strength with continuing displacement.

Patton, in his study of the shear strength of rock, found that with large displacements originally polished rock surfaces become

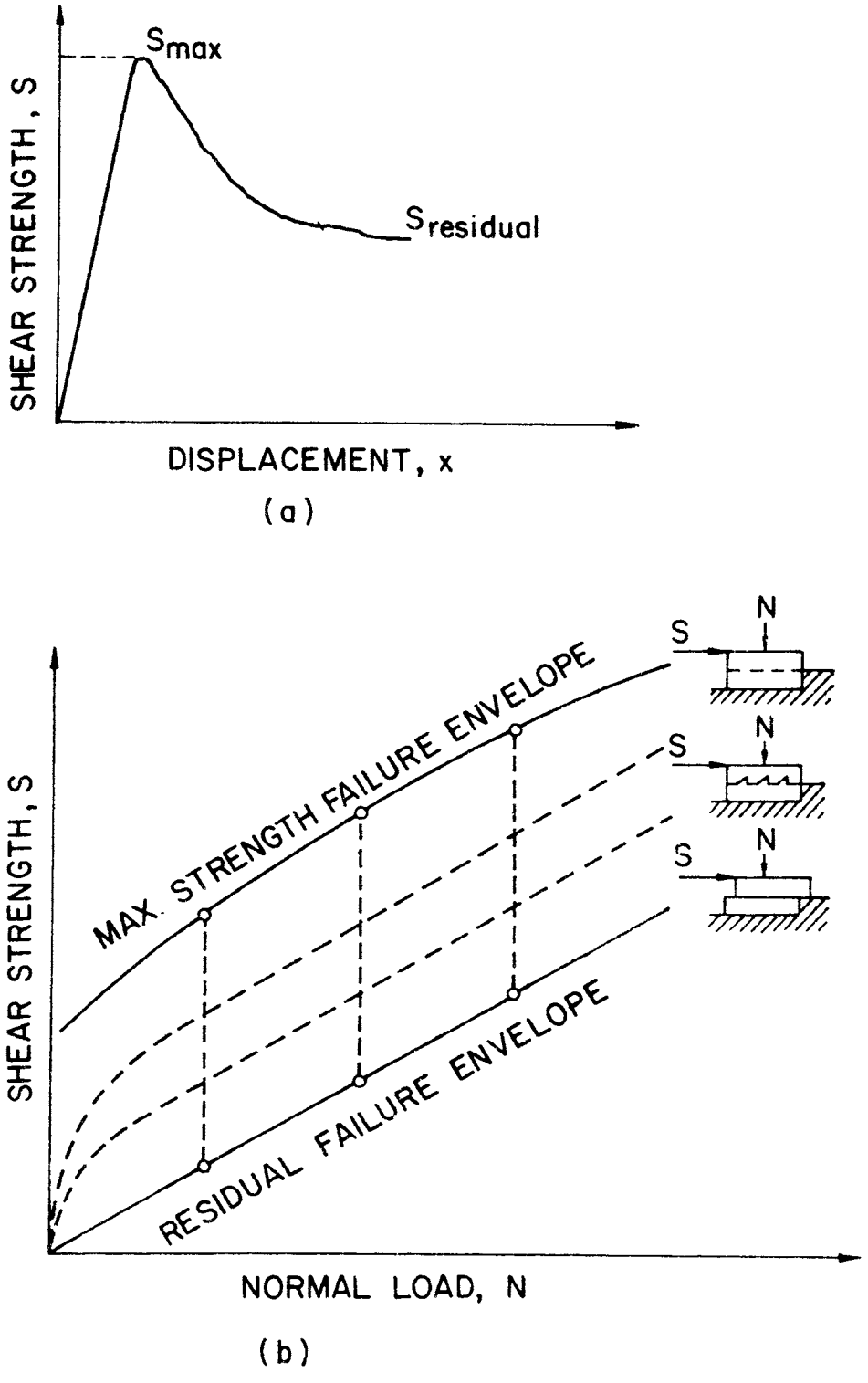

Figure 8. (a) Shear Strength Versus Displacement Showing Maximum and Residual Stresses, (b) Maximum Strength and Residual Failure Envelopes for Initially Intact Specimens (After Deere[25])

scratched and gouged[26]. The frictional resistance increases from some initial low value to a higher residual value. On the other hand, if the original surfaces are rough, they become smooth with continued displacements, and the frictional resistance progressively approaches the above mentioned residual value. He also used specimens containing a number of irregular 'teeth', representing various degrees of rough surfaces, in direct shear tests and obtained different failure envelopes lying between the two extreme failure conditions as shown in Fig. 8b.

D. Rock Behavior under Combined Loading

In triaxial compression tests, the state of confinement influences rock properties of intact rock. An increase in confining pressure could result in an increase in ultimate strength, strain and stiffness. Under sufficiently high pressure, as the cases in deep oil wells, rock becomes ductile.

One convenient way to summarize the results of triaxial tests is to plot the data in terms of major and minor principal stresses at failure on a Mohr diagram as shown in Fig. 9a. A curve tangent to the family of Mohr circles for tests conducted at various confining pressures is the failure envelope for the particular intact rock tested. Bieniawski in a survey of published rock fracture data concluded that Mohr envelopes are approximately linear over a wide range of confining pressure[21].

Although the post-failure behavior of rock under triaxial loading is not well tested, it is agreed that the falling branches of the stress-strain curves in triaxial tests follow the same trend

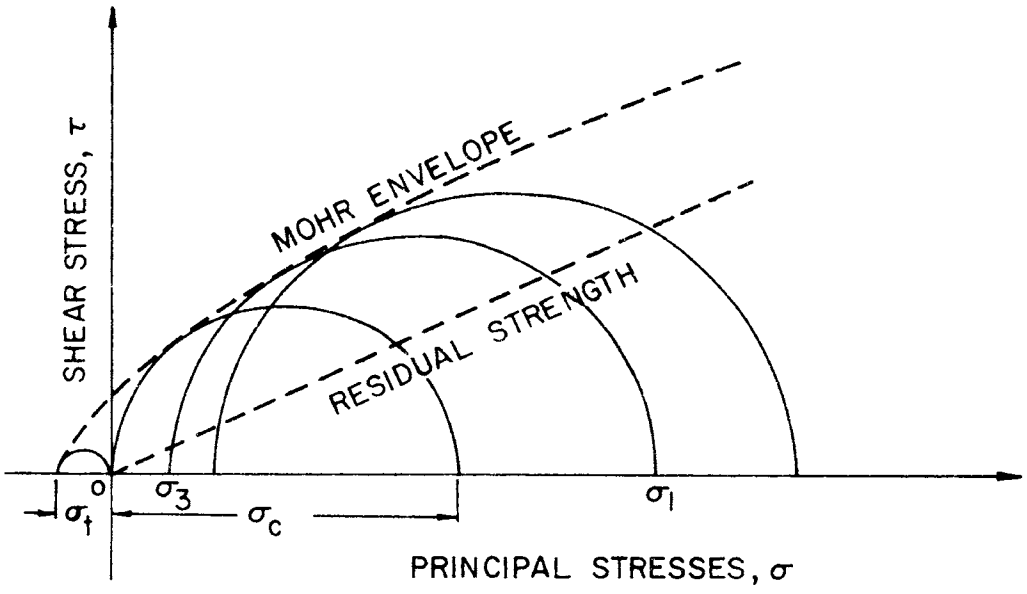

(a)

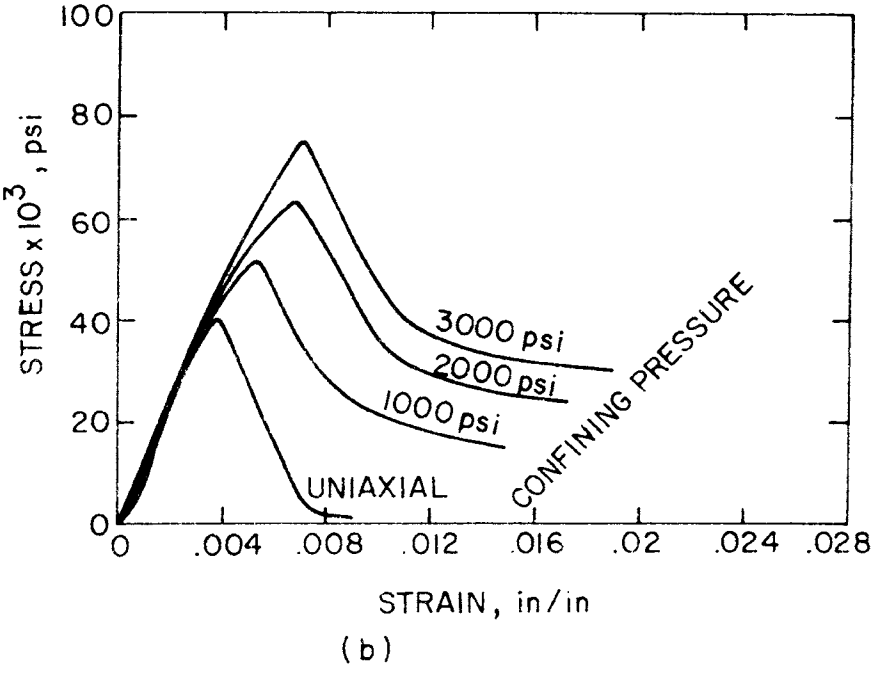

(b)

Figure 9. (a) Mohr Envelope for Rock, (b) Typical Stress-Strain Curves for Norite in Triaxial Compression (After Bieniawski[27])

as observed in the uniaxial compression or direct shear tests (Fig. 9b)[24,27]. The residual strength of pulverized rock after a large displacement could be approximated by a linear Mohr envelope with no cohesive strength as given in Fig. 9a.

E. Failure Theories

Griffith was the first to formulate a theoretical study on fracture initiation based on energy considerations[21,28]. Later on, an alternative approach, which considered the stress concentration at the crack tip, was adopted because of the difficulty of experimentally evaluating the surface energy of a material. Griffith postulated that the presence of small cracks or flaws existing in almost every rock causes large stress concentrations at the tips of these cracks when the material is stressed. He derived the relationship between the applied stress field and the tensile stress at the crack tip, assuming the crack has the shape of a flat ellipse. When the tensile stress at or near its tip reaches a critical value, the crack will start to extend. This critical value may be expressed by a corresponding critical value of the applied stress for the case of uniaxial tension. Therefore, a fracture initiation criterion is formulated, which relates the principal stress components of an applied stress field to the uniaxial tensile strength of the material*, as

$$(\sigma_1 - \sigma_3)^2 / (\sigma_1 + \sigma_3) = - 8 \sigma_t \qquad (1)$$

---

*Note that the uniaxial tensile strength is negative in this study. Hence, in substituting a numerical value for σ_t, the negative sign must be shown, e.g. σ_t = -800 psi.

Where σ_1 and σ_3 are the major and minor principal components of the applied stress and σ_t is the axial tensile strength of the material.

Griffith's original theory does not consider the closure of cracks. Under compressive stress conditions, however, closure may occur before the tensile stress at the crack tip is high enough to initiate fracture. When closure takes place the shear resistance, resulting from the contact pressure between the crack faces, has to be overcome before propagation of the crack can occur. McClintock and Walsh modified Griffith's original theory to account for this effect and obtained a relationship between the principal stresses required to initiate fracture. When the normal stress on the crack surface is compressive, the equation is

$$\sigma_1 = \sigma_3 \frac{(1 + f^2)^{\frac{1}{2}} + f}{(1 + f^2)^{\frac{1}{2}} - f} + \sigma_c \qquad (2)$$

Where f is the coefficient of friction between the crack faces and σ_c is the uniaxial compressive strength of the material.

As discussed above, original and modified Griffith theories refer to fracture initiation only. The fracture propagation path and its associated stress redistribution are very difficult to predict. Furthermore, the theories assumed a single flaw in a semi-infinite elastic media, i.e., the intersection of adjacent flaws has been neglected. Therefore, Griffith's hypothesis, based on a genetic concept, cannot represent a complete rock failure mechanism. Nevertheless, if a modified friction coefficient is assumed, which is different from the internal crack friction, then the modified

Griffith theory almost coincides with the experimental failure envelope of an intact rock[28].

F. Mathematical Material Failure Model for Rock

Obviously, rock failure is too complicated to be expressed by a single criterion. In the interest of the study of practical engineering problems, a mathematical model based on observations of experimental results is proposed as follows:

1. Before the stress state reaches the maximum failure strength, rock is considered linear-elastic, isotropic and homogeneous.

2. The simplified failure criterion for an intact rock is assumed to be a linear Mohr envelope as shown in Fig. 10[24]. Tensile rupture occurs when the minor principal stress equals the uniaxial tensile strength of the material. When the normal stress on the potential shear surface is compressive, i.e., where the modified Griffith theory applies, a linear envelope is chosen. The transition between tensile and compressive failures can be approximated by the relationship between intrinsic shear strength τ_o and uniaxial tensile strength σ_t as:

$$\sigma = \frac{1}{2\ \tau_o\ \mu}\ \tau^2 + \sigma_t \qquad (3)$$

μ is the slope of the Mohr envelope.

3. After tensile fracture, rock loses its cohesion on the newly created surface and still retains its strength in the direction parallel to the fracture surface. This situation can be approximately simulated in a computer code using the finite element method, which

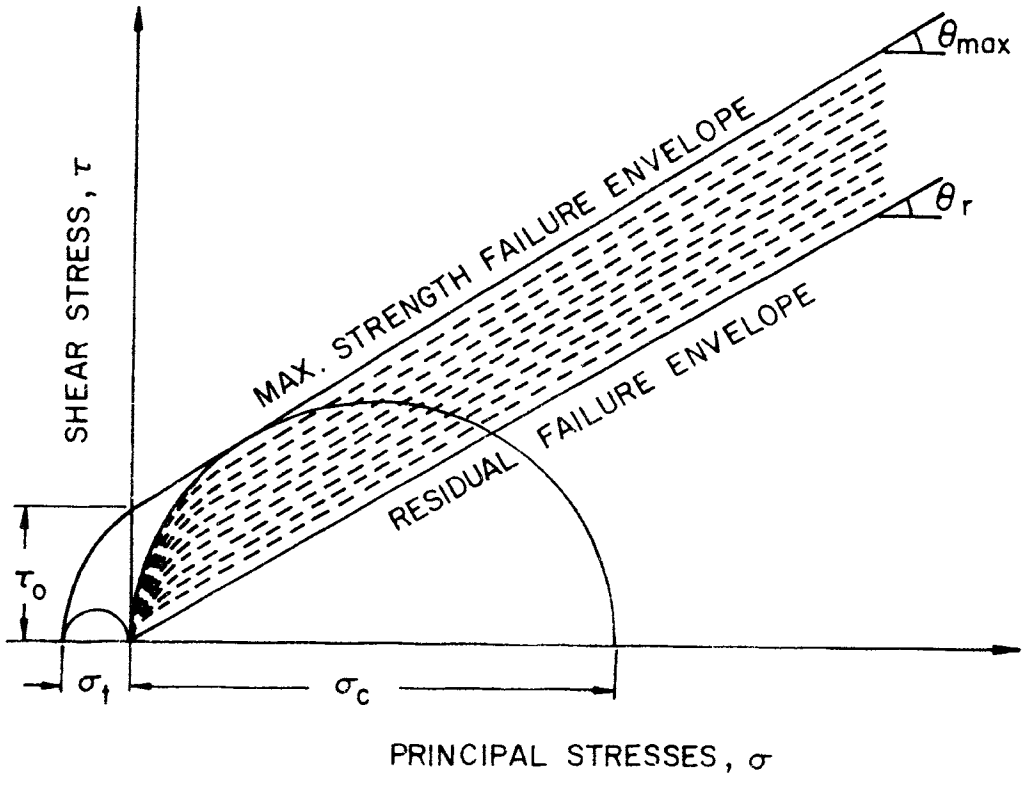

Figure 10. Idealized Failure Envelope for Rock

will be discussed in detail in the next chapter.

4. After compressive failure, rock strength and stiffness decrease gradually along with the displacements until they finally reach the residual values. Degrees of failure are represented by dividing the space between two extreme envelopes, intact and residual, into many levels. On each level, i.e., the same failure envelope, the degree of failure and material properties are assumed the same.

The slope of the Mohr envelopes for maximum and residual failure strength, the shapes of the falling branch of stress-strain curves as well as the variations of rock properties during the process of progressive rock failure are different from rock to rock. Therefore, extensive tests along with refined experimental methods are needed for a better understanding of the post-failure behavior of a particular rock used in a penetration study.

In order to compare the results from computer simulation with experimental tests, a particular rock, Salem (Indiana) Limestone, will be used for this study. Its properties are[18]:

Tensile strength, σ_t	-759 psi
Compressive strength, σ_c	6,370 psi
Young's modulus, E	3,660,000 psi
Poisson's ratio, ν	0.272
Angle of maximum Mohr envelope, θ_{max}	30 degrees

Because the study of the post-failure behavior of rock is still in the developing stage, the information for Salem Limestone needed to establish a mathematical failure model as suggested above is still

incomplete. Some interpolations between bounded values and extrapolations from the available properties are necessary.

The angle of the residual Mohr envelope θ_r has not been well tested. Therefore, two estimated values, 25 and 30 degrees, will be used in the simulations.

Since the stiffness of rock decreases with the displacements, the instantaneous value of Young's modulus for a fractured rock is assumed to be the slope of the chord of the stress-strain curve as shown in Fig. 11.

The post-failure curves, as shown in the previous sections, display a fast strength loss at the beginning of rock failure and a gradually flattening toward their residual levels. A simple mathematical relation, representing this characteristic, is given as:

$$E_i = EP^c, \quad P = \frac{\sigma_i - \sigma_r}{\sigma_{max} - \sigma_r} \tag{4}$$

Where E_i instantaneous stiffness

c slope constant

P ratio of strength

σ_i instantaneous strength

σ_{max} maximum strength

σ_r residual strength

Figure 11 shows two post-failure stress-strain curves with constants c = 2 and 2.5. These two constants will be used in the analytical study.

While the stiffness of rock decreases in progressive failure, Poisson's ratio should also be changed accordingly. Since Poisson's

ratio for fractured rock is not available, an alternative approach is suggested. The compressibility β of an intact rock is defined as:

$$\frac{\Delta V}{V} = \beta \, \Delta p \tag{5}$$

Where V volume

ΔV volumetric change, for plane strain problems

$$\frac{\Delta V}{V} = \frac{3}{E} (1 - 2\nu) \, p$$

p pressure, $p = \frac{1}{3} (\sigma_x + \sigma_y + \sigma_z)$

Δp pressure change

If we assume that the relationship of Eq. (5) can also be applied to the post-failure state with a constant compressibility, then Poisson's ratio becomes a function of the instantaneous stiffness E_i. The variable Poisson's ratio ν_i can be expressed as:

$$\nu_i = \frac{1}{2} \left[1 - \frac{Ei}{E} (1 - 2\nu)\right] \tag{6}$$

Figure 11 illustrates the change of Poisson's ratio along the stress-strain curve.

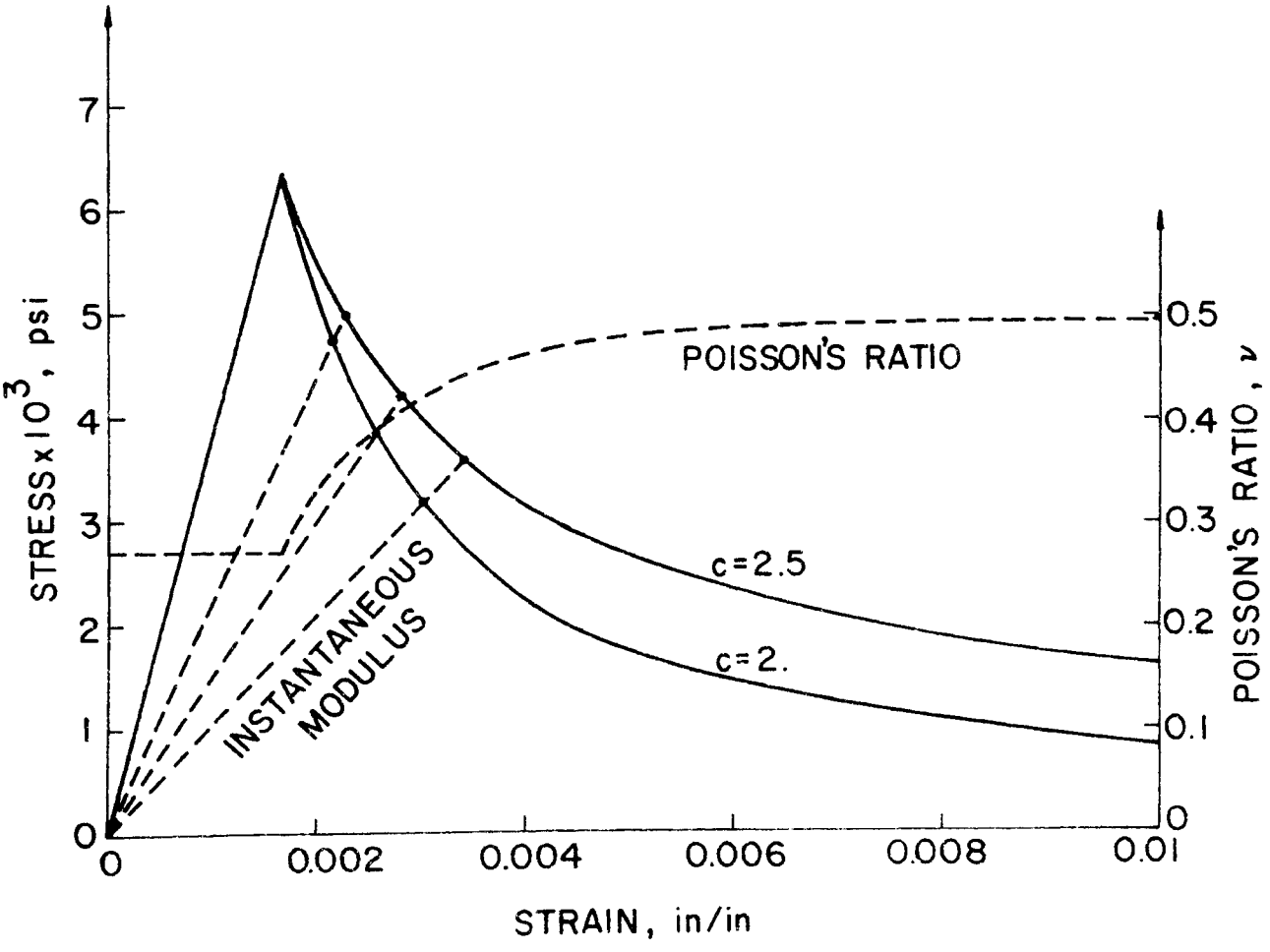

Figure 11. Idealized Stress-Strain Curves for Salem Limestone

IV. THE FINITE ELEMENT METHOD AND ITS APPLICATION FOR PENETRATION SIMULATION

A. General

The finite element method has advanced rapidly with the advent and improvement of electronic digital computers. A considerable volume of literature and text books has accumulated over a relatively short period. The general philosophy and mathematical background of this method can be obtained from many publications. Therefore, in this chapter, discussions will be concentrated on specific methods applied in the simulation of bit penetration.

In order to associate the finite element method with the proposed mathematical material failure model as described in the previous chapter, some finite element techniques will be used in the simulation. An anisotropic element is introduced to represent an element after tensile failure. Variable stiffness is used in the simulation of progressive strength failure of rock. A stress release technique and iteration method are applied during the process of successive penetration.

Bit penetration studies of a long wedge (or blunt point) bit acting on a large block of rock can be considered a plane strain problem, without considering the end effect. The finite element program developed for the penetration study is based on this assumption. Mathematical derivation of the method, using the displacement approach, has been illustrated in detail in the text by Zienkiewicz[29], and basic relations are listed in appendix A for reference.

B. Anisotropic Element

When the minor principal stress of an element reaches its critical value in tension, a fracture surface is created perpendicular to the principal direction. This newly developed surface imposes an additional boundary to the system and results in a significant stress redistribution in the immediate vicinity as well as a change in the structure stiffness. The simulation procedure can be accomplished by regriding the whole structure including the crack surface as a free boundary. However, the amount of work for this procedure is considerable and the continuing modification of successive failures of the structure may be too complicated and costly to be practical. An alternative method, using an anisotropic element to represent a tensile fractured element, has been recommended by Sandhu et al. in their study on tensile fracture propagation[24]. The method assumes that the crack plane is a principal plane for the anisotropic element. In the direction normal to the plane, Young's modulus and Poisson's ratio are reduced to very small values. Nevertheless, the element is still capable of withstanding stress parallel to the crack plane. The plane strain elasticity matrix, $[D]$, for a symmetric anisotropic element can be expressed as

$$[D] = \frac{E_2}{(1+\nu_1)(1-\nu_1-2n\nu_2^2)} \begin{bmatrix} n(1-n\nu_2^2) & n\nu_2(1+\nu_1) & 0 \\ n\nu_2(1+\nu_1) & (1-\nu_1^2) & 0 \\ 0 & 0 & m(1+\nu_1)(1-\nu_1-2n\nu_2^2) \end{bmatrix} \quad (7)$$

Where

$$n = \frac{E_1}{E_2} \quad , \text{ and } \quad m = \frac{1}{2\ (1 + \nu_2)}$$

The constants E_1 and ν_1 are associated with the behavior in the fracture plane, and E_2 and ν_2 with a direction normal to these.

When the direction of the fracture surface is inclined at an angle, β, to the global coordinates, a transformation for the matrix is necessary. If $[D']$ represents the local matrix, then it is easy to show that

$$[D] = [T][D'][T]^T \tag{8}$$

Where $[T]$ is the transformation matrix and $[D]$ is now the elasticity matrix in global coordinates.

C. Non-linear Material Properties

In small strain linearly elastic problems, using the displacement approach, we have always arrived at the final answer by solving the system of equilibrium equations:

$$[K]\{\delta\} = \{R\} \tag{9}$$

Where $\{R\}$ and $\{\delta\}$ list respectively all the external forces acting at nodes and all the nodal displacements, and $[K]$ is the assembled stiffness matrix.

For non-linear material problems, the stiffness matrix of each element is a function of its stress or strain level. Therefore, the final stiffness matrix $[K]$ of the whole structure can be expressed as

$$[K(\{\sigma\})]\{\delta\} = \{R\}$$

$$\text{or } [K(\{\varepsilon\})]\{\delta\} = \{R\} \tag{10}$$

The above equations can be solved by iterative methods. In order to study successive penetration, the incremental displacement method is used. Rewriting the above equation in terms of small penetration increments, we obtain

$$[K]_{n-1}\{\Delta\delta\}_n = \{\Delta R\}_n \tag{11}$$

Where $[K]_{n-1}$ is the stiffness matrix at the previous stress state, and $\{\Delta\delta\}_n$ and $\{\Delta R\}_n$ are matrices of small incremental displacements and nodal loads.

D. Geometric Non-linearity

In the previous section, Eq. (11) has been derived based on small displacements with non-linear material properties. For problems with large displacements or strains, assuming the geometry of elements remains unchanged and using first-order, infinitesimal linear strain approximations may yield an inaccurate solution. Practical engineering structures such as plates, columns and other relatively slender designs decrease their load-carrying capacity with continuing deformation. Modifications of the structure stiffness become necessary for large displacement problems. In bit penetration studies, although action is conducted on a large block of rock, the relative material movement around a bit could cause serious errors after a certain depth of penetration. Using the iteration method as suggested in Eq. (11), adjustment for this geometric non-linearity can be accomplished by redefining element coordinates in the computation of stiffnesses. Rewriting Eq. (11), we have

$$[K(\delta,\sigma)]_{n-1}\ \{\Delta\delta\}_n = \{\Delta R\}_n \tag{12}$$

Where $[K(\delta,\sigma)]_{n-1}$ is the stiffness matrix formulated by the most recent coordinates of the elements.

It should be noted that not all non-linearities are accounted for in this study. But since large strains in rock are not possible without fracture significant errors are not introduced[29].

E. Stress Release

Zienkiewicz, et al. have suggested a so called 'stress transfer' method to study linear elastic rock behavior by considering rock as a 'no tension' material[19]. The method converts excessive stresses that an element cannot bear to nodal loads and reapplies these nodal loads to the element nodes and thereby to the system, i.e., excessive stresses can be released from an over stressed element to neighboring elements. Assuming $\{\Delta\sigma\}^e$ are the excessive stresses in an element, then the transformation for nodal loads $\{\Delta R\}^e$ is given by

$$\{\Delta R\}^e = \int_e [B]^T \{\Delta\sigma\}^e dV \qquad (13)$$

Where $[B]$ is the strain-displacement coefficient matrix.

Stress releases can basically be divided into two cases, tensile and compressive releases. When the minor principal stress σ_3 of an element reaches its critical value, tensile fracture occurs and the critical tensile stress should be released. Figures 12a and 12b show the stress states of an element before and after stress release. Figure 12c represents the stress relationship on Mohr's circles. In the process of successive penetration, tensile or shear stresses may be accumulated on the tensile fractured surface. These small stress increments are released by a similar procedure as illustrated in Fig. 13. The above release method can also be applied for an

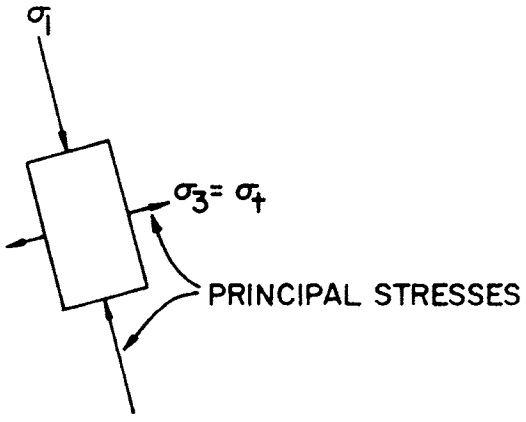

a. BEFORE STRESS RELEASE

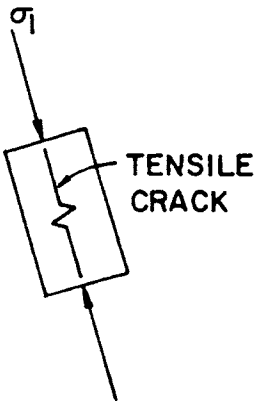

b. AFTER STRESS RELEASE

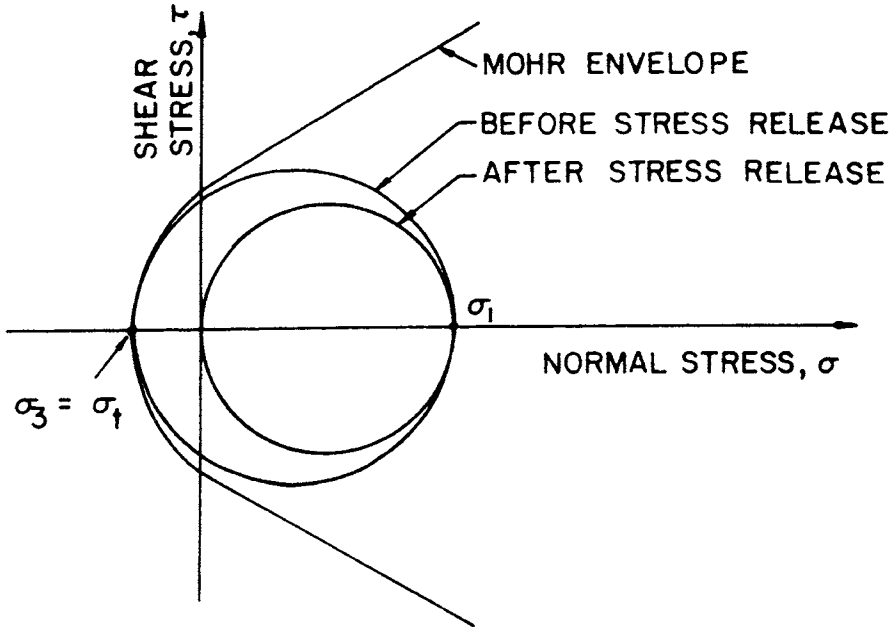

c. STRESS RELEASE RELATIONSHIP ON MOHR CIRCLES

Figure 12. Tensile Stress Release at Tensile Failure

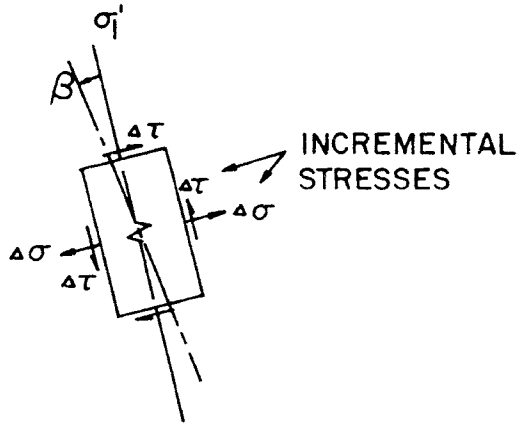

a. BEFORE STRESS RELEASE

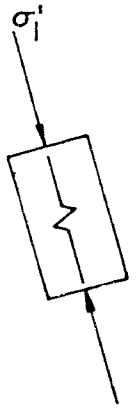

b. AFTER STRESS RELEASE

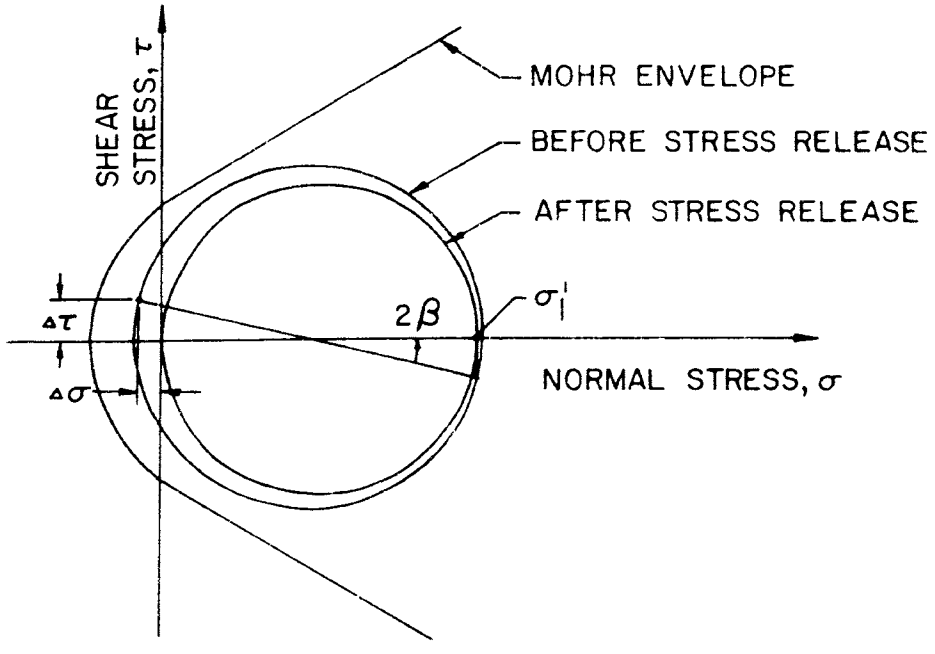

c. STRESS RELEASE RELATIONSHIP ON MOHR CIRCLES

Figure 13. Incremental Stress Release after Tensile Failure

element which has failed in compression with its minor principal stress in tension, which according to the assumption in the mathematical material failure model the tensile stress should be released.

In the case of compressive stress release, when the stress state of an element reaches the failure envelope in compression, a small amount of major principal stress, σ_1, is released as shown in Fig. 14. At point A the element reaches its maximum strength before the stress release, and point B represents the released stress state with a reduction in major principal stress $\Delta\sigma_1$ from point A. In the process of incremental bit penetration the stress state of an element may increase again to its new failure point C. A similar stress release procedure, as started at point A, is repeated. If the incremental displacement of bit penetration and the amount of stress release are sufficiently small values, then the falling branch of the stress-strain curve as shown in Fig. 14 can be closely followed.

F. Iteration Process

Simulation of bit penetration starts from the initial contact of a bit and an intact rock without pre-existing stresses. A small assigned incremental penetration is imposed in each iteration. With the assigned small displacement on the boundary and the current structure stiffness, the incremental stresses can be obtained by solving the matrix equations as given in Eq. (12). If the displacement increment is sufficiently small, then each incremental solution may be considered linear and could be accomplished accurately in one step. In order to trace actual fracture propagation during penetration, the computer program is designed to adjust penetration

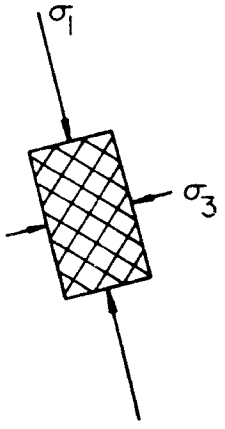

a. BEFORE STRESS RELEASE

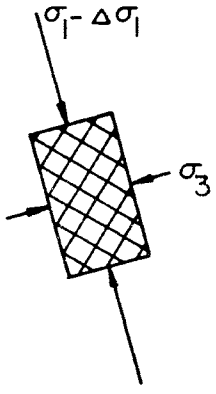

b. AFTER STRESS RELEASE

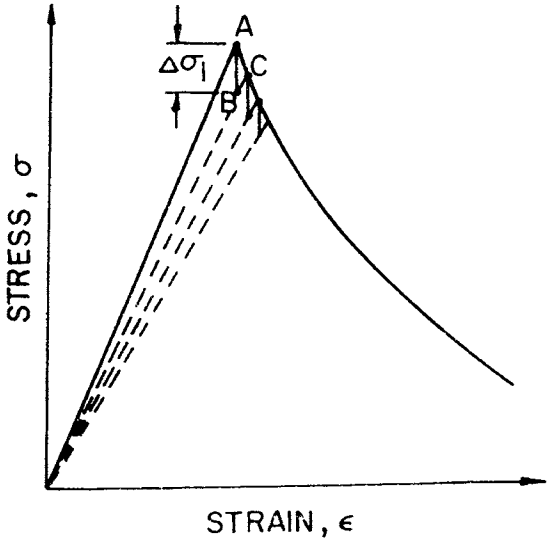

c. STRESS RELEASE RELATIONSHIP ON STRESS-STRAIN CURVE

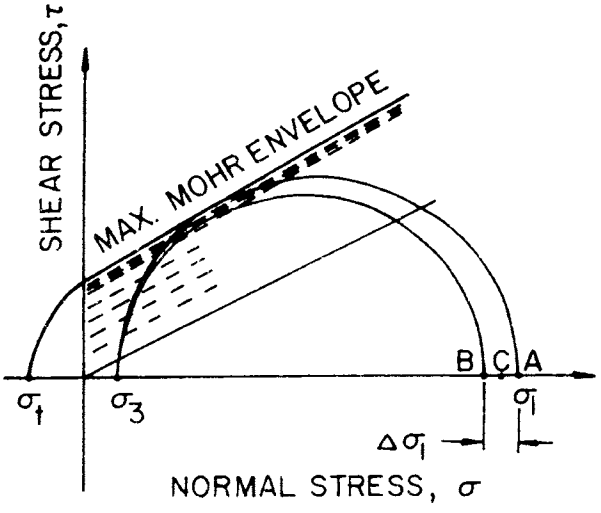

d. STRESS RELEASE RELATIONSHIP ON MOHR CIRCLES

Figure 14. Successive Compressive Stress Release

magnitude in each iteration by allowing no more than one unfailed element to reach the failure envelope. The ratio of the adjustment is used in calculating actual incremental stresses. After the accumulated total stresses for each element are obtained, the stress states of all failed elements are checked to determine their current situation. Further modifications for material properties and releases for excessive stresses follow, if necessary. An additional loop within the same iteration is performed to release these excessive stresses. In this loop, transformation from stresses to nodal loads is accomplished using Eq. (13), and the penetration boundary is adjusted to keep the bit stationary. Stress redistribution is accomplished at the end of this loop by adding the incremental stresses, generated from the transferred nodal loads, to the total stresses of all elements.

Since the incremental penetration is small, modification for geometric non-linearity is taken after a specified number of iterations. Before each execution of the program, the number of iterations n and coordinate modifications m have to be specified. With these numbers, the computer program can automatically iterate n times before modifing the node coordinates and formulating the new structure stiffness. At the end of every n iterations, node and element data are punched on cards for plotting and continuation of simulation. A simplified flow chart of the program is shown in Fig. 15, also, a computer program list with input instructions is given in appendix B.

In order to make a proper modification of the failed elements, a simplified classification is introduced:

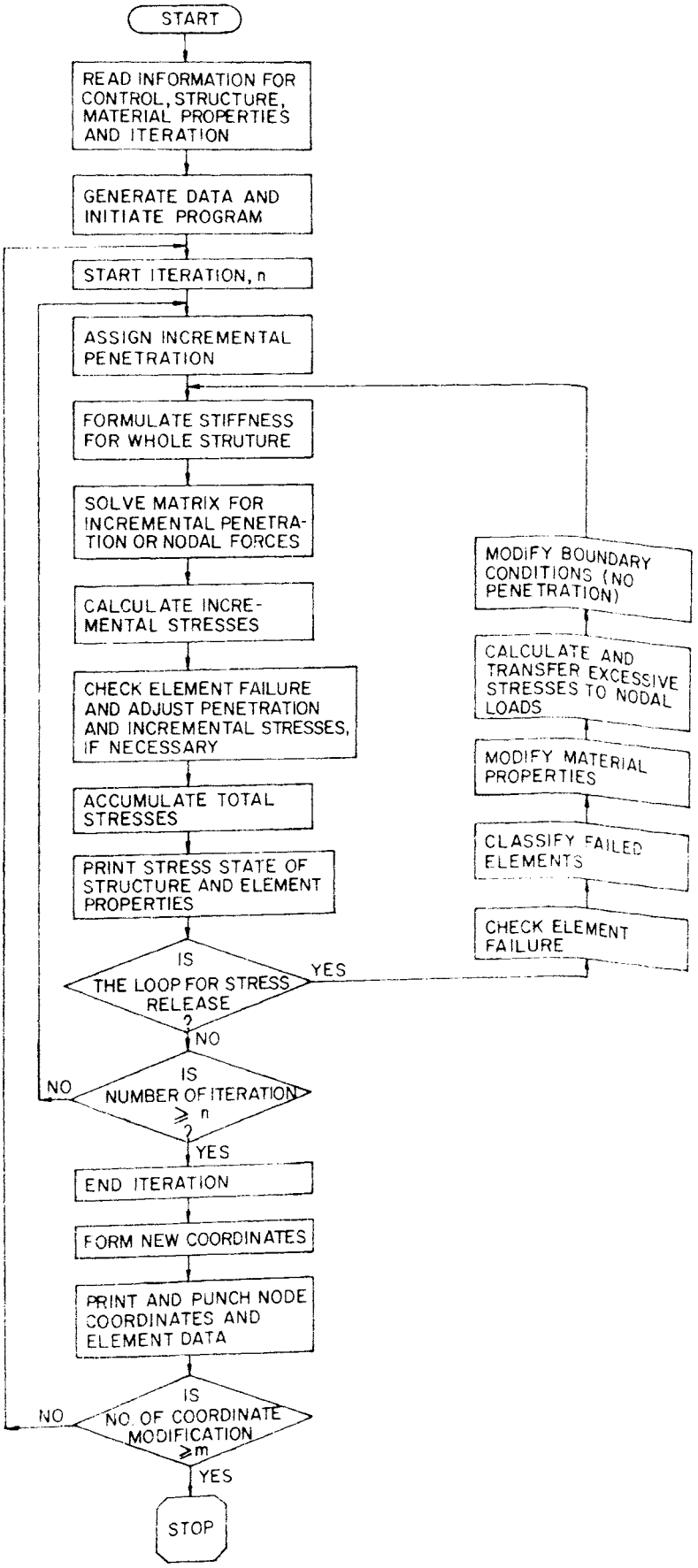

Figure 15. Flow Chart for Bit Penetration Simulation

Class 1: tensile fracture with an open crack. An anisotropic element is used for this class. Incremental stresses generated on the crack surface should be released. Tensile or compressive stresses in the crack direction are checked for possible further failure. If the stress in that direction reaches the tensile or compressive strength, then the failed element becomes class 4 or class 3, respectively. These classes are introduced in the following paragraphs.

Class 2: tensile fracture with closed crack. If the crack was closed, then the normal stress on the crack surface becomes compressive. Therefore, anisotropic material properties are abandoned. However, the crack direction is recorded in case of crack reopening. Compressive failure is checked for a possible change of failure state.

The above crack opening is determined by comparing the current element volume with a testing volume which is obtained by applying the current major principal stress on the element. If the volume of the current element is greater, then the crack is open.

Class 3: compressive failure. Elements in this class follow the progressive strength failure as discussed in the previous sections. When the sum of the principal stresses of an element is in tension, the element is classified as class 4.

Class 4: loose fragments. All the stresses in the element are released. Young's modulus and Poisson's ratio are assigned small values. The element volume at the beginning of this class is recorded. If the current volume is smaller than the recorded value, the element becomes class 3.

In practical penetration simulations, most elements stay in

class 3. Some fractured tensile elements may change their classifications from class 1 to class 3 as penetration continues. Only very few elements near the edge of a bit become class 4.

G. Simulations

Blunt point, sharp wedge and cylindrical bits, representing different degrees of dullness, are used in the penetration simulations as shown in Fig. 16 with dimensions.

As proposed in the previous chapter, two material failure models with different stress-strain slopes and residual angles of the Mohr envelope are chosen. The first model, with c = 2.0 and θ_r = 25, is used for all bits; and the second model, with c = 2.5 and θ_r = 30, is applied only with the blunt point bit for the purpose of comparison.

A rough bit-rock interface is assumed for all cases, i.e., no relative movement on the contact surface between bit and rock. Figure 17 shows a finite element grid which is typical of the type used in this study. The overall size and the imposed boundary conditions of the grid are comparable with the experimental test conducted by Maurer, which will be used to compare with the analytical results[9].

1. Blunt point bit

A series of plots showing principal stresses, degrees and types of element failure and position of elements at various stages of penetration of the blunt point bit, using the first material model, is illustrated in Fig. 18. As shown in Fig. 18a, rock begins to fail after a small elastic deformation at the boundary of the cutting

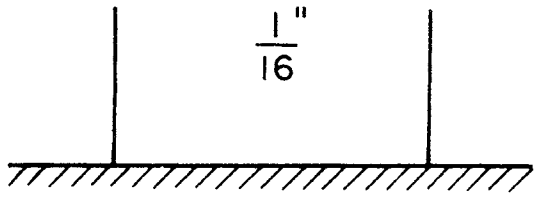

a. BLUNT POINT BIT

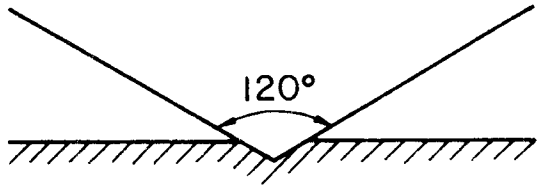

b. SHARP WEDGE BIT

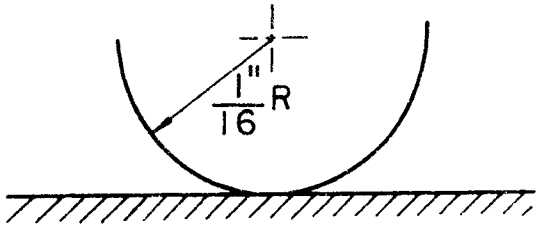

c. CYLINDRICAL BIT

Figure 16. Bits for the Penetration Simulations

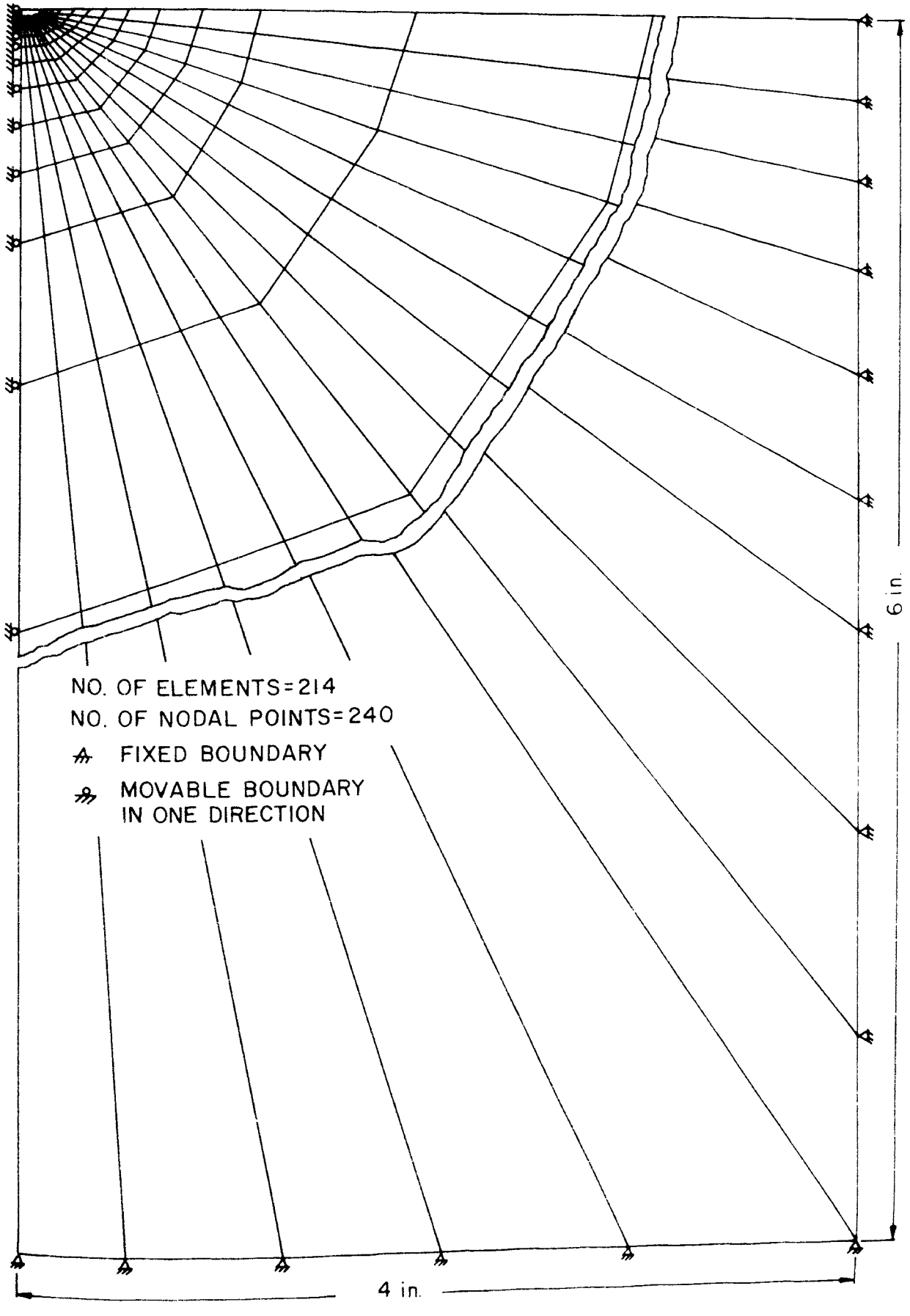

Figure 17. Typical Finite Element Grid for the Penetration Simulations

edge, where high stress intensity exists. Major principal stresses in all elements are in compression with directions toward the penetrating bit. Elements immediately under the bit have high compressive minor principal stresses which keep these elements in the elastic state. The highest stress intensity elements at this stage are under the cutting edge. Fracture in the rock propagates from the edge downward to a certain distance creating a central high compressive zone and separating it from two sides of the rock as shown in Fig. 18b. As the penetration continues, the failed area expands toward the symmetric center of the rock and forms a compressive failure zone surrounding a small portion of the high compressive elastic area immediately under the bit, as shown in Fig. 18c. Increasing penetration at this point has little effect on the side elements, but gradually reduces material strength and stiffness of the compressive zone as shown in Fig. 18c and 18d. The elements which have failed in compression, under the pressure of the penetrating bit, are squeezed into lateral movement, as a consequence, tensile fractures start from the bottom of the compressive zone and gradually spread to both sides, as shown in Fig. 18c, 18d and 18e. If the penetration is further increased, the increasing pressure on the side elements will reach the point that fractures start to propagate in these elements and finally form a chip. At this point, the upward movement of the chip away from the original free surface becomes obvious. The sequence of the chip formation is shown from Fig. 18f to 18h. The downward tensile crack, which has not been fully shown in Fig. 18 due to the limited space, reaches

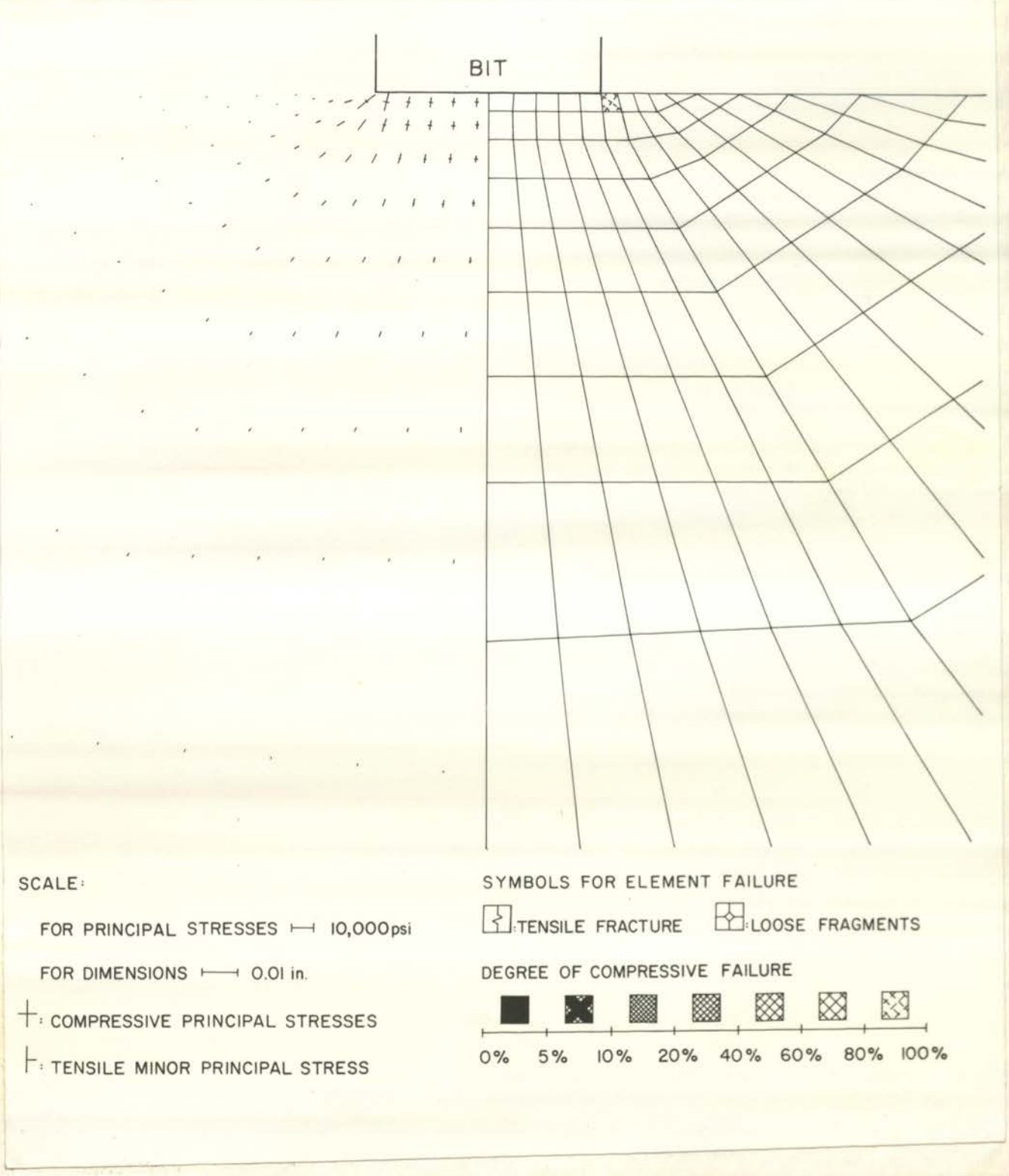

Figure 18a. Blunt Point Bit Penetration Using the First Material Model

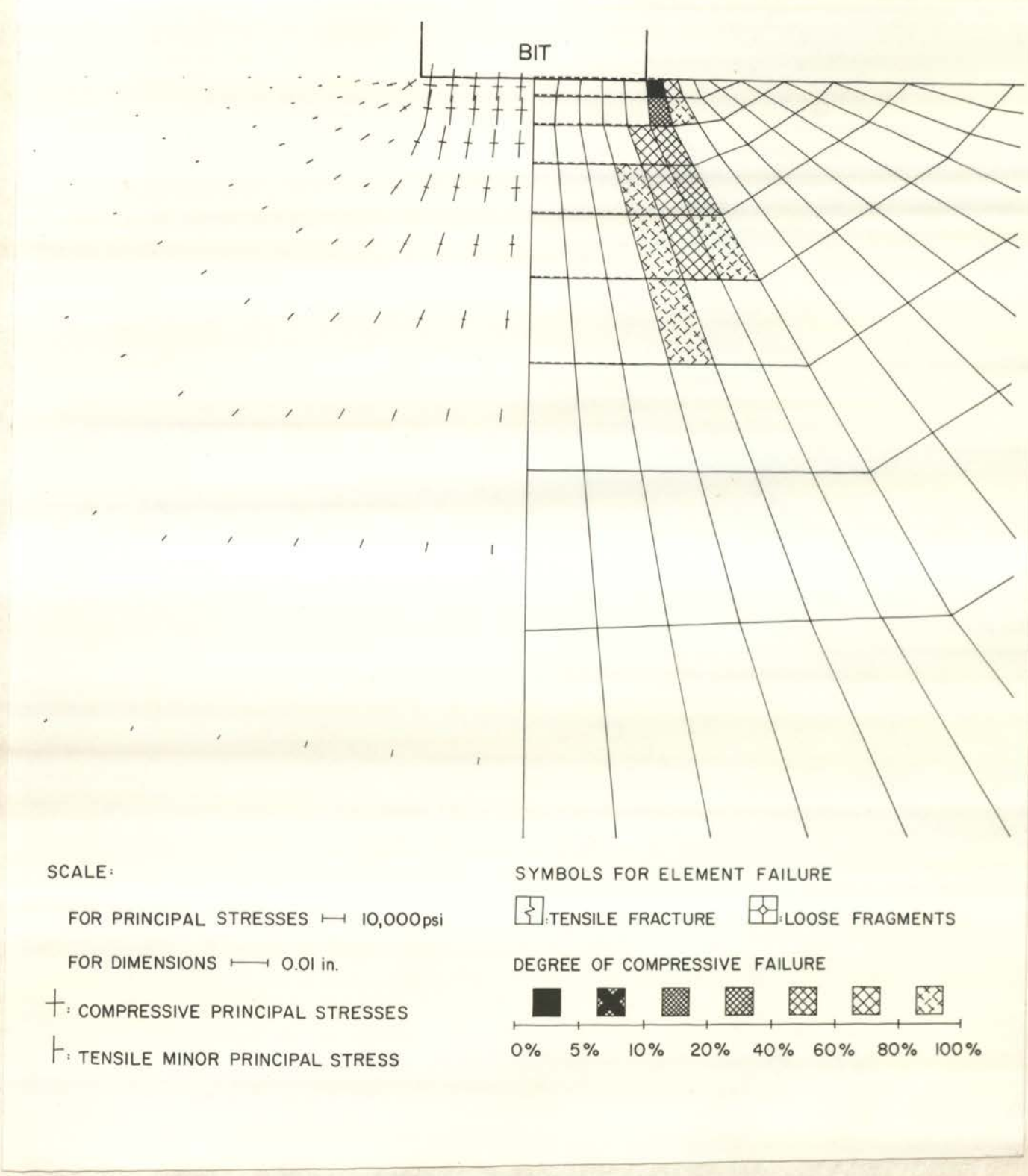

Figure 18b. Blunt Point Bit Penetration Using the First Material Model

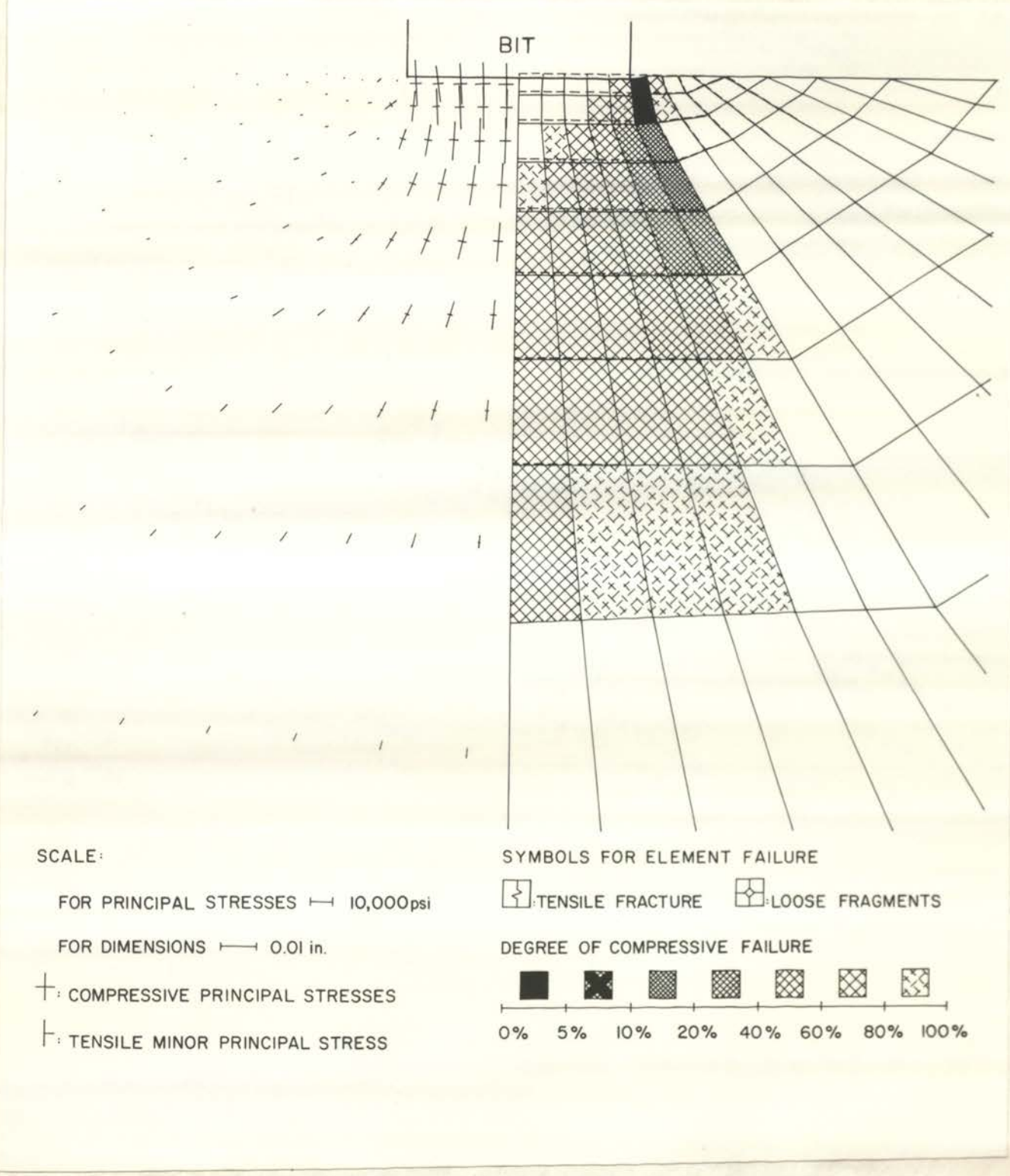

Figure 18c. Blunt Point Bit Penetration Using the First Material Model

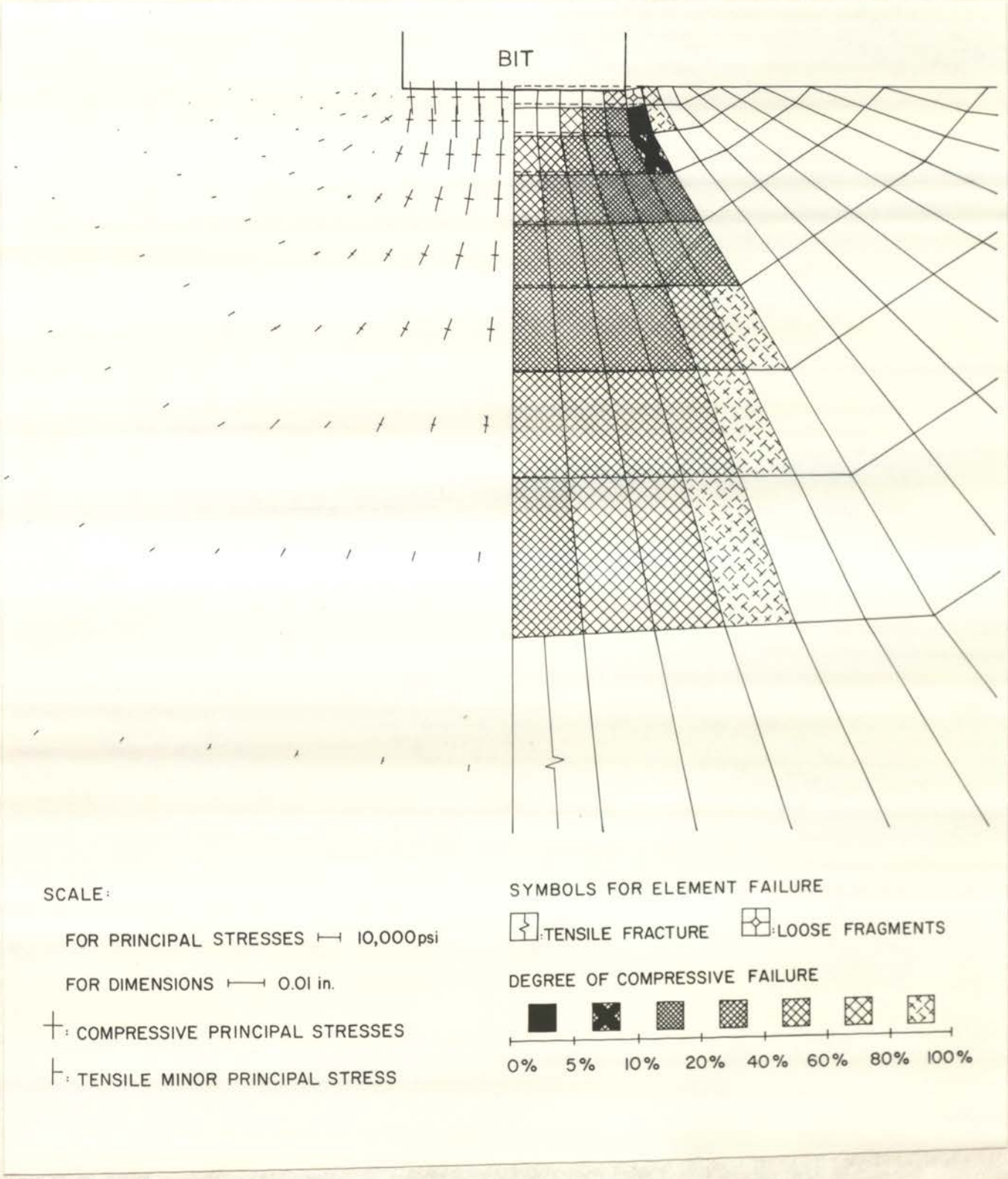

Figure 18d Blunt Point Bit Penetration Using the First Material Model

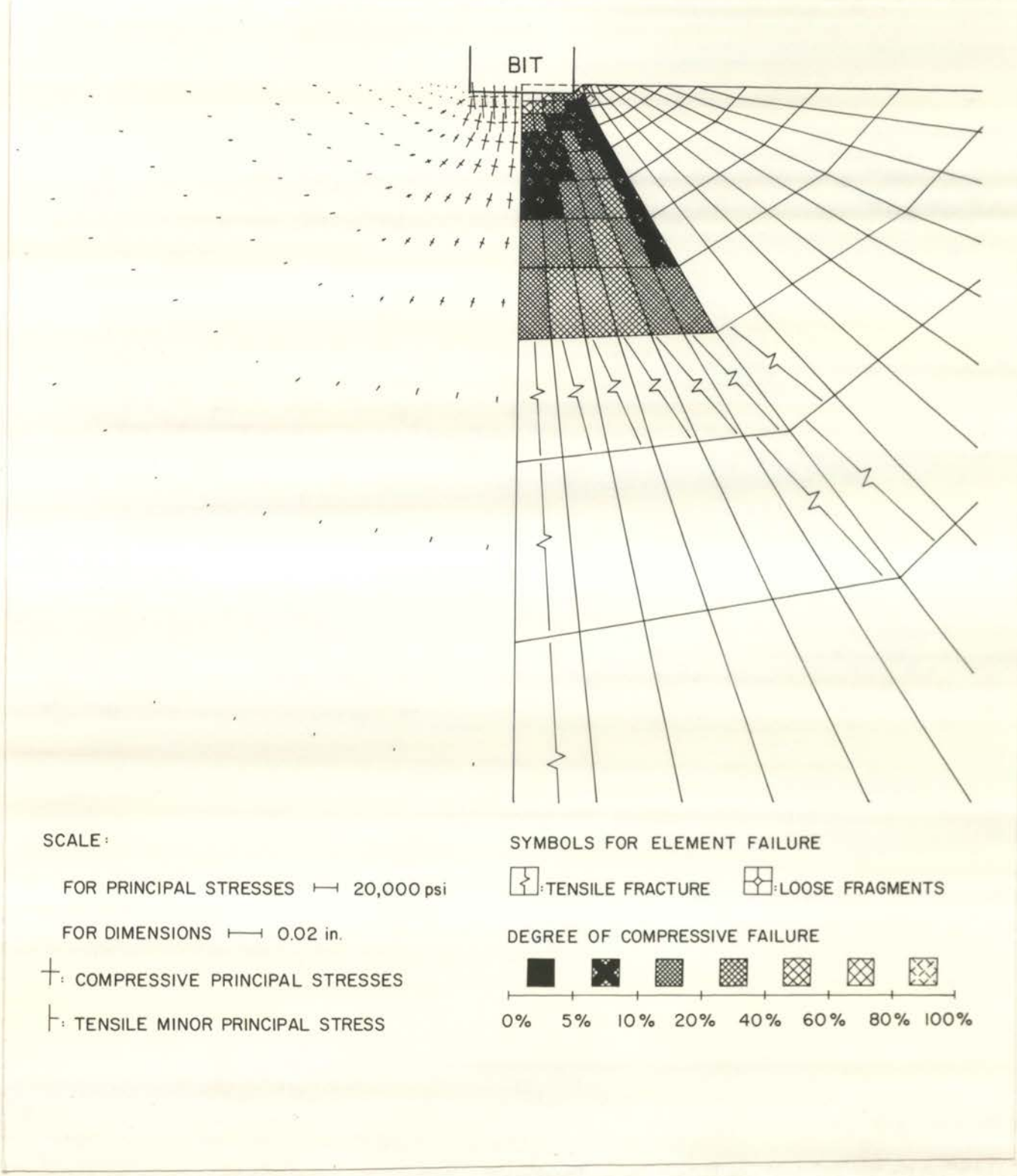

Figure 18e. Blunt Point Bit Penetration Using the First Material Model

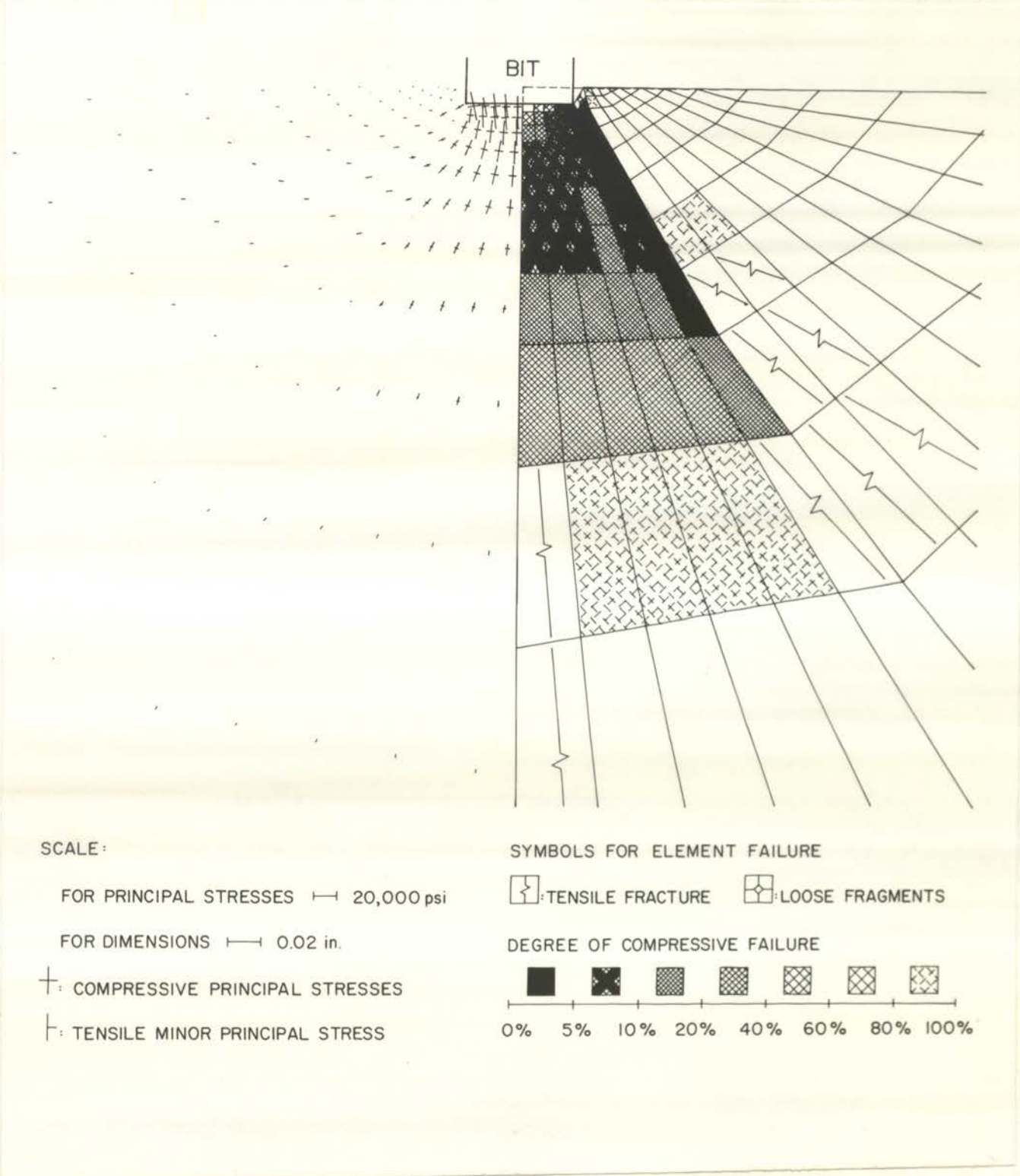

Figure 18f. Blunt Point Bit Penetration Using the First Material Model

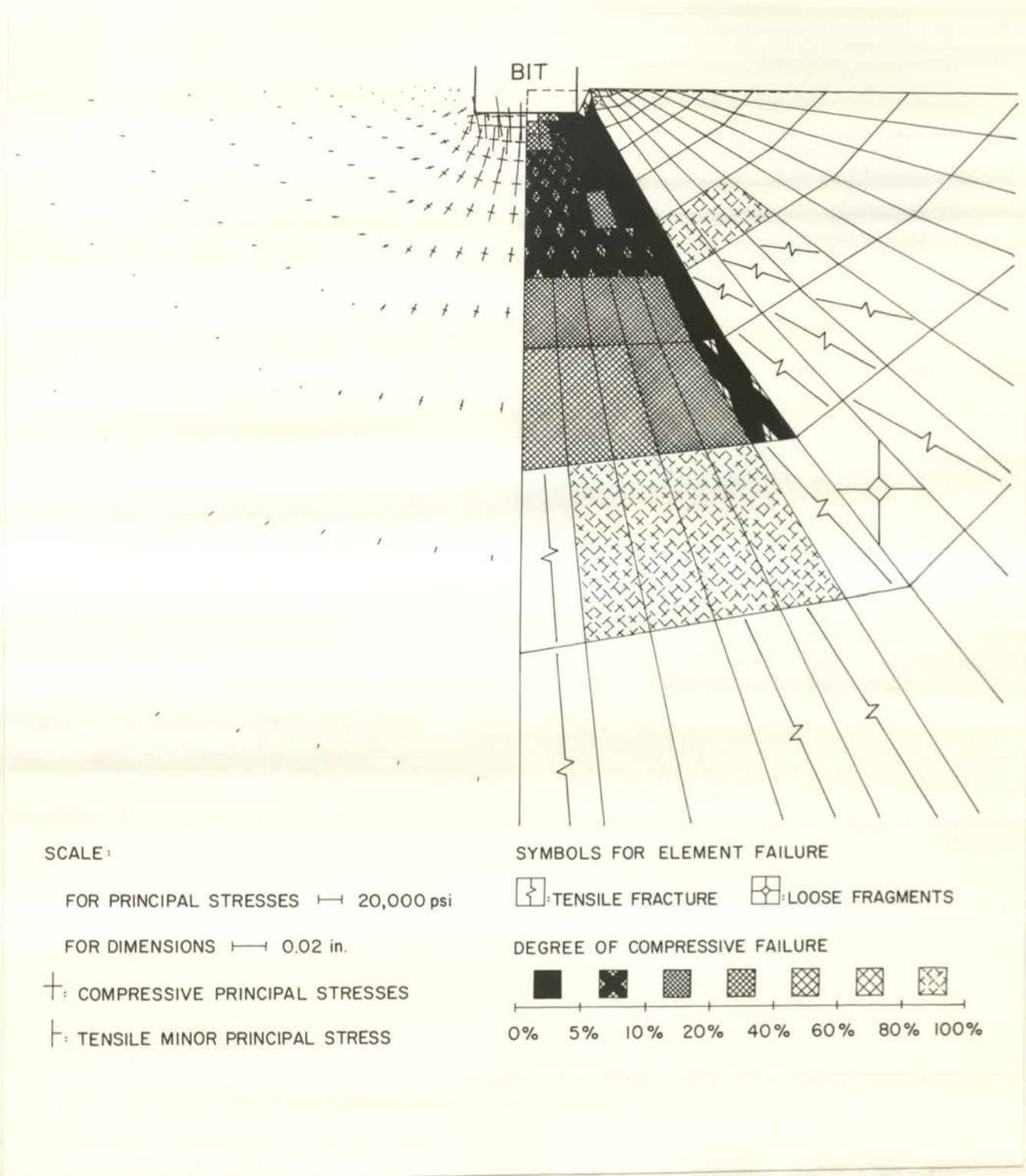

Figure 18g. Blunt Point Bit Penetration Using the First Material Model

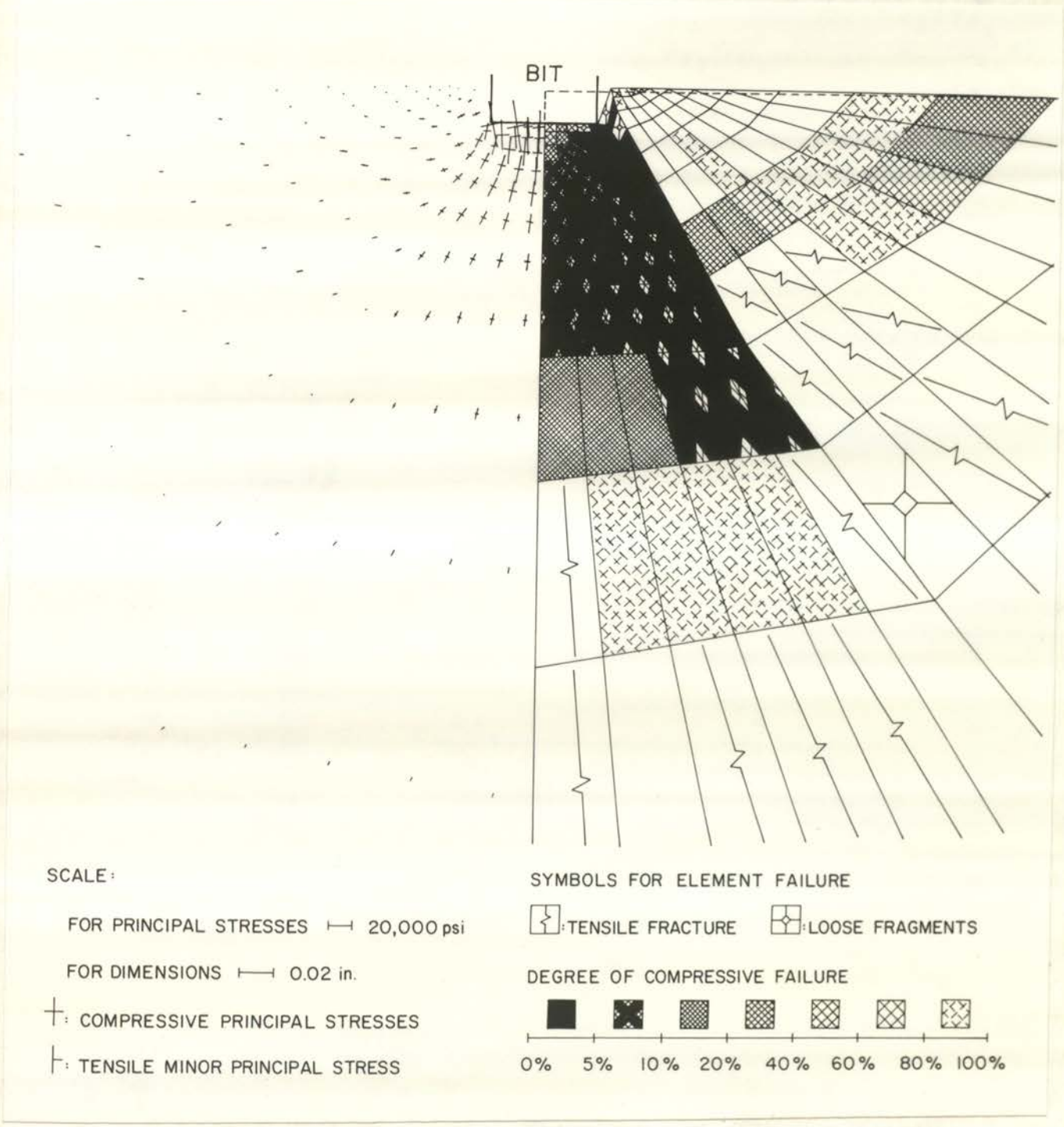

Figure 18h. Blunt Point Bit Penetration Using the First Material Model

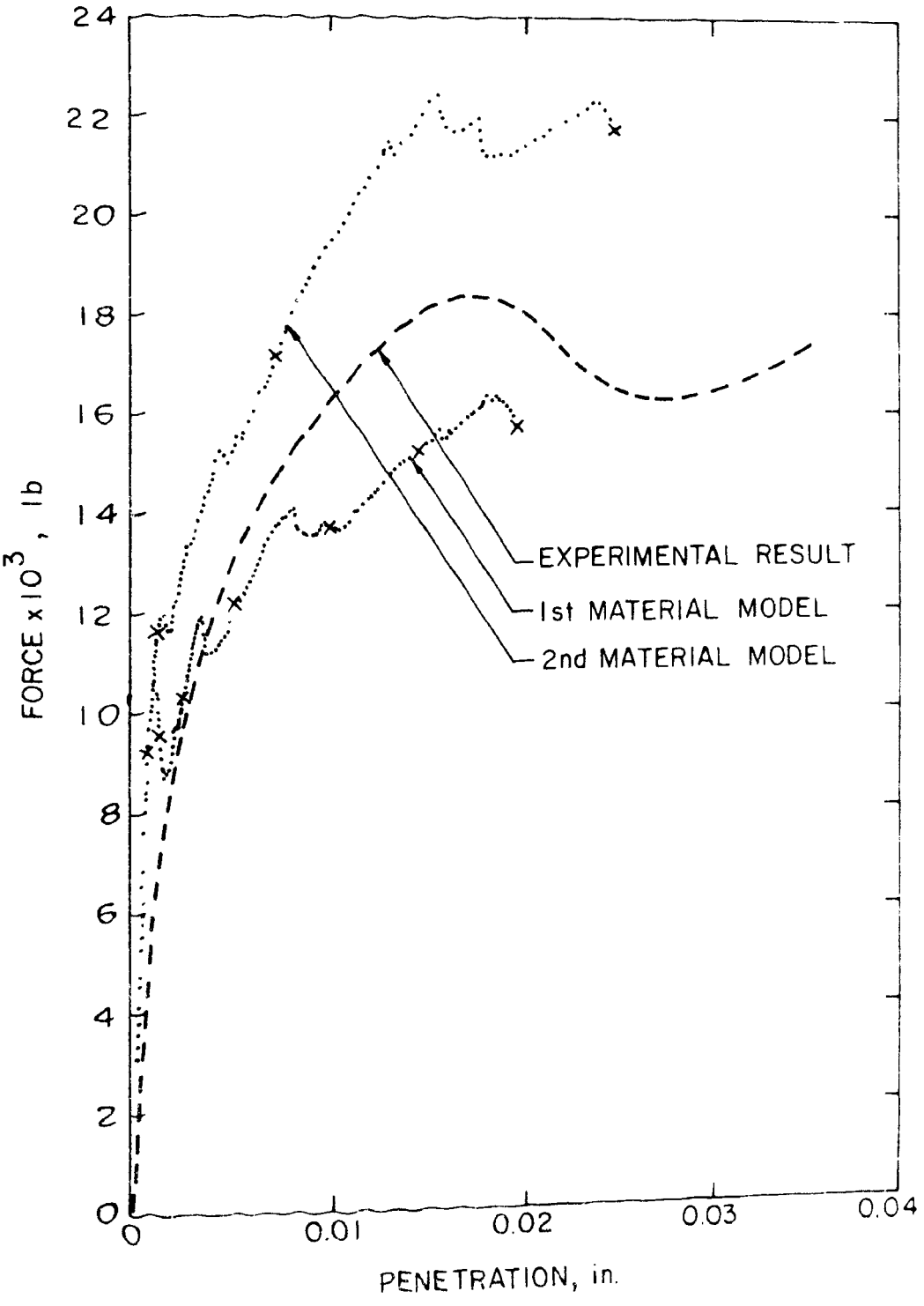

Figure 19. Force-Penetration Curves for Blunt Point Bit

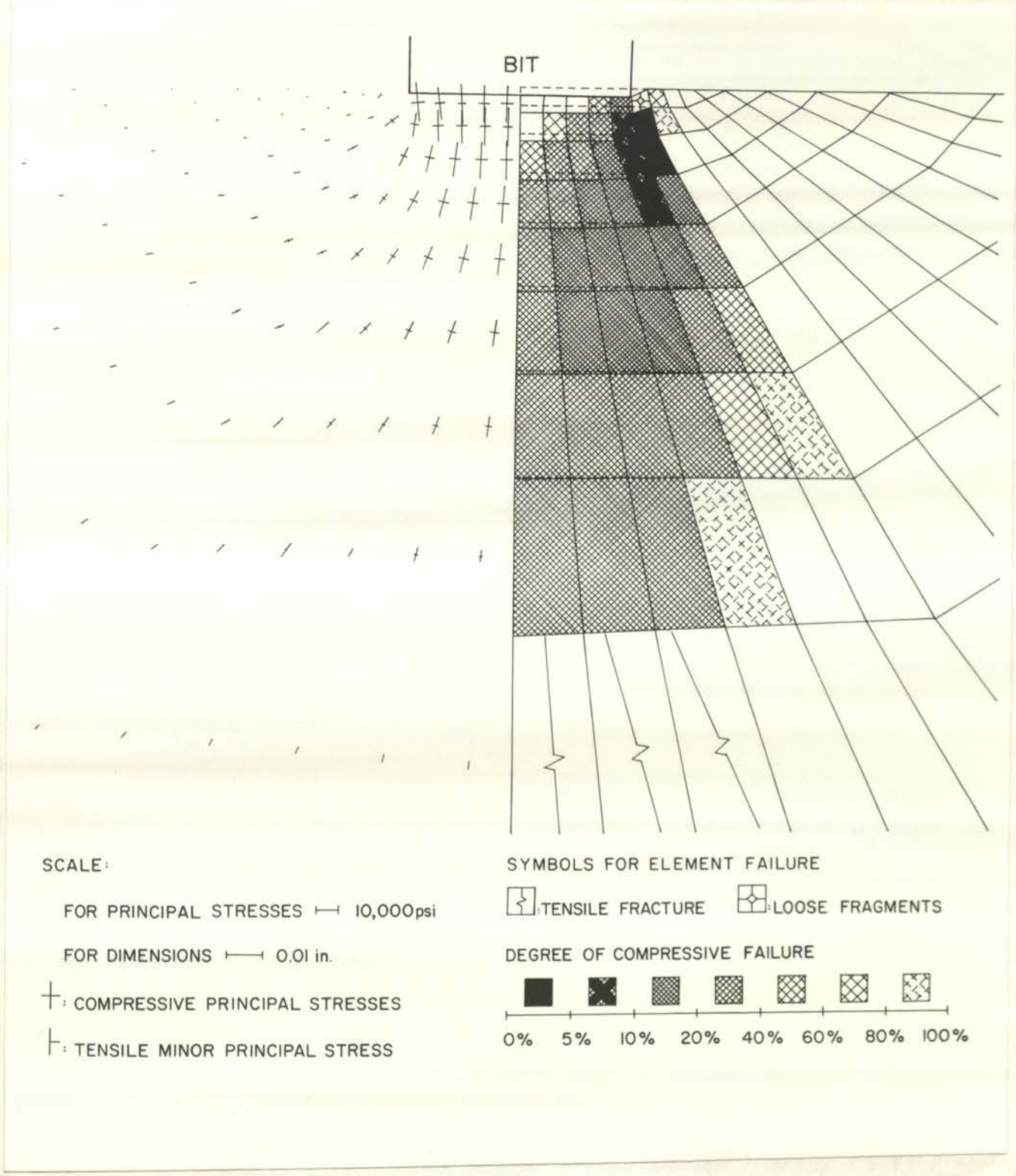

Figure 20a. Blunt Point Bit Penetration Using the Second Material Model

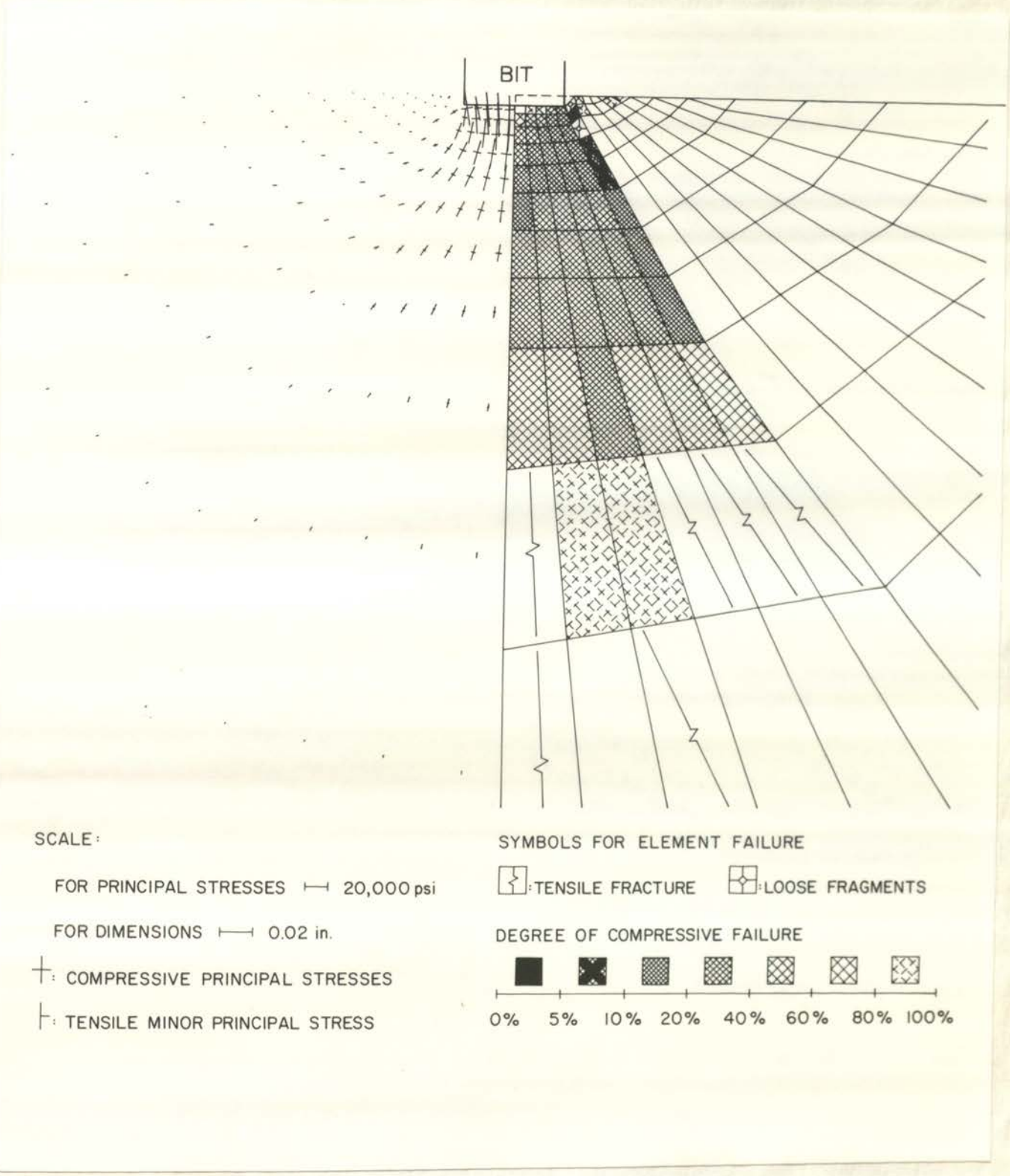

Figure 20b. Blunt Point Bit Penetration Using the Second Material Model

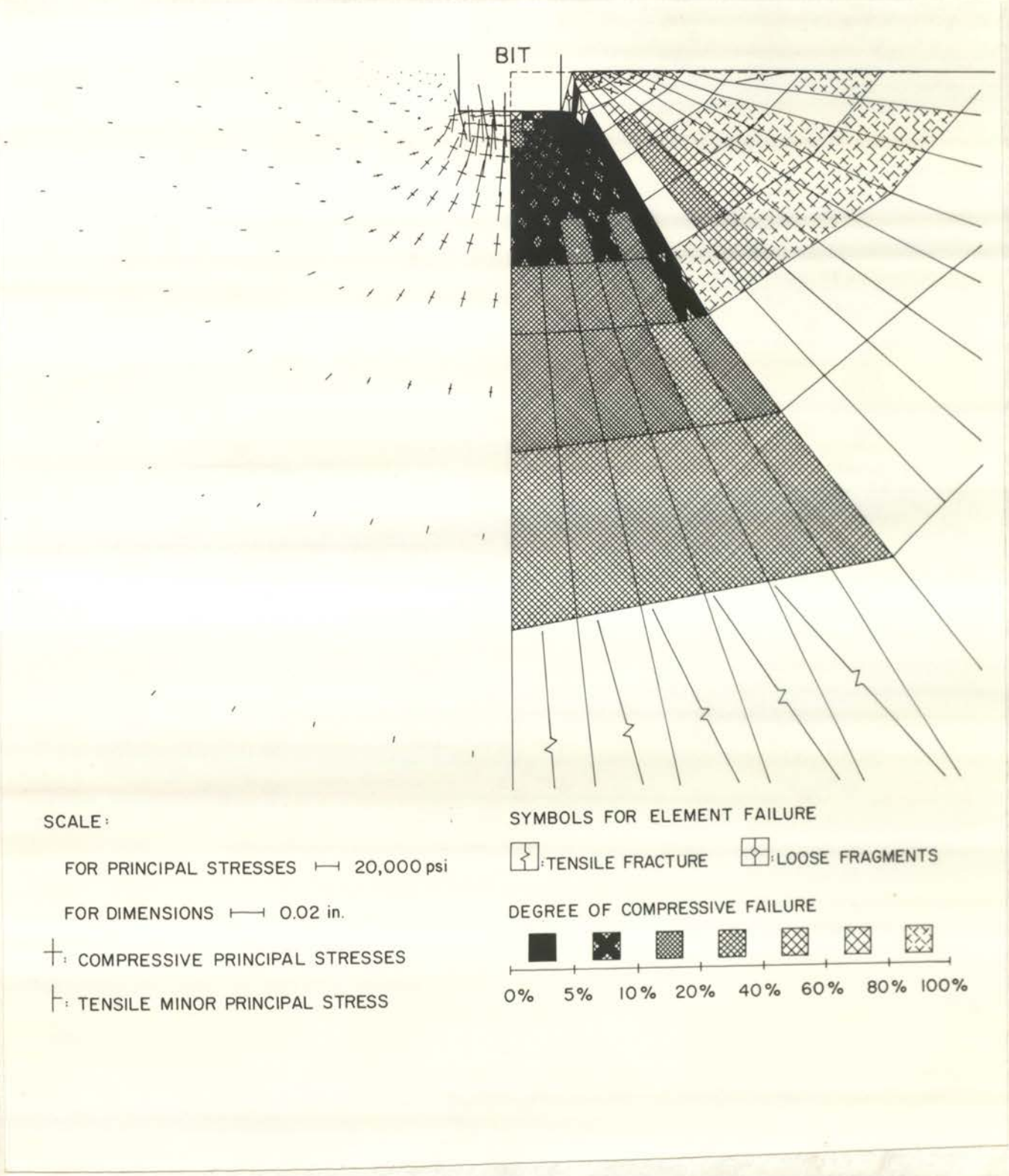

Figure 20c. Blunt Point Bit Penetration Using the Second Material Model

about 1" depth from the free surface at the final stage of the penetration. The corresponding F-P curve of this penetration simulation is plotted in Fig. 19. Cross marks on the curve indicate the positions of the bit penetration, where stress field and element failure are plotted. Every dot represents an iteration in the computer program. As shown in Fig. 19, the F-P curve of this simulation is lower than the experimental result, however, the depths of bit penetration at the peaks of both curves, where the first chip is formed, are close. The analytical F-P curve at the beginning of the penetration showing a steeper slope is probably due to the linear-elastic assumption on rock before failure.

Figure 20 shows the sequence of the blunt point bit penetration using the second material failure model of higher post-failure strength. Some differences between two simulations are observed: a) the depth of penetration to form the chip is deeper in the second simulation, b) the degrees of failure of the elements in the compressive zone are more homogeneous, c) the F-P curve in Fig. 19 for the second simulation is higher than the curves of the first simulation and the experimental result. These results demonstrate the influence of the post-failure rock behavior and properties on bit penetration.

2. Sharp wedge bit

Initial position of the bit is given in Fig. 16 with a small dent in the rock. At the beginning of this simulation, the finite element grid is arranged to have only one element making contact with the bit. After the successive penetration, if the wedge starts

to reach the next element, a second contact element is assigned, etc.

As shown in Fig. 21 the compressive failure zone quickly spreads from the edge of the wedge to the area under the bit. The tensile crack under the compressive failure zone starts to propagate before the side elements have developed high enough pressure to form a chip. When the penetration reaches a depth as shown in Fig. 21c, chip formation is in process. The F-P curve of this bit penetration, as shown in Fig. 22, almost reaches its peak at this stage. Further penetration will complete the chip and pulverize the compressively failed elements as shown in Fig. 21d.

A wedge bit, with the action of the inclined bit surfaces, creates quicker lateral pressure on the side elements than the other dull bits in a small penetration, which results in early chip formation and more effective bit penetration as shown in the simulation.

Because of the quick chip formation in this simulation, the contact boundary has not been modified.

3. Cylindrical bit

Penetration simulation begins at the contact of the first element with the cylindrical bit. In the process of continuing penetration, the contact area of the interface is gradually modified as described in the wedge bit simulation.

Figures 23a and 23b show the failure propagation at the early stage of penetration. Along with the continuing penetration and increasing contact surface with the bit, the compressive failure zone of the rock keeps expanding in lateral and vertical directions

as shown from Fig. 23c to 23e. Tensile cracks and lateral pressure are also increasing simultaneously. Final chip formation and additional radical cracks are shown in Fig. 23f.

For every new element to contact the bit, the F-P curve of this simulation shows a jump in applied force with small penetration as illustrated in Fig. 22. The number at each jump indicates the order of the new contact element. After the element at the edge of the contact zone gradually decreases its strength with penetration, the increased force starts to fall as shown in the figure.

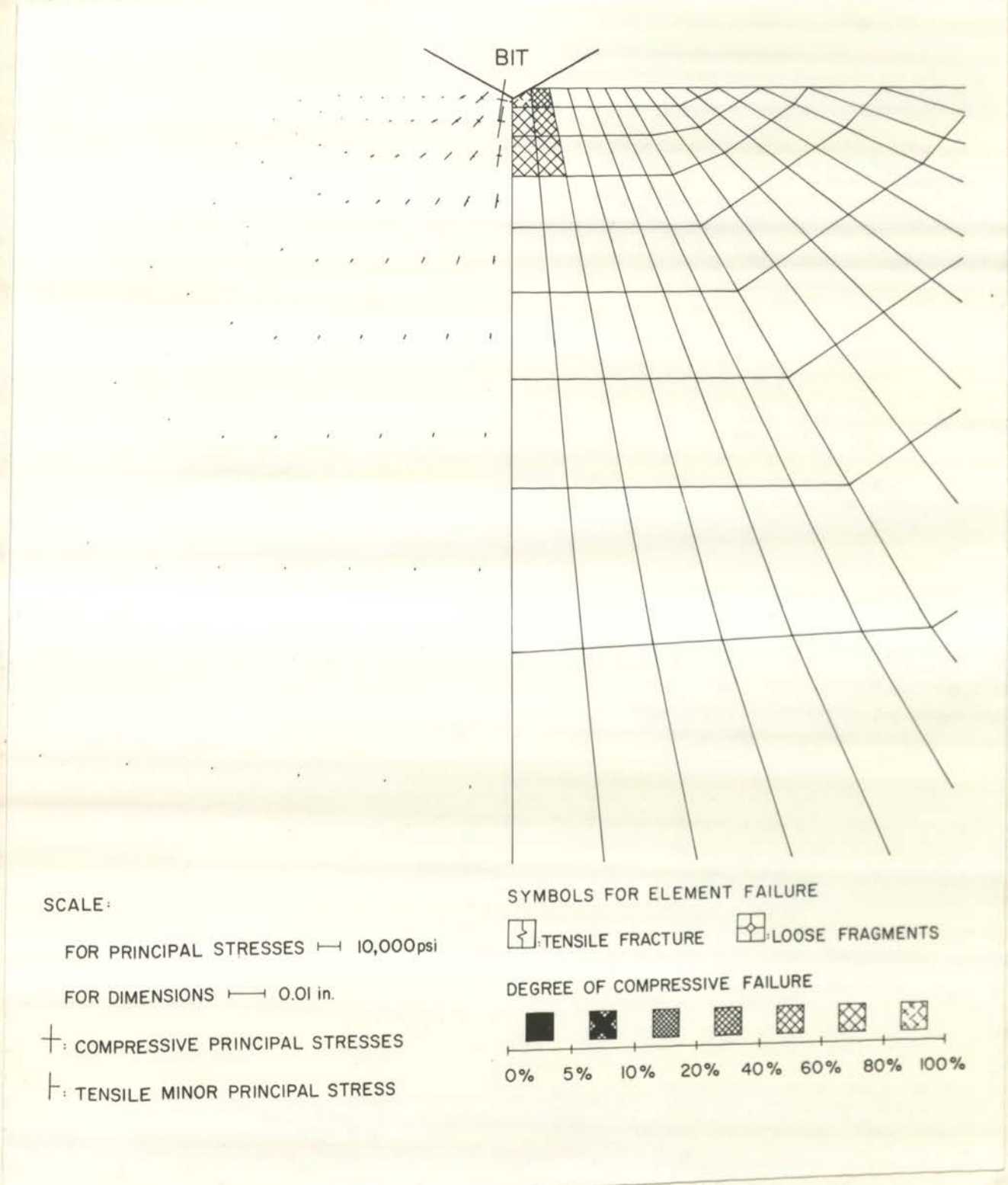

Figure 21a. Sharp Wedge Bit Penetration

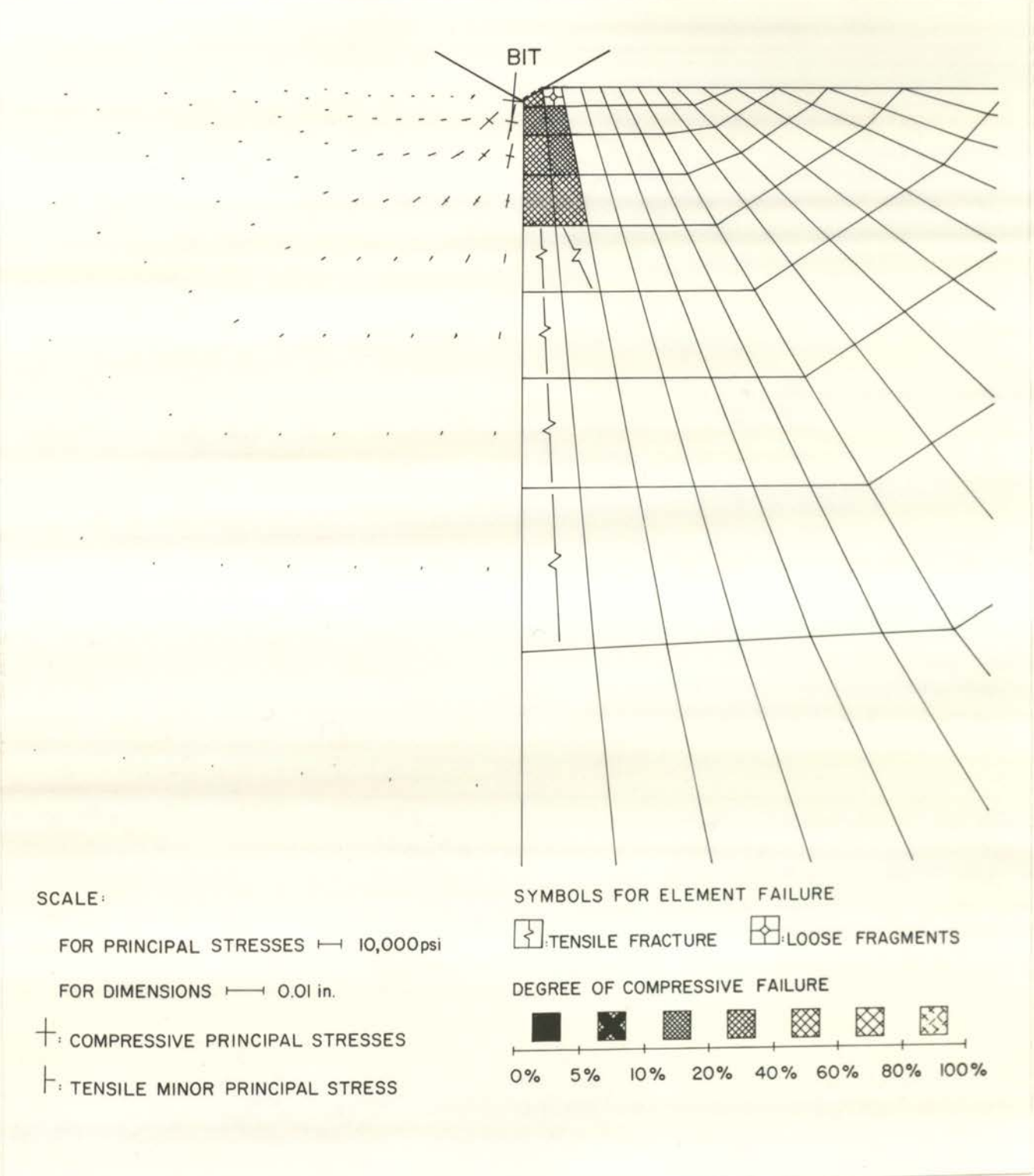

Figure 21b. Sharp Wedge Bit Penetration

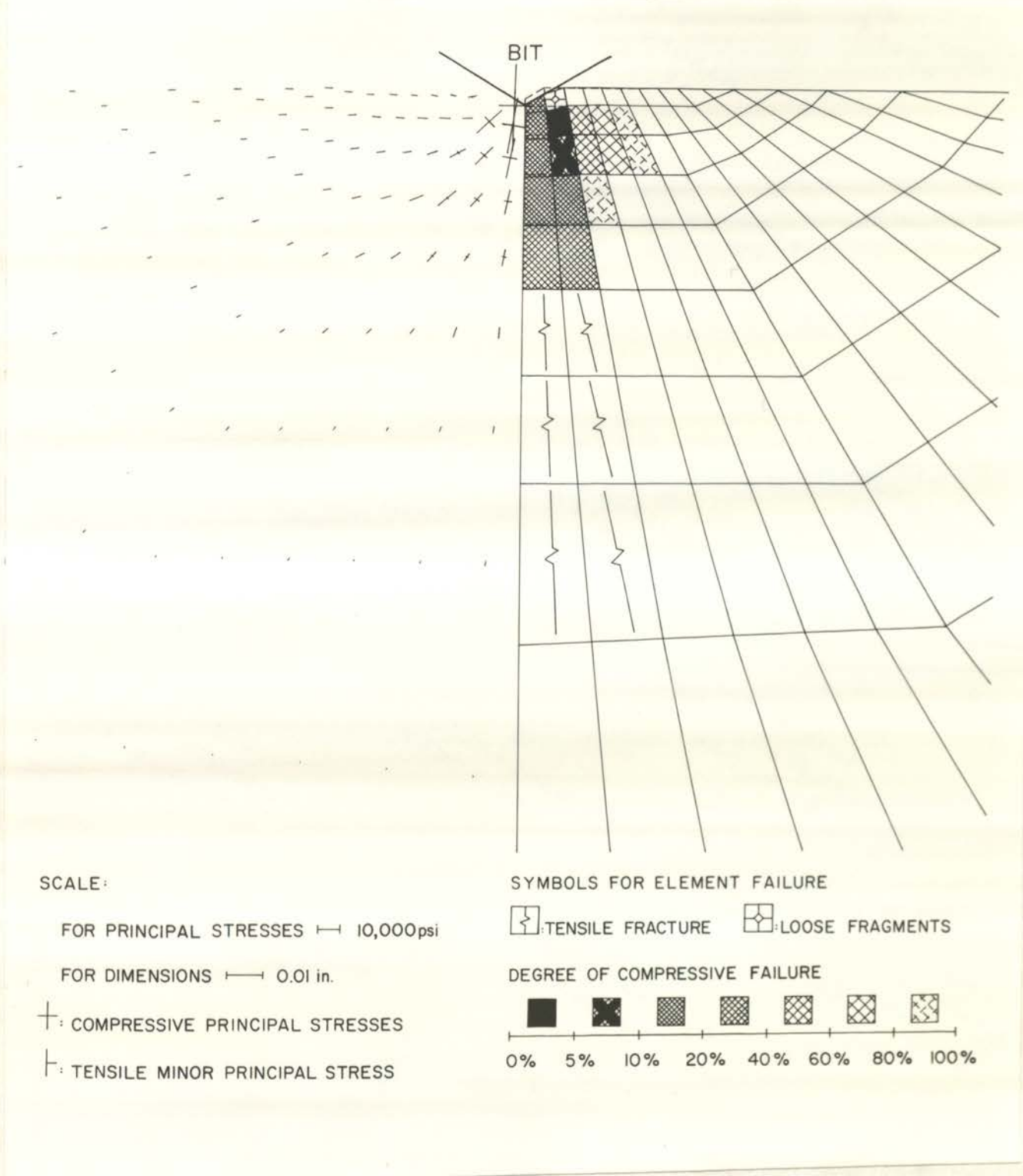

Figure 21c. Sharp Wedge Bit Penetration

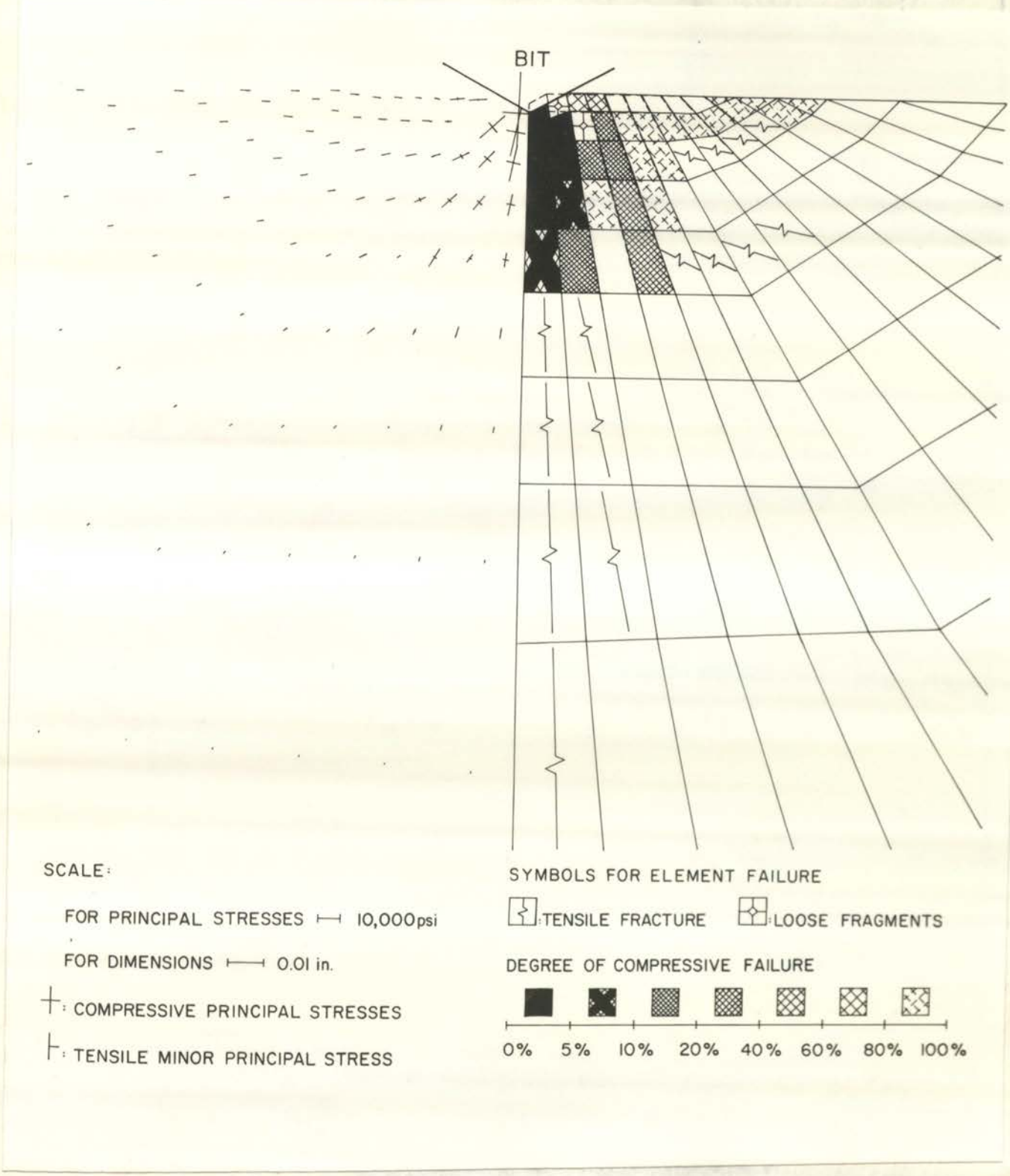

Figure 21d. Sharp Wedge Bit Penetration

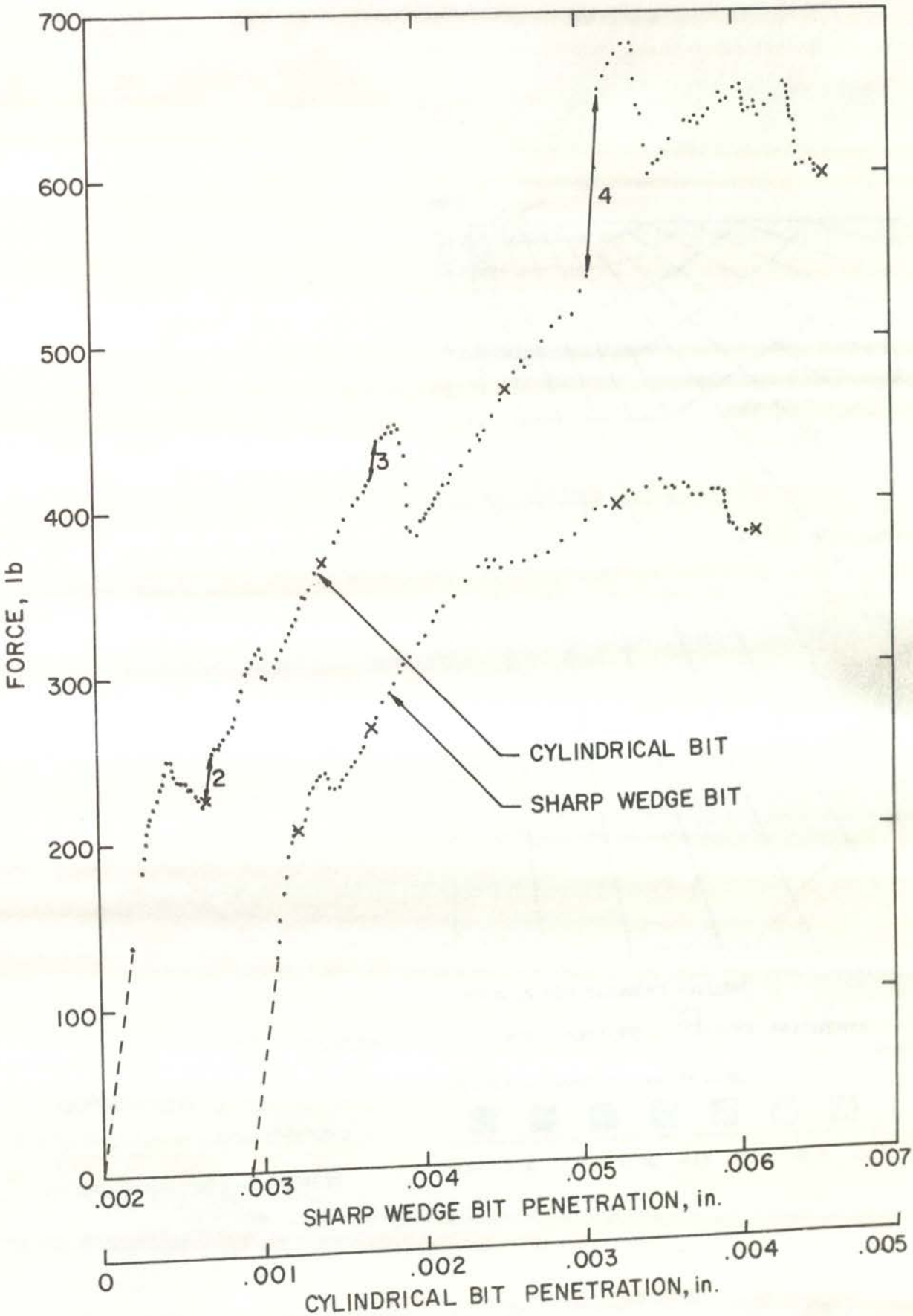

Figure 22. Force-Penetration Curves for Sharp Wedge and Cylindrical Bits

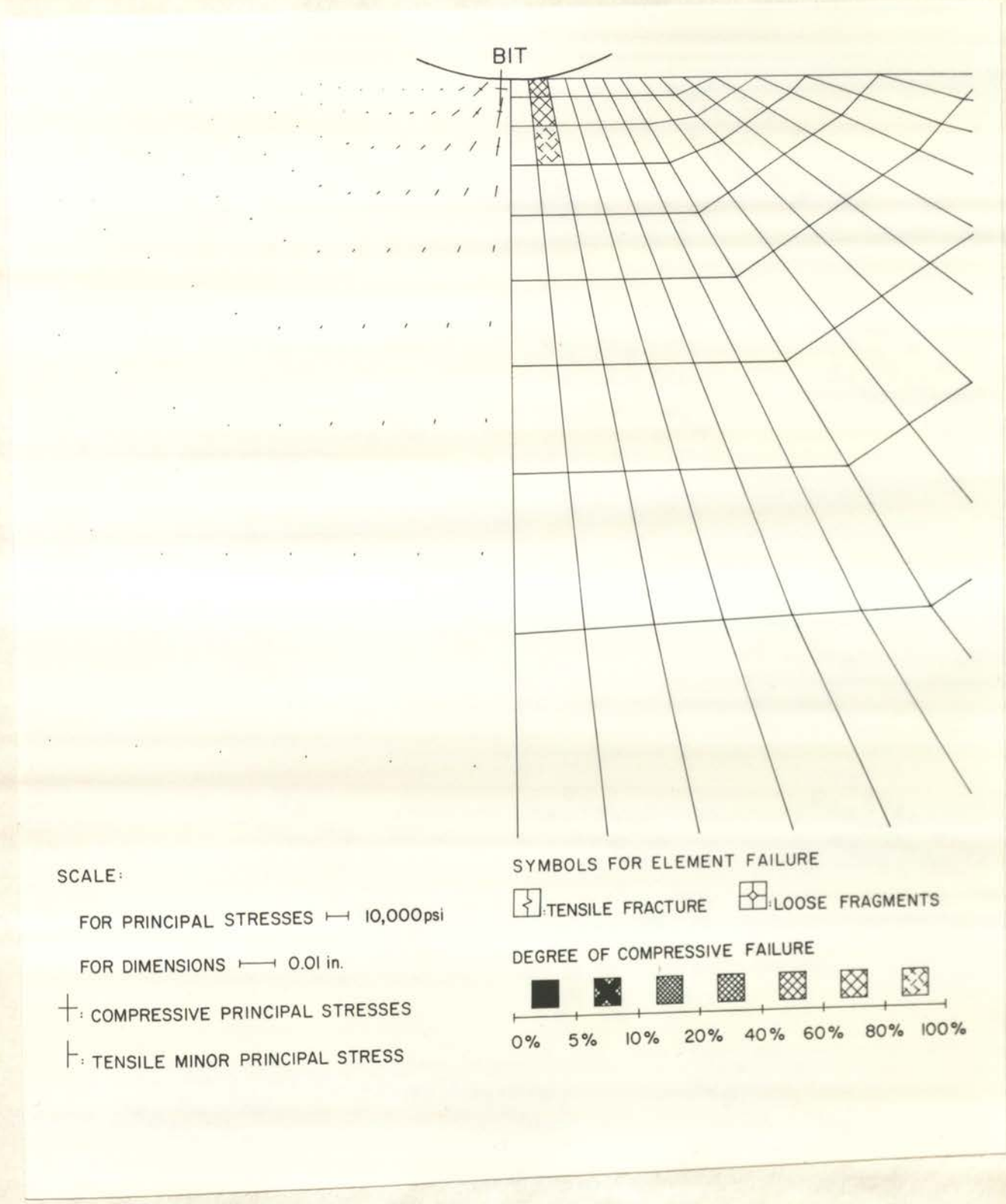

Figure 23a. Cylindrical Bit Penetration

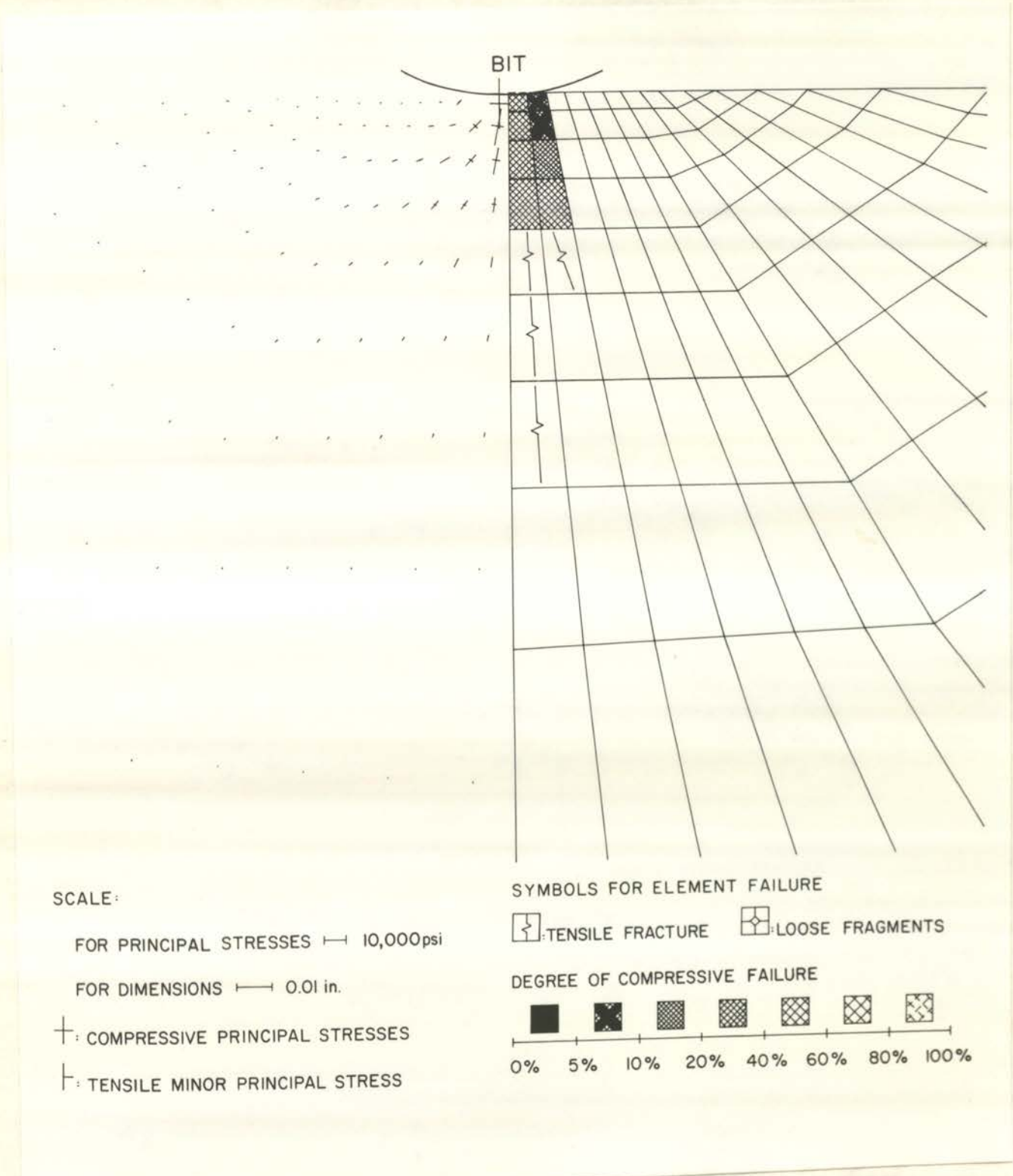

Figure 23b. Cylindrical Bit Penetration

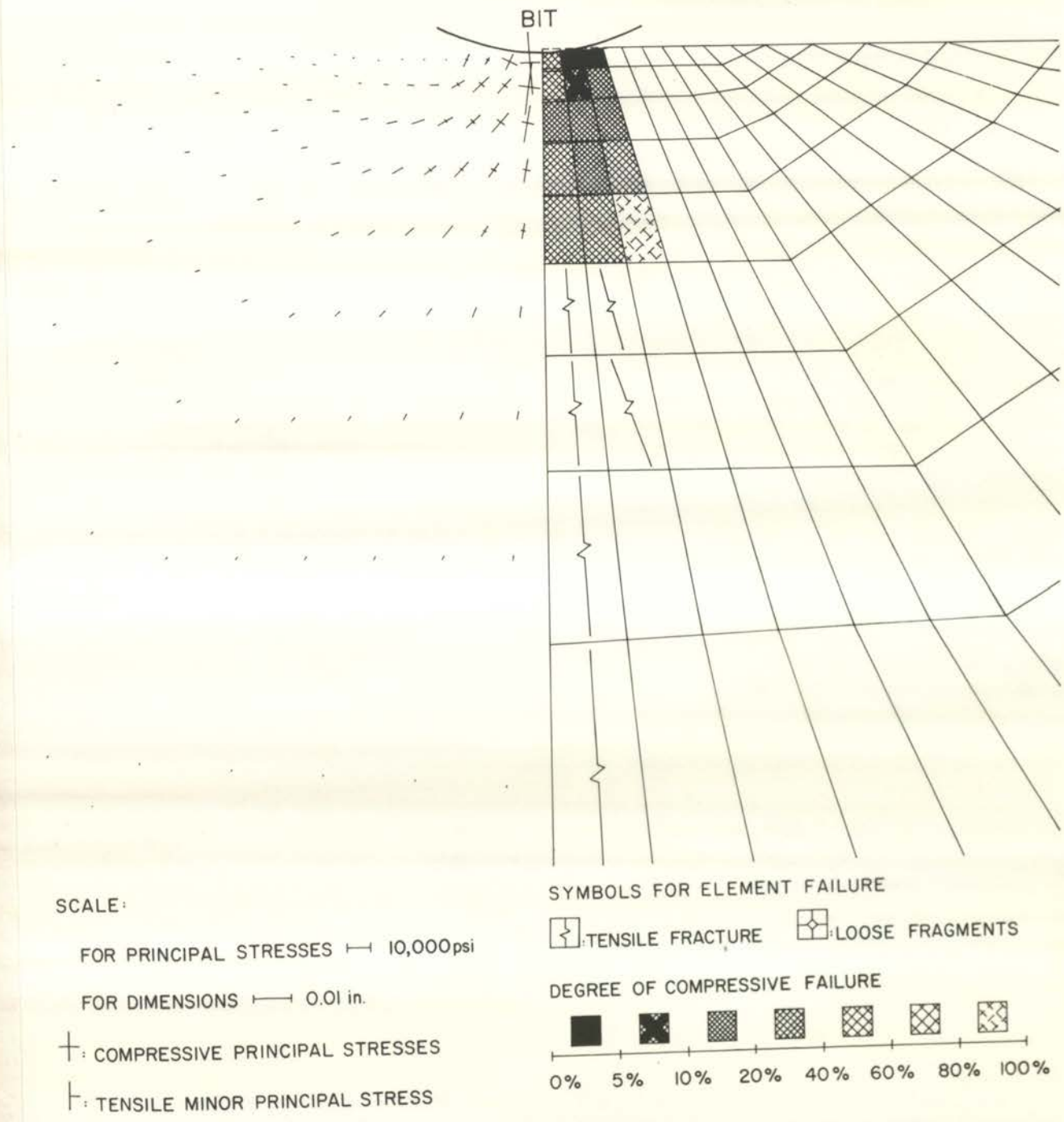

Figure 23c. Cylindrical Bit Penetration

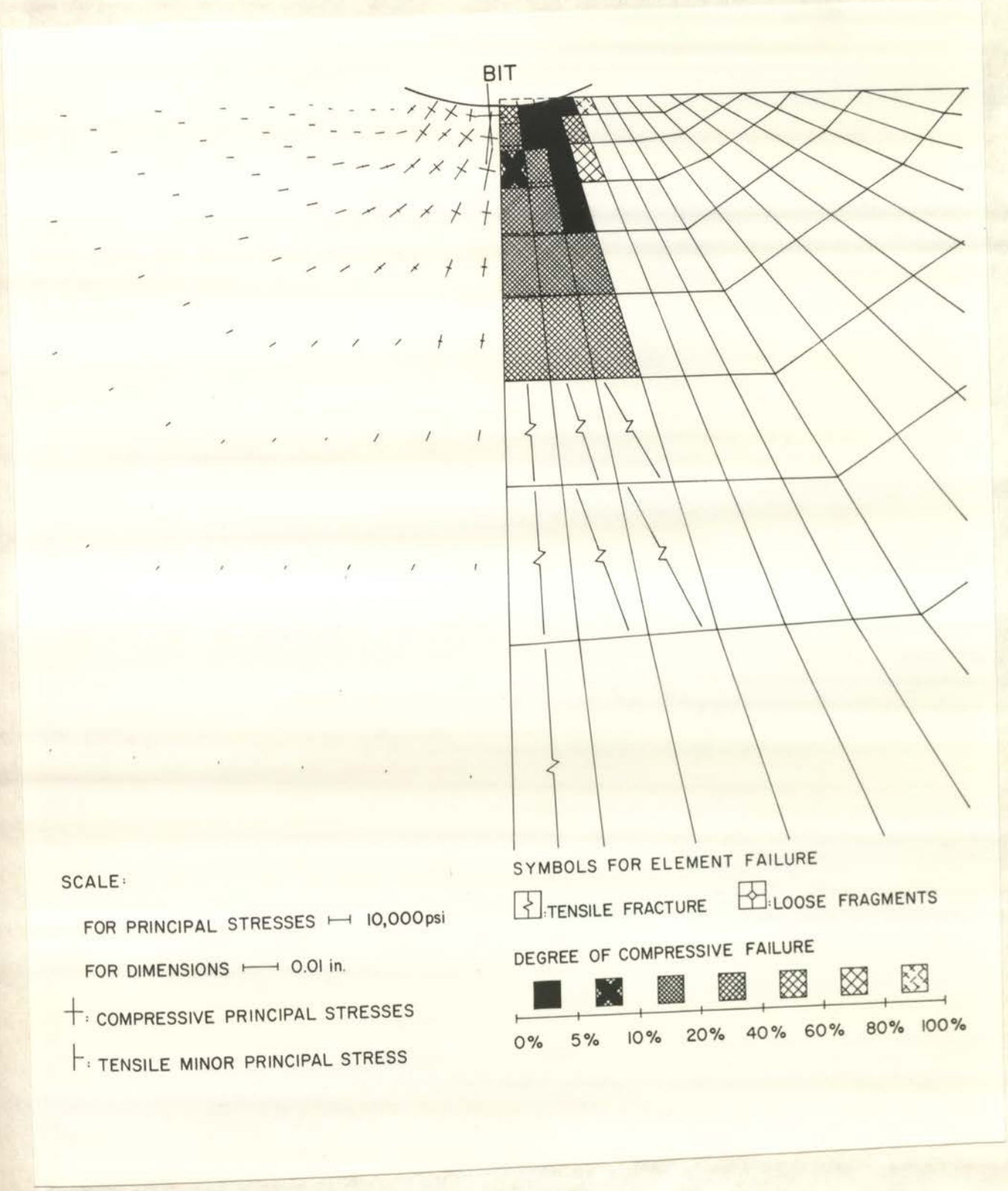

Figure 23d. Cylindrical Bit Penetration

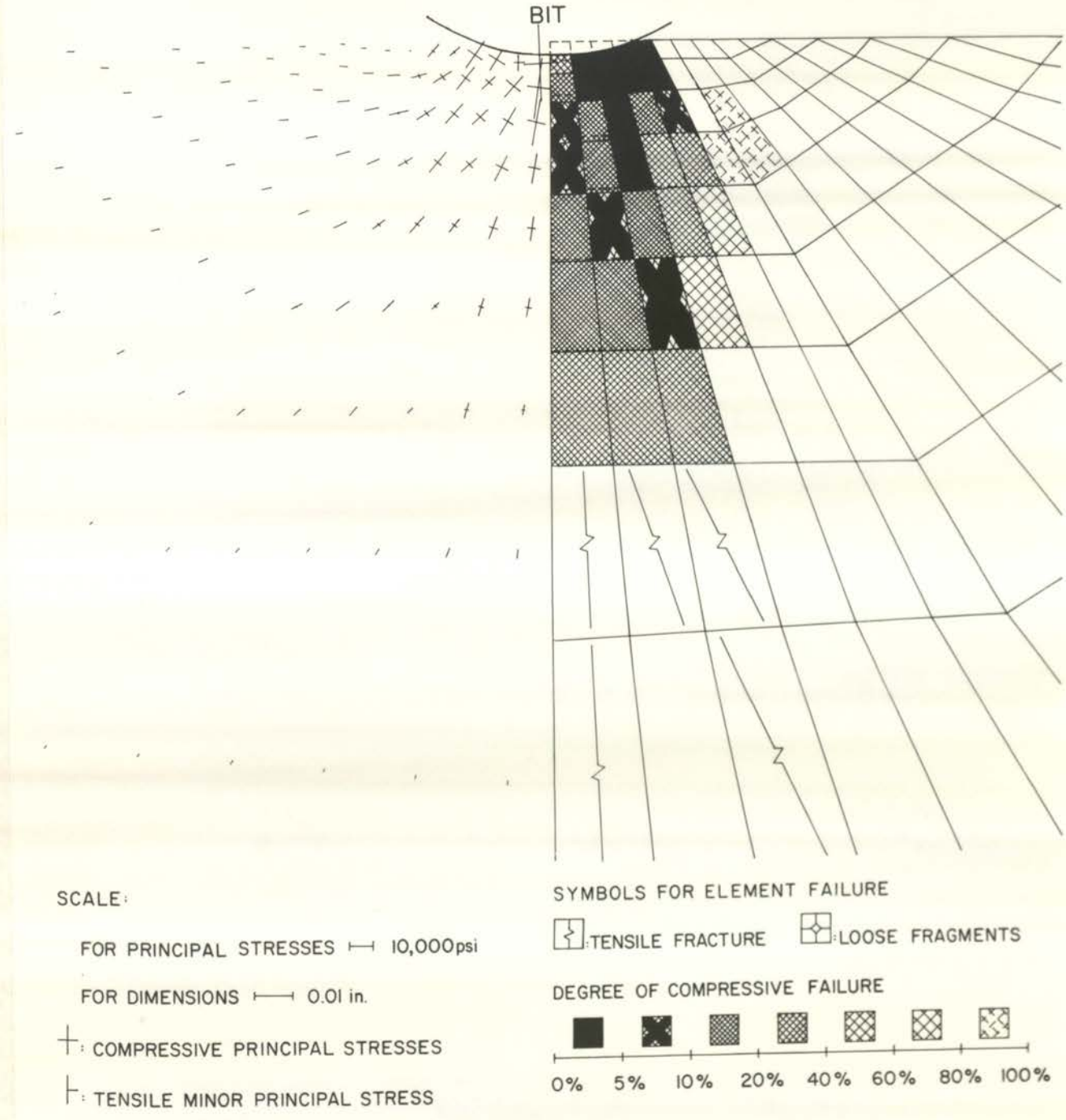

Figure 23e. Cylindrical Bit Penetration

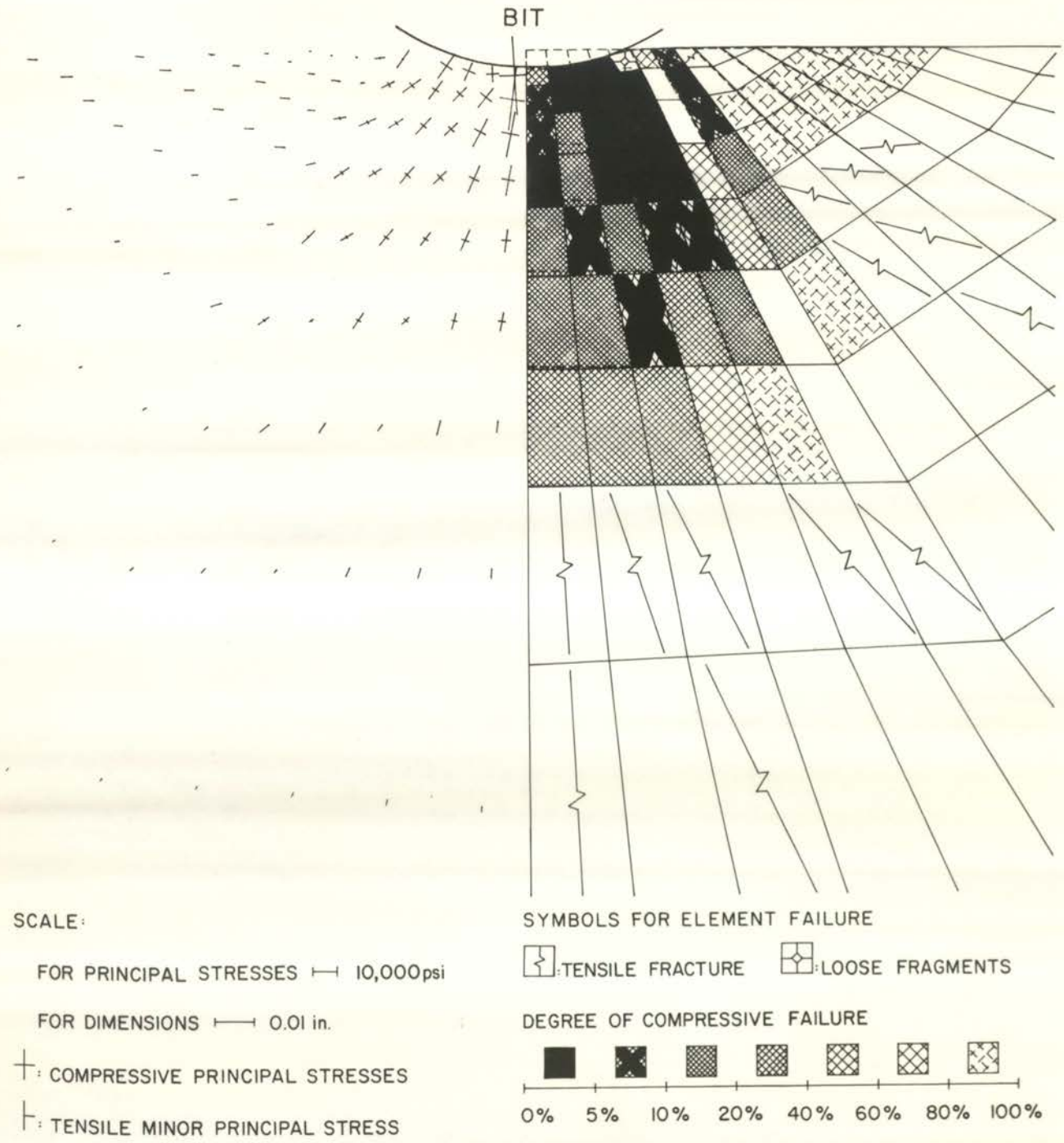

Figure 23f. Cylindrical Bit Penetration

V. CONCLUSIONS AND RECOMMENDATIONS

A. Conclusions

The sequence of rock failure mechanisms and the quantitative information on stress, displacement and material failure in the process of bit penetration can be obtained through computer simulation. Using the proposed mathematical rock failure models and the developed finite element code, the analytical results presented in this study have shown a reasonable agreement with experimental observations. Three tool profiles have been simulated to demonstrate their shape effects on the penetration mechanism. The special suitability of the finite element method has also been shown in the study of the influence of the post-failure rock strength and properties on bit penetration.

B. Recommendations

1. Extensive study along with refined experimental methods are needed for a better understanding of the post-failure behavior of rock. Stress-strain relationships, residual Mohr envelopes as well as the variations of rock properties in progressive strength failure must be known to improve the analysis.

2. With better understanding of the post-failure behavior of rock, present computer codes can be modified to adapt a more complicated non-linear rock behavior such as a non-linear Mohr envelope and variable stress-strain curve as a function of confining pressure. Constitutive equations for rock properties in the failure state can also be applied to yield better results.

3. This bit penetration program can be generalized for the

studies of various bit-rock interface conditions, different tool actions and other related rock failure problems.

4. Wedge type penetrators with increasing edge radii could give some of the effects of wear.

BIBLIOGRAPHY

1. Maurer, W. C., "The State of Rock Mechanics Knowledge in Drilling," Proc. 8th Sym. Rock Mech., Univ. of Minn., Sept. 1966, p. 355-395.

2. Paul, B., and Sikarskie, D. L., "A Preliminary Theory of Static Penetration by a Rigid Wedge into a Brittle Material," Trans. AIME, Vol. 232, 1965, p. 372-383.

3. Sikarskie, D. L., and Altiero, N. J., "The Formation of Chips in the Penetration of Elastic-Brittle Materials (Rock)," Trans. ASME, J. of Applied Mech., Sept. 1973, p. 791-797.

4. Sikarskie, D. L., and Cheatham, J. B., Jr., "Penetration Problems in Rock Mechanics," Rock Mech. Sym., ASME, AMD, Vol. 3, 1974, p. 41-71.

5. Hartman, H. L., "Basic Studies of Percussion Drilling," Mining Engineer, Jan. 1959, p. 68-75.

6. Reichmuth, D. R., "Correlation of Force-Displacement Data with Physical Properties of Rock for Percussive Drilling Systems," 5th Sym. Rock Mech., 1963, p. 33-60.

7. Singh, M. M., and Johnson, A. M., "Static and Dynamic Failure of Rock under Chisel Loads," Trans. AIME, Vol. 38, 1967, p. 366-373.

8. Ladanyi, B., "Rock Failure under Concentrated Loading," 10th Sym. Rock Mech., 1972, p. 363-387.

9. Maurer, W. C., "Bit Tooth Penetration under Simulated Borehole Conditions," J. of Pet. Tech., Dec. 1965, p. 1433-1442.

10. Gnirk, P. F., and Cheatham, J. B., Jr., "An Experimental Study of Single Bit-Tooth Penetration into Dry Rock at Confining Pressures of 0 to 5,000 psi," J. of SPE, Vol. 5, No. 2, June 1965, p. 117-130.

11. Dutta, P. K., "A Theory of Percussive Drill Bit Penetration," Int. J. Rock Mech. Min. Sci., Vol. 9, 1972, p. 543-567.

12. Hill, R., "Mathematical Theory of Plasticity," Clarendon Press, Oxford, 1950.

13. Courant, R., and Friedrichs, K. O., "Supersonic Flow and Shock Waves," Interscience, Inc., N. Y., 1948.

14. Cheatham, J. B., Jr., "An Analytical Study of Rock Penetration by a Single Bit Tooth," Proc. of 8th Annual Drilling and

Blasting Sym., Univ. of Minn., Minn., 1958.

15. Pariseau, W. G., and Fairhurst, C., "The Force-Penetration Characteristic for Wedge Penetration into Rock," Int. J. Rock Mech. Min. Sci., Vol. 4, No. 2, 1967, p. 165-180.

16. Johnson, Sowerby, and Haddow, "Plane-Strain Slip-Line Fields," American Elsevier Publishing Co., Inc., N. Y., 1970.

17. Clark, G. B., et al., "An Investigation of Thermal-Mechanical Fragmentation of Rock," Univ. of Mo.-Rolla, RMERC, Annual Report, July 1972.

18. Krech, W. W., et al., "A Standard Rock Suite for Rapid Excavation Research," BuMines RI 7865, 1974.

19. Zienkiewicz, O. C., et al., "Stress Analysis of Rock as a 'no Tension' Material," Geotechnique, 18, 1968, p. 56-66.

20. Sandhu, R. S., Wu, T. H., and Hooper, J. R., "Stresses, Deformations and Progressive Failure of Non-Homogeneous Fissured Rock," The Ohio St. Univ., Final Report, ARPA Order No. 1579, Mar. 1973.

21. Bieniawski, Z. T., "Mechanism of Brittle Fracture of Rock," Int. J. Rock Mech. Min. Sci., Vol. 4, 1967, p. 407-423.

22. Barnard, P. R., "Researches into the Complete Stress-Strain Curve for Concrete," Mag. Concrete Res., Vol. 16, No. 49, 1964, p. 203-210.

23. Cook, N. G. W., and Hojem, J. P. M., "A Rigid 50-Ton Compression and Tension Testing Machine," South African Mech. Engr., Nov. 1966.

24. Wawersik, W. R., "Detailed Analysis of Rock Failure in Laboratory Compression Tests," Ph. D. Thesis, Univ. of Minn. 1968.

25. Deere, D. V., et al., "Design of Surface and Near-Surface Construction in Rock," 8th Sym. Rock Mech., Minn., 1966.

26. Patton, F. D., "Multiple Modes of Shear Failure in Rock and Related Materials," Ph. D. Thesis, Univ. of Ill., 1966.

27. Bieniawski, Z. T., "Propagation of Brittle Fracture in Rock," 10th Sym. Rock Mech., Univ. of Texas-Austin, 1968.

28. Hoek, E., and Bieniawski, Z. T., "Brittle Fracture Propagation in Rock under Compression," Int. J. Fracture Mech. 1, (3), 1965, p. 137-155.

29. Zienkiewicz, O. C., "The Finite Element Method," McGraw Hill Co., London, 1971.

30. Stagg, K. G., and Zienkiewicz, O. C., "Rock Mechanics in Engineering Practice," John Wiley & Sons, Ltd., 1968.

31. Jaeger, C., "Rock Mechanics and Engineering," Cambridge University Press, 1972.

VITA

Jaw-Kuang Wang was born in June 14, 1943, in Taiwan, Republic of China. He received a Bachelor of Science degree in Mechanical Engineering from Cheng Kung University in June 1966.

He served in the Chinese Air Force from July 1966 to July 1967, then worked as a Mechanical Engineer at the Bureau of Inspection and Quarantine from July 1967 to August 1968.

In September 1968 he enrolled in the Graduate School of the University of Missouri-Rolla, where he received his Master of Science degree in May 1970.

In March 1975 he married Miss Shu-Huei Li in Rolla, Missouri.

APPENDIX A

FUNDAMENTAL EQUATIONS FOR PLANE-STRAIN PENETRATION PROBLEMS

Displacement Function:

$$\{f\} = [N]\{\delta\}^e , \quad [N] = \text{general function of position}$$

$$\{\delta\}^e = \text{nodal displacements}$$

Strain-Displacement Relations:

$$\{\varepsilon\} = [B]\{\delta\}^e = \begin{Bmatrix} \frac{\partial u}{\partial x} \\ \frac{\partial v}{\partial y} \\ \frac{\partial u}{\partial y} + \frac{\partial v}{\partial x} \end{Bmatrix}$$

Stress-Strain Relations:

$$\{\sigma\} = [D]\{\varepsilon\} = [D][B]\{\delta\}^e$$

$$[D] = \frac{E\,(1-\nu)}{(1+\nu)(1-2\nu)} \begin{bmatrix} 1 & \nu/(1-\nu) & 0 \\ \nu/(1-\nu) & 1 & 0 \\ 0 & 0 & (1-2\nu)/2(1-\nu) \end{bmatrix}$$

Force-Displacement Relations:

(without initial stress, initial strain and body force)

$$\{R\}^e = [K]\{\delta\}^e , \quad \{R\}^e = \text{nodal forces}$$

$$[K] = \int_e [B]^T [D][D][B]\,dV$$

Force-Stress Relations:

$$\{R\}^e = \int_e [B]^T \{\sigma\}\,dV$$

APPENDIX B

PROGRAM INPUT INSTRUCTIONS AND LISTING

This computer program is applicable to plane strain analysis of stress, deformation and progressive failure in rock, using the proposed mathematical rock failure model as presented in this thesis. Incremental boundary displacement is used for simulation of fracture initiation and propagation in an arbitrary elastic rock structure. The program is capable of terminating or continuing at any specific stage of simulation.

The following set of cards is required for the start of each problem.

1. Identification Card (20A4):

Cols.	1-80	This card contains information to be printed with results.

2. Control Card (7I5, 3F10.0):

Cols.	1-5	Number of nodal points (350 maximum)
	6-10	Number of elements (350 Maximum)
	11-15	Number of displacement boundary cards (100 maximum)
	16-20	Number of iterations per coordinate modification
	21-25	Number of coordinate modifications
	30	Data check option, 0 run complete program, 1 test data only
	35	Continuation option, 0 new program, 1 continuation

36-45 Incremental displacement, in.

46-55 Initial displacement, in.

56-65 Anistropic ratio, ratio = E_2 / E_1

3. Material Properties Information (7F10.0):

Cols. 1-10 Young's modulus, psi

11-20 Poisson's ratio

21-30 Compressive stress (+), psi

31-40 Tensile stress (-), psi

41-50 Angle of maximum Mohr envelope, degree

51-60 Angle of residual Mohr envelope, degree

61-70 Post-failure stress-strain slope, c

4. Element Cards (5I5):

One card for each element

Cols. 1-5 Element Number

6-10 Nodal point, I

11-15 Nodal point, J

16-20 Nodal point, K

21-25 Nodal point, L

Maximum difference between nodes around an element must be less than 30. Element cards must be in numerical sequence. If element cards are omitted, the program automatically generates the omitted information by incrementing by one the preceding I, J, K, and L. The last element card must be supplied.

5. Displacement Boundary Cards (3I5):

One card for each boundary element which is subject to incremental displacements.

Cols. 1-5 Nodal point, I

6-10 Nodal point, J

11-15 Element number

6. Nodal Point Cards (2I5, 2F10.0):

One card for each node with the following information:

Cols. 1-5 Nodal point number

10 Number which indicates which displacements are to be specified

11-20 X-coordinate

21-30 Y-coordinate

The number in column 10 is defined as:

0 No specified displacement

1 Specified displacement in X direction

2 Specified displacement in Y direction

3 Specified displacements in X and Y directions

Nodal points must be in numerical sequence. If the cards are omitted, the omitted nodal points are generated at equal intervals along a straight line between the defined nodal points.

7. Continuation:

a) Change column 35 in the control card.

b) Change identification card, number of iteration, incremental displacements, etc., if necessary.

c) Element volumes of the original coordinates will be punched on output cards at the start of each new problem. These cards should be placed after the displacement boundary cards in the continuation. Original nodal point information is abandoned.

d) After a specified number of iterations, information on nodal points and elements will be punched on cards. The most recent set of cards will be used for the next run. It is placed after element volume cards.

```
C*************************************************************
C
C   STRESS ANALYSIS OF PLANE STRAIN SOLID
C   WITH INCREMENTAL DISPLACEMENT BOUNDARY
C
C*************************************************************
      COMMON E(7,10),NUMNP,NUMEL,NUMPC,MTYPE,NP,ANI,HED(20),
     1R(350),Z(350),UR(350),UZ(350),CODE(350),IBC(100),
     2JBC(100),PR(100),ANGLE(4),SIG(10),NDEG,IFF(350),
     3VOLM(350),NEWRZ,INN,ICHEK,KONTD,IND,FK(350),IFH(350),
     4BETA(350)
      COMMON/ARG/RRR(5),ZZZ(5),S(10,10),P(10),LM(4),DD(3,3),
     1HH(10,10),RR(4),ZZ(4),C(3,3),H(6,10),D(6,6),F(10,10),
     2TP(6),XI(10),EE(5),IX(350,5),EMOD(350)
      COMMON/BANARG/MBAND,NUMBLK,B(120),A(120,60)
      COMMON/PLANE/EE2P,EE2PP,FFKK
      COMMON/ITT/URR(350),UZZ(350),SIGG(350,4),DVOL(350)
      COMMON/IO/IN,IOUT,NUM1,NDAT1,NDAT2,NREC1
      DIMENSION IB(20)
      DEFINE FILE 4(350,250,U,NREC1)
C
C   NTEST=0    RUN COMPLETE PROGRAM
C   NTEST=1    TEST DATA ONLY
C
C
C*************************************************************
C   READ INFORMATION FOR CONTROL, STRUCTURE,
C   MATERIAL PROPERTIES, AND ITERATION
C*************************************************************
C
C
C   DATA SET REFERENCE NUMBERS
C
      DATA NO1,NO2,NO3,NO4,NO8,NO9/5,7,6,4,8,9/
      IN=NO1
      IOUTP=NO2
      IOUT=NO3
      NUM1=NO4
      NDAT1=NO8
      NDAT2=NO9
C
      MAXB=60
C
      READ(IN,1000) HED,NUMNP,NUMEL,NUMPC,NP,NRZ,NTEST,KONTD
     1,DP,DPI,ANI
C
C   KONTD=0, NEW PROGRAM
C   KONTD=1, CONTINUATION
C
      WRITE(IOUT,2000) HED,NUMNP,NUMEL,NUMPC,NP,NRZ,
     1KONTD,DP,DPI,ANI
      NDEG=2*NUMNP
      IF(NTEST) 53,57,53
```

```
    53 WRITE(IOUT,2014)
    57 READ(IN,1005)(E(I,1),I=1,7)
       WRITE(IOUT,2001) (E(I,1),I=1,7)
C
       E(5,1)=E(5,1)/57.296
       E(6,1)=E(6,1)/57.296
       E51=TAN(E(5,1))
       E61=TAN(E(6,1))
       E55=SQRT(1.+E51*E51)
       E(1,2)=0.5*E(3,1)*(E55+1.-E51)/(E55+1.+E51)
       E(3,2)=2.*(1.+SIN(E(5,1)))/COS(E(5,1))*E51
       EE(2)=E(2,1)
C
C*****************************************************************
C  READ AND PRINT ELEMENT DATA
C*****************************************************************
C
       N=0
  130 READ(IN,1003) M,(IX(M,I),I=1,4)
  140 N=N+1
       IF(M-N) 170,170,150
  150 NN=N-1
       IX(N,1)=IX(NN,1)+1
       IX(N,2)=IX(NN,2)+1
       IX(N,3)=IX(NN,3)+1
       IX(N,4)=IX(NN,4)+1
  170 IX(N,5)=1
       IF(M-N) 180,180,140
  180 IF(NUMEL-N) 190,190,130
  190 CONTINUE
C
C*****************************************************************
C  READ AND PRINT NODAL POINT DATA
C*****************************************************************
C
       IF(KONTD .EQ. 1) GO TO 110
       L=0
    60 READ(IN,1002) N,CODE(N),R(N),Z(N)
       NL=L+1
       ZX=N-L
       IF(L) 65,70,65
    65 DR=(R(N)-R(L))/ZX
       DZ=(Z(N)-Z(L))/ZX
    70 L=L+1
       IF(N-L) 100,90,80
    80 CODE(L)=0.0
       R(L)=R(L-1)+DR
       Z(L)=Z(L-1)+DZ
       GO TO 70
    90 CONTINUE
       IF(NUMNP-N) 100,110,60
   100 WRITE(IOUT,2009) N
       NTEST=1
```

```
  110 CONTINUE
C
C*****************************************************************
C  READ AND PRINT DISPLACEMENT BOUNDARY CONDITION
C*****************************************************************
C
      IF(NUMPC) 290,310,290
  290 WRITE(IOUT,2005)
      DO 300 L=1,NUMPC
      READ(IN,1004)IBC(L*2-1),IBC(L*2),JBC(L)
  300 WRITE(IOUT,2007)IBC(L*2-1),IBC(L*2),JBC(L)
      I=NUMPC+1
      JBC(I)=0
  310 CONTINUE
C
C*****************************************************************
C     DETERMINE THE BANDWIDTH OF THE STIFFNESS MATRIX
C*****************************************************************
C
      J=0
      DO 340 N=1,NUMEL
      DO 340 I=1,4
      DO 325 L=1,4
      KK=IABS(IX(N,I)-IX(N,L))
      IF(KK-J) 325,325,320
  320 J=KK
  325 CONTINUE
  340 CONTINUE
C
C  CHECK BANDWIDTH
C
      MBAND=2*J+2
      IF(MBAND-MAXB) 345,345,346
  346 WRITE(IOUT,2013) MAXB
      CALL EXIT
  345 IF(NTEST) 505,347,505
 2013 FORMAT(5X,'BANDWIDTH OF STIFFNESS MATRIX EXCEEDS',I3)
C*****************************************************************
C  SOLVE STRUCTURE BY CALLING SUBROUTINES
C*****************************************************************
C
  347 CONTINUE
C
      DO 350 N=1,NUMNP
      URR(N)=0.
  350 UZZ(N)=0.
      DO 360 I=1,NUMEL
      IFF(I)=0
      IFH(I)=0
      DVOL(I)=0.
      FK(I)=1.
      BETA(I)=0.
      DO 360 J=1,4
```

```
  360 SIGG(I,J)=0.
      IND=0
C
      IF(KONTD .EQ. 0) GO TO 390
      READ(IN,1111)(VOLM(I),I=1,NUMEL)
      READ(IN,1010)(CODE(I),R(I),Z(I),I=1,NUMNP)
      READ(IN,1011)(IBH(I),FK(I),EMOD(I),BETA(I),SIGG(I,1),
     1SIGG(I,2),SIGG(I,4),I=1,NUMEL)
      IND=1
C
  390 DO 370 I=1,NUMNP
      UR(I)=0.
  370 UZ(I)=0.
C
      NEWRZ=0
C
  555 DO 500 NNN=1,NP
      INN=NNN
      ICHEK=0
C
      IND=IND+1
C
C  ASSIGN INCREMENTAL DISPLACEMENT
C
      DO 301 I=1,NUMPC
  301 UZ(IBC(I*2-1))=DP+DPI
      UZ(IBC(NUMPC*2))=DP+DPI
      DPI=0.
      GO TO 516
C
  510 CONTINUE
      DO 515 I=1,NUMNP
      IF(CODE(I) .EQ. 0.) GO TO 515
      IF(CODE(I)-2.) 512,513,514
  512 UR(I)=0.
      GO TO 515
  513 UZ(I)=0.
      GO TO 515
  514 UR(I)=0.
      UZ(I)=0.
  515 CONTINUE
  516 CONTINUE
C
C  FORM STIFFNESS MATRIX
C
      CALL STIFF
C
C  SOLVE FOR DISPLACEMENTS
C
      CALL BANSOL
C
C  COMPUTE STRESSES
C
```

```
      IND=IND+1
      INN=2
      CALL STRESS
C
      IF(ICHEK-1)503,500,500
  503 ICHEK=1+ICHEK
      GO TO 510
C
  500 CONTINUE
C
C*****************************************************************
C  MODIFY COORDINATES
C*****************************************************************
      NEWRZ=NEWRZ+1
      DO 600 I=1,NUMNP
      R(I)=R(I)+URR(I)
  600 Z(I)=Z(I)+UZZ(I)
      IF(KONTD .NE. 0) GO TO 601
      WRITE(ICUT,1111)(VCLM(I),I=1,NUMEL)
      WRITE(IOUTP,1111)(VCLM(I),I=1,NUMEL)
  601 WRITE(IOUT,2018) (I,CODE(I),R(I),Z(I),I=1,NUMNP)
      WRITE(IOUTP,1010)(CODE(I),R(I),Z(I),I=1,NUMNP)
      WRITE(IOUT,2019)(I,IFH(I),FK(I),EMOD(I),BETA(I),
     1SIGG(I,1),SIGG(I,2),SIGG(I,4),I=1,NUMEL)
      WRITE(IOUTP,1011)(IFH(I),FK(I),EMOD(I),BETA(I),
     1SIGG(I,1),SIGG(I,2),SIGG(I,4),I=1,NUMEL)
      IF(NEWRZ-NRZ)525,504,504
C
  525 DO 526 I=1,NUMNP
      URR(I)=0.
  526 UZZ(I)=0.
      GO TO 555
  504 CONTINUE
C
C*****************************************************************
  505 CALL EXIT
C*****************************************************************
C
 1000 FORMAT(20A4/7I5,3F10.0)
 1002 FORMAT(I5,F5.0,4F10.0)
 1003 FORMAT(5I5)
 1004 FORMAT(3I5)
 1005 FORMAT(8F10.0)
 1010 FORMAT(3(F3.0,2F11.8))
 1011 FORMAT(I3,F7.4,1P5E13.6)
 1111 FORMAT(1P6E13.6)
 2000 FORMAT(1H0 20A4///5X,'NO. OF NODAL POINTS=',I3/5X,
     1'NO. OF ELEMENTS=',I3/5X,'NO. OF DISP. B. C. =',I3/
     25X,'NO. OF ITERATIONS=',I3/5X,'NO. OF MODIFICATIONS=',
     3I3/5X,'CONTINUATION=',I3/5X,'DP=',F10.5/5X,'DPI=',
     4F10.5/5X,'ANI=',F10.5//)
 2001 FORMAT(5X,'E=',E20.8/5X,'POISSONS RATIO=',E20.8/5X,
     1'STRESS(C)=',E20.8/5X,'STRESS(T)=',E20.8/5X,
```

```
     2'MAX. ANGLE=',F10.5/5X,'RES. ANGLE=',F10.5/5X,
     3'SLOPE=',F10.5//)
2005 FORMAT(//5X,'DISPLACEMENT B. C.'/14X,'I',14X,'J',4X,
     1'ELEMENT NO.')
2007 FORMAT(3I15)
2009 FORMAT(5X,'NODAL POINT CARD ERROR N=',I5,
     1'. EXECUTION TERMINATED.')
2014 FORMAT(5X,'PROGRAM WILL NOT BE EXECUTED. ONLY DATA',
     1' WILL BE TESTED.')
2018 FORMAT(5H1N.P.,6X,'TYPE',16X,'R(I)',16X,'Z(I)'/(I5,
     1E10.0,2F20.7))
2019 FORMAT(10H1ELEM. NO.,'    IFH(I)', 10X,'FK(I)',8X,
     1'EMOD(I)',8X,'BETA(I)',6X,'SIGG(I,1)',6X,'SIGG(I,2)',
     26X,'SIGG(I,4)'/(2I10,6E15.5))
      STOP
      END



      SUBROUTINE STIFF
      COMMON F(7,10),NUMNP,NUMEL,NUMPC,MTYPE,NP,ANI,HED(20),
     1R(350),Z(350),UR(350),UZ(350),CODE(350),IBC(100),
     2JBC(100),PR(100),ANGLE(4),SIG(10),NDEG,IFF(350),
     3VOLM(350),NEWRZ,INN,ICHEK,KONTD,IND,FK(350),IFH(350),
     4BETA(350)
      COMMON/ARG/RRR(5),ZZZ(5),S(10,10),P(10),LM(4),DD(3,3),
     1HH(10,10),RR(4),ZZ(4),C(3,3),H(6,10),D(6,6),F(10,10),
     2TP(6),XI(10),EE(5),IX(350,5),EMOD(350)
      COMMON/BANARG/MBAND,NUMBLK,B(120),A(120,60)
      COMMON/IO/IN,IOUT,NUM1,NDAT1,NDAT2,NREC1
C
C   INITIALIZATION
C
      REWIND NDAT2
      NB=30
      ND=2*NB
      ND2=2*ND
      STOP=0.0
      NUMBLK=0
C
      DO 50 N=1,ND2
      B(N)=0.0
      DO 50 M=1,ND
   50 A(N,M)=0.0
C
C   FORM STIFFNESS MATRIX IN BLOCKS
C
   60 NUMBLK=NUMBLK+1
      NH=NB*(NUMBLK+1)
      NM=NH-NB
      NL=NM-NB+1
      KSHIFT=2*NL-2
C
```

```
      DO 210 N=1,NUMEL
      NREC1=N
C
      IF(IX(N,5)) 210,210,65
   65 DO 80 I=1,4
      IF(IX(N,I)-NL) 80,70,70
   70 IF(IX(N,I)-NM) 90,90,80
   80 CONTINUE
      GO TO 210
C
   90 IX(N,5)=-IX(N,5)
      IF(INN .EQ. 1) GO TO 100
      READ(NUM1'NREC1) HH,C,RRR(5),ZZZ(5),EE(2),S,VOL
   94 EM=EMOD(N)
      GO TO 130
  100 IF(IND .EQ. 1 ) GO TO 101
      IF(IFH(N)) 98,98,99
   98 EE(2)=E(2,1)
      GO TO 102
   99 VOLL=0.
      IF(IX(N,3) .EQ. IX(N,4)) GO TO 30
      RRR(5)=(R(IX(N,1))+R(IX(N,2))+R(IX(N,3))+R(IX(N,4)))*
     1.25
      ZZZ(5)=(Z(IX(N,1))+Z(IX(N,2))+Z(IX(N,3))+Z(IX(N,4)))*
     1.25
      IIX=IX(N,5)
      IX(N,5)=IX(N,1)
      J=4
      GO TO 31
   30 RRR(5)=(R(IX(N,1))+R(IX(N,2))+R(IX(N,3)))/3.
      ZZZ(5)=(Z(IX(N,1))+Z(IX(N,2))+Z(IX(N,3)))/3.
      IIX=IX(N,4)
      IX(N,4)=IX(N,1)
      J=3
   31 DO 35 I=1,J
      R1=R(IX(N,I))
      Z1=Z(IX(N,I))
      R2=R(IX(N,I+1))
      Z2=Z(IX(N,I+1))
      CCMM=.5*(R2*(ZZZ(5)-Z1)+R1*(Z2-ZZZ(5))+RRR(5)*(Z1-Z2))
   35 VOLL=VOLL+CCMM
      IF(IX(N,4) .EQ. IX(N,1)) IX(N,4)=IIX
      IF(IX(N,5) .EQ. IX(N,1)) IX(N,5)=IIX
      EE(2)=.5-(.5-E(2,1))*EMOD(N)/E(1,1)
      IF(EE(2) .GT. 0.49977)EE(2)=0.49977
      IF(IFH(N) .EQ. 1 .OR. IFH(N) .EQ. 4) EE(2)=.1*E(2,1)
      IF(IFH(N) .EQ. 2) EE(2)=E(2,1)
      GO TO 102
  101 MMM=NUMEL
      EE(2)=E(2,1)
  102 CALL QUAD(N,VOL,N)
      IF(VOL) 105,105,106
  105 WRITE(ICUT,2003) N
```

```
      STOP=1.
  106 EM=E(1,1)
      IF(IND .EQ. 1) GO TO 110
      EM=EMOD(N)
      IF(IFH(N) .NE. 3 .OR. VOL .LT. VOLM(N)) GO TO 115
      EE(2)=0.10*E(2,1)
      CALL QUAD(N,VOL,N)
      GO TO 115
  110 VOLM(N)=VOL
      EMOD(N)=E(1,1)
  115 WRITE(NUM1'NREC1) FH,C,RRR(5),ZZZ(5),EE(2),S,VOL
C
  130 IF(EE(2) .EQ. .1*E(2,1) .AND. EM .GT. ANI*E(1,1))
     1EM=ANI*E(1,1)
  131 DO 140 J=1,10
      DO 140 K=1,10
  140 S(J,K)=EM*S(J,K)
C
      IF(IX(N,3)-IX(N,4)) 145,156,145
  145 DO 150 II=1,9
      CC=S(II,10)/S(10,10)
      DO 150 JJ=1,9
  150 S(II,JJ)=S(II,JJ)-CC*S(10,JJ)
C
      DO 155 II=1,8
      CC=S(II,9)/S(9,9)
      DO 155 JJ=1,8
  155 S(II,JJ)=S(II,JJ)-CC*S(9,JJ)
  156 CONTINUE
C
C  ADD ELEMENT STIFFNESS TO TOTAL STIFFNESS
C
      DO 166 I=1,4
  166 LM(I)=2*IX(N,I)-2
C
      DO 200 I=1,4
      DO 200 K=1,2
      II=LM(I)+K-KSHIFT
      KK=2*I-2+K
      DO 200 J=1,4
      DO 200 L=1,2
      JJ=LM(J)+L-II+1-KSHIFT
      LL=2*J-2+L
      IF(JJ) 200,200,175
  175 IF(ND-JJ) 180,195,195
  180 WRITE(ICUT,2004) N
      STOP=1.0
      GO TO 210
  195 A(II,JJ)=A(II,JJ)+S(KK,LL)
  200 CONTINUE
  210 CONTINUE
C
C  ADD CONCENTRATED FORCES WITHIN BLOCK
```

```
C
      IF(NM-NUMNP) 211,211,212
  211 NSTOP=NM
      GO TO 213
  212 NSTOP=NUMNP
  213 DO 250 N=NL,NSTOP
      K=2*N- KSHIFT
      B(K)=B(K)+UZ(N)
  250 B(K-1)=B(K-1)+UR(N)
C
C   DISPLACEMENT B. C.
C
  310 DO 400 M=NL,NH
      IF(M-NUMNP) 315,315,400
  315 U=UR(M)
      N=2*M-1-KSHIFT
      IF(CODE(M)) 390,400,316
  316 IF(CODE(M)-1.) 317,370,317
  317 IF(CODE(M)-2.) 318,390,318
  318 IF(CODE(M)-3.) 390,380,390
  370 CALL MODIFY(A,B,ND2,MBAND,N,U)
      GO TO 400
  380 CALL MODIFY(A,B,ND2,MBAND,N,U)
  390 U=UZ(M)
      N=N+1
      CALL MODIFY(A,B,ND2,MBAND,N,U)
  400 CONTINUE
C
C   WRITE BLOCK OF EQUATIONS ON TAPE AND SHIFT UP LOWER BLOCK
C
      WRITE(NDAT2)(B(N),(A(N,M),M=1,MBAND),N=1,ND)
      DO 420 N=1,ND
      K=N+ND
      B(N)=B(K)
      B(K)=0.0
      DO 420 M=1,ND
      A(N,M)=A(K,M)
  420 A(K,M)=0.0
C
C   CHECK FOR LAST BLOCK
C
      IF(NM-NUMNP) 60,480,480
  480 CONTINUE
      IF(STOP) 490,500,490
  490 CALL EXIT
  500 RETURN
C
 2003 FORMAT(26HONEGATIVE AREA ELEMENT NO. I4)
 2004 FORMAT(29HOBAND WIDTH EXCEEDS ALLOWABLE I4)
      END
```

```
      SUBROUTINE QUAD(N,VEL,MMM)
      COMMON E(7,10),NUMNP,NUMEL,NUMPC,MTYPE,NP,ANI,HED(20),
     1R(350),Z(350),UR(350),UZ(350),CODE(350),IBC(100),
     2JBC(100),PR(100),ANGLE(4),SIG(10),NDEG,IFF(350),
     3VOLM(350),NEWRZ,INN,ICHEK,KONTD,IND,FK(350),IFH(350),
     4BETA(350)
      COMMON/ARG/RRR(5),ZZZ(5),S(10,10),P(10),LM(4),DD(3,3),
     1HH(10,10),RR(4),ZZ(4),C(3,3),H(6,10),D(6,6),F(10,10),
     2TP(6),XI(10),EE(5),IX(350,5),EMOD(350)
      COMMON/BANARG/MBAND,NUMBLK,B(120),A(120,60)
      COMMON/IO/IN,IOUT,NUM1,NDAT1,NDAT2,NREC1
C
   90 I=IX(N,1)
      J=IX(N,2)
      K=IX(N,3)
      L=IX(N,4)
C
C   FORM STRESS-STRAIN RELATIONSHIP
C
   10 IF(IFH(MMM) .NE. 1) GO TO 20
C
C   ANISOTROPIC ELEMENTS
C
      E2=1./ANI
      COMM=1./((1.+E(2,1))*(1.-E(2,1)-2.*E2*EE(2)*EE(2)))
C
      C11=E2*(1.-E2*EE(2)*EE(2))*COMM
      C12=E2*EE(2)*(1.+E(2,1))*COMM
      C22=(1.-E(2,1)*E(2,1))*COMM
      C33=.5/(1.+EE(2))
C
      BETAA=(BETA(MMM)+90.)/57.296
      SINB=SIN(BETAA)
      COSB=COS(BETAA)
      SINB2=SINB*SINB
      SINB4=SINB2*SINB2
      COSB2=COSB*COSB
      COSB4=COSB2*COSB2
      SINBC=SINB*COSB
      SINBC2=SINB2*COSB2
C
      C(1,1)=C11*COSB4+2.*C12*SINBC2+C22*SINB4-4.*C33*SINBC2
      C(1,2)=C11*SINBC2+C12*(SINB4+COSB4)+C22*SINBC2-4.*C33*
     1SINBC2
      C(1,3)=SINBC*(C11*COSB2-C22*SINB2+(SINB2-COSB2)*(C12+
     12.*C33))
      C(2,1)=C(1,2)
      C(2,2)=C11*SINB4+2.*C12*SINBC2+C22*COSB4+4.*C33*SINBC2
      C(2,3)=SINBC*(C11*SINB2-C22*COSB2+(COSB2-SINB2)*(C12+
     12.*C33))
      C(3,1)=C(1,3)
      C(3,2)=C(2,3)
      C(3,3)=SINBC2*(C11-2.*C12+C22)+C33*(COSB4-2.*SINBC2+
```

```
     1SINB4)
       GO TO 30
  20 COMM=(1.-EE(2))/((1.+EE(2))*(1.-2.*EE(2)))
       C(1,1)=COMM
       C(1,2)=COMM*EE(2)/(1.-EE(2))
       C(1,3)=0.0
       C(2,1)=C(1,2)
       C(2,2)=COMM
       C(2,3)=0.0
       C(3,1)=0.0
       C(3,2)=0.0
       C(3,3)=.5/(1.+EE(2))
C
C   FORM QUADRILATERAL STIFFNESS MATRIX
C
  30 RRR(5)=(R(I)+R(J)+R(K)+R(L))/4.0
       ZZZ(5)=(Z(I)+Z(J)+Z(K)+Z(L))/4.0
       DO 97 M=1,4
       MM=IX(N,M)
       IF(R(MM)) 96,94,96
  94 R(MM)=.01*(RRR(5)*4.-R(L))/3.
  96 RRR(M)=R(MM)
  97 ZZZ(M)=Z(MM)
C
       DO 100 II=1,10
       DO 100 JJ=1,10
       HH(JJ,II)=0.0
 100 S(II,JJ)=0.0
       DO 119 II=1,4
       JJ=IX(N,II)
 119 ANGLE(II)=CODE(JJ)/57.3
C
C   CHECK FOR TRIANGULAR ELEMENT
C
       IF(K-L) 125,120,125
 120 CALL TRISTF(1,2,3,MMM)
       RRR(5)=(RRR(1)+RRR(2)+RRR(3))/3.0
       ZZZ(5)=(ZZZ(1)+ZZZ(2)+ZZZ(3))/3.0
       VOL=XI(1)
       GO TO 130
C
C   QUADRILATERAL ELEMENT
C
 125 VOL=0.0
       CALL TRISTF(4,1,5,MMM)
       VOL=VOL+XI(1)
 127 CALL TRISTF(1,2,5,MMM)
       VOL=VOL+XI(1)
 129 CALL TRISTF(2,3,5,MMM)
       VOL=VOL+XI(1)
 132 CALL TRISTF(3,4,5,MMM)
       VOL=VOL+XI(1)
       DO 140 II=1,6
```

```
      DO 140 JJ=1,10
  140 HH(II,JJ)=HH(II,JJ)/4.0
C
  130 RETURN
      END



      SUBROUTINE TRISTF(II,JJ,KK,MMM)
      COMMON F(7,10),NUMNP,NUMEL,NUMPC,MTYPE,NP,ANI,HED(20),
     1R(350),Z(350),UR(350),UZ(350),CODE(350),IBC(100),
     2JBC(100),PR(100),ANGLE(4),SIG(10),NDEG,IFF(350),
     3VOLM(350),NEWRZ,INN,ICHEK,KONTD,IND,FK(350),IFH(350),
     4BETA(350)
      COMMON/ARG/RRR(5),ZZZ(5),S(10,10),P(10),LM(4),DD(3,3),
     1HH(10,10),RR(4),ZZ(4),C(3,3),H(6,10),D(6,6),F(10,10),
     2TP(6),XI(10),EE(5),IX(350,5),EMOD(350)
      COMMON/IO/IN,IOUT,NUM1,NDAT1,NDAT2,NREC1
      DOUBLE PRECISION COMM,DPRR(3),DPZZ(3)
C
C
C   INITIALIZATION
C
      LM(1)=II
      LM(2)=JJ
      LM(3)=KK
C
      RR(1)=RRR(II)
      RR(2)=RRR(JJ)
      RR(3)=RRR(KK)
      RR(4)=RRR(II)
      ZZ(1)=ZZZ(II)
      ZZ(2)=ZZZ(JJ)
      ZZ(3)=ZZZ(KK)
      ZZ(4)=ZZZ(II)
      DO 115 I=1,3
      DPRR(I)=RR(I)
  115 DPZZ(I)=ZZ(I)
C
   85 DO 100 I=1,6
      DO 90 J=1,10
      F(I,J)=0.0
   90 H(I,J)=0.0
      DO 100 J=1,6
  100 D(I,J)=0.0
C
C   FORM INTEGRAL(G)T*(C)*(G)
C
      COMM=DPRR(2)*(DPZZ(3)-DPZZ(1))+DPRR(1)*(DPZZ(2)-
     1DPZZ(3))+DPRR(3)*(DPZZ(1)-DPZZ(2))
      XI(1)=COMM/2.
C
      D(2,6)=XI(1)*C(1,2)
```

```
      D(3,5)=XI(1)*C(3,3)
      D(5,5)=XI(1)*C(3,3)
      D(6,6)=XI(1)*C(2,2)
      D(2,2)=XI(1)*C(1,1)
      D(3,3)=XI(1)*C(3,3)
      IF(IFH(MMM) .NE. 1) GO TO 108
C
C   ANISOTROPIC ELEMENTS
C
      D(2,3)=XI(1)*C(1,3)
      D(2,5)=XI(1)*C(1,3)
      D(3,6)=XI(1)*C(2,3)
      D(5,6)=XI(1)*C(2,3)
C
  108 DO 110 I=1,6
      DO 110 J=I,6
  110 D(J,I)=D(I,J)
C
C   FORM COEFFICIENT-DISPLACEMENT TRANSFORMATION MATRIX
C
      DD(1,1)=(DPRR(2)*DPZZ(3)-DPRR(3)*DPZZ(2))/COMM
      DD(1,2)=(DPRR(3)*DPZZ(1)-DPRR(1)*DPZZ(3))/COMM
      DD(1,3)=(DPRR(1)*DPZZ(2)-DPRR(2)*DPZZ(1))/COMM
      DD(2,1)=(DPZZ(2)-DPZZ(3))/COMM
      DD(2,2)=(DPZZ(3)-DPZZ(1))/COMM
      DD(2,3)=(DPZZ(1)-DPZZ(2))/COMM
      DD(3,1)=(DPRR(3)-DPRR(2))/COMM
      DD(3,2)=(DPRR(1)-DPRR(3))/COMM
      DD(3,3)=(DPRR(2)-DPRR(1))/COMM
C
      DO 120 I=1,3
      J=2*LM(I)-1
      H(1,J)=DD(1,I)
      H(2,J)=DD(2,I)
      H(3,J)=DD(3,I)
      H(4,J+1)=DD(1,I)
      H(5,J+1)=DD(2,I)
  120 H(6,J+1)=DD(3,I)
C
C   FORM ELEMENT STIFFNESS MATRIX (H)T*(D)*(H)
C
      DO 130 J=1,10
      DO 130 K=1,6
      IF(H(K,J)) 128,130,128
  128 DO 129 I=1,6
  129 F(I,J)=F(I,J)+D(I,K)*H(K,J)
  130 CONTINUE
C
      DO 140 I=1,10
      DO 140 K=1,6
      IF(H(K,I)) 138,140,138
  138 DO 139 J=1,10
  139 S(I,J)=S(I,J)+H(K,I)*F(K,J)
```

```
  140 CONTINUE
C
C     FORM STRAIN TRANSFORMATION MATRIX
C
      DO 410 I=1,6
      DO 410 J=1,10
  410 BB(I,J)=BB(I,J)+H(I,J)
C
      RETURN
      END



      SUBROUTINE MODIFY(A,B,NEQ,MBAND,N,U)

      DIMENSION A(120,60),B(120)
C
      DO 250 M=2,MBAND
      K=N-M+1
      IF(K) 235,235,230
  230 B(K)=B(K)-A(K,M)*U
      A(K,M)=0.0
  235 K=N+M-1
      IF(NEQ-K) 250,240,240
  240 B(K)=B(K)-A(N,M)*U
      A(N,M)=0.0
  250 CONTINUE
      A(N,1)=1.0
      B(N)=U
      RETURN
      END



      SUBROUTINE BANSOL
      COMMON/BANARG/MM,    NUMBLK,B(120),A(120,60)
      COMMON/IO/IN,IOUT,NUM1,NDAT1,NDAT2,NREC1
C
C   REDUCE EQUATIONS BY BLOCKS
C
      NN=60
      NL=NN+1
      NH=NN+NN
      REWIND NDAT1
      REWIND NDAT2
      NB=0
      GO TO 150
C
C   SHIFT BLOCK OF EQUATIONS
C
  100 NB=NB+1
      DO 125 N=1,NN
      NM=NN+N
```

```
      B(N)=B(NM)
      B(NM)=0.0
      DO 125 M=1,MM
      A(N,M)=A(NM,M)
  125 A(NM,M)=0.0
C
C   READ NEXT BLOCK OF EQUATIONS INTO CORE
C
      IF(NUMBLK-NB) 150,200,150
  150 READ (NDAT2)  (B(N),(A(N,M),M=1,MM),N=NL,NH)
      IF(NB) 200,100,200
C
C   REDUCE BLOCK OF EQUATIONS
C
  200 DO 300 N=1,NN
      IF(A(N,1)) 225,300,225
  225 B(N)=B(N)/A(N,1)
      DO 275 L=2,MM
      IF(A(N,L)) 230,275,230
  230 C=A(N,L)/A(N,1)
      I=N+L-1
      J=0
      DO 250 K=L,MM
      J=J+1
  250 A(I,J)=A(I,J)-C*A(N,K)
      B(I)=B(I)-A(N,L)*B(N)
      A(N,L)=C
  275 CONTINUE
  300 CONTINUE
C
C   WRITE BLOCK OF REDUCED EQUATIONS ON TAPE 1
C
      IF(NUMBLK-NB) 375,400,375
  375 WRITE (NDAT1) (B(N),(A(N,M),M=2,MM),N=1,NN)
      GO TO 100
C
C   BACK-SUBSTITUTION
C
  400 DO 450 M=1,NN
      N=NN+1-M
      DO 425 K=2,MM
      L=N+K-1
  425 B(N)=B(N)-A(N,K)*B(L)
      NM=N+NN
      B(NM)=B(N)
  450 A(NM,NB)=B(N)
      NB=NB-1
      IF(NB) 475,500,475
  475 BACKSPACE NDAT1
      READ (NDAT1) (B(N),(A(N,M),M=2,MM),N=1,NN)
      BACKSPACE NDAT1
      GO TO 400
C
```

```
C  ORDER UNKNOWNS IN B ARRAY
C
  500 K=0
      DO 600 NB=1,NUMBLK
      DO 600 N=1,NN
      NM=N+NN
      K=K+1
  600 B(K)=A(NM,NB)
      RETURN
      END



      SUBROUTINE STRESS
      COMMON E(7,10),NUMNP,NUMEL,NUMPC,MTYPE,NP,ANI,HED(20),
     1R(350),Z(350),UR(350),UZ(350),CODE(350),IBC(100),
     2JBC(100),PR(100),ANGLE(4),SIG(10),NDFG,IFF(350),
     3VOLM(350),NEWRZ,INN,ICHEK,KONTO,IND,FK(350),IFH(350),
     4BETA(350)
      COMMON/ARG/RRR(5),ZZZ(5),S(10,10),P(10),LM(4),DD(3,3),
     1HH(10,10),RR(4),ZZ(4),C(3,3),H(6,10),D(6,6),F(10,10),
     2TP(6),XI(10),EE(5),IX(350,5),EMOD(350)
      COMMON/BANARG/MBAND,NUMBLK,B(120),A(120,60)
      COMMON/III/URR(350),UZZ(350),SIGG(350,4),DVOL(350)
      COMMON/IO/IN,IOUT,NUM1,NDAT1,NDAT2,NREC1
C
      DIMENSION SIG1(350),SIG2(350),SIG4(350),FSS(10)
C
      UCON=0.
      IIBC=1
      PN=0.
      EE2P=E(2,1)
      DO 9 I=1,NUMEL
    9 IX(I,5)=IABS(IX(I,5))
      DO 10 I=1,NUMNP
      UR(I)=0.
   10 UZ(I)=0.
C
      IF(ICHEK-1)12,15,15
   12 WRITE(IOUT,2000)
C
C*****************************************************************
C  CALCULATE STRESSES
C*****************************************************************
C
   15 DO 200 N=1,NUMEL
      EM=EMOD(N)
      NREC1=N
   16 READ(NUM1'NREC1) HH,C,RRR(5),ZZZ(5),EE(2),S,VOL
      IF(EE(2) .EQ. .1*E(2,1) .AND. EM .GT. ANI*E(1,1))
     1EM=ANI*E(1,1)
   17 DO 120 I=1,4
      II=2*I
```

```
      JJ=2*IX(N,I)
      P(II-1)=R(JJ-1)
   10 P(II)=R(JJ)
      DO 20 I=9,10
      DO 20 J=1,10
   20 S(I,J)=S(I,J)*EM
      DO 150 I=1,2
      RR(I)=0.
      DO 150 K=1,8
  150 RR(I)=RR(I)-S(I+8,K)*P(K)
C
      COMM=S(9,9)*S(10,10)-S(9,10)*S(10,9)
      IF(COMM) 155,160,155
  155 P(9)=(S(10,10)*RR(1)-S(9,10)*RR(2))/COMM
      P(10)=(-S(10,9)*RR(1)+S(9,9)*RR(2))/COMM
C
  160 DO 170 I=1,6
      TP(I)=0.
      DO 170 K=1,10
  170 TP(I)=TP(I)+EM(I,K)*P(K)
      RR(1)=TP(2)
      RR(2)=TP(4)
      RR(3)=TP(3)+TP(5)
C
      DO 180 I=1,3
      SUM=0.
      DO 180 K=1,3
      SUM=SUM+C(I,K)*RR(K)*EM
  180 SIG(I)=SUM
      SIG(4)=SIG(3)
      IF(ICHEK .EQ. 0) GO TO 190
C
C  ACCUMULATE STRESSES
C
      SIGG(N,1)=SIG(1)+SIGG(N,1)
      SIGG(N,2)=SIG(2)+SIGG(N,2)
      SIGG(N,4)=SIG(4)+SIGG(N,4)
      GO TO 200
  190 SIG1(N)=SIG(1)
      SIG2(N)=SIG(2)
      SIG4(N)=SIG(4)
      IF(IFP(N) .GT. 0) GO TO 200
      SIGG1=SIG(1)+SIGG(N,1)
      SIGG2=SIG(2)+SIGG(N,2)
      SIGG4=SIG(4)+SIGG(N,4)
      CC=(SIGG1+SIGG2)/2.
      BB=(SIGG1-SIGG2)/2.
      CR=SQRT(BB**2+SIGG4**2)
      SIG(5)=CC+CR
      SIG(6)=CC-CR
      SIG(7)=28.648*ATAN2(SIGG4,BB)
      S1=-SIG(6)
      S3=-SIG(5)
```

```
C
C   CHECK ELEMENT FAILURE
C
      CALL FRT(S1,S3,IKOD,UCC,PT1,PCC)
      IF(UCC-UCCN) 195,194,194
  194 UCCN=UCC
      IF(UCC .EQ. PCC) IIKC=3
      IF(UCC .EQ. PT1) IIKC=1
      IUCC=N
      MM=N
  195 WRITE(ICUT,2001)N,IKOD,PT1,PCC,SIG(5),SIG(6),SIG(7),
     1SIG(1),SIG(2),SIG(4),SIGG1,SIGG2,SIGG4
  200 CONTINUE
C
      IF(ICHEK .GT. 0) GO TO 800
C
C
C   ADJUST INCREMENTAL DISPLACEMENT
C
      N=IUCC
      CC=(SIGG(N,1)+SIGG(N,2))/2.
      BB=(SIGG(N,1)-SIGG(N,2))/2.
      CR=SQRT(BB**2+SIGG(N,4)**2)
      S1=-CC+CR
      S3=-CC-CR
      CALL FRT(S1,S3,IKOD,UCC,PT1,PCC)
      IF(IIKC .EQ. 3) UUCC=PCC
      IF(IIKC .EQ. 1) UUCC=PT1
C
      IF(UUCC .GE. 1.) GO TO 205
      IF((UCCN-UUCC) .LT. 0.01) GO TO 207
      GO TO 206
  205 RATIO=0.
      IFH(N)=IIKC
      GO TO 209
  206 RATIO=(1.-UUCC)/(UCCN-UUCC)
      IF(RATIO .GT. 1.1) GO TO 208
      IFH(N)=IIKC
      GO TO 209
  207 RATIO=1.1
      IF(UCCN-1.001) 209,204,204
  204 RATIO=1.
      IFH(N)=IIKC
      GO TO 209
  208 RATIO=1.1
  209 WRITE(ICUT,3000)    MM,IIKC,UCCN,UUCC,RATIO
C
      DO 220 I=1,NUMNP
      URR(I)=R(2*I-1)*RATIO+URR(I)
  220 UZZ(I)=R(2*I)*RATIO+UZZ(I)
C
      WRITE(ICUT,3003)
      DO 700 N=1,NUMEL
```

```
C
C   ACCUMULATE TOTAL STRESSES
C
      SIGG(N,1)=SIG1(N)*RATIO+SIGG(N,1)
      SIGG(N,2)=SIG2(N)*RATIO+SIGG(N,2)
      SIGG(N,4)=SIG4(N)*RATIO+SIGG(N,4)
C
C   INDENTOR PRESSURE
C
      IF(N-JBC(IIBC))211,210,211
  210 RJ=R(IBC(IIBC*2))
      ZJ=Z(IBC(IIBC*2))
      RI=R(IBC(IIBC*2-1))
      ZI=Z(IBC(IIBC*2-1))
      PL1=SQRT((RJ-RI)*(RJ-RI)+(ZJ-ZI)*(ZJ-ZI))
      PL2=ATAN2((ZJ-ZI),(RJ-RI))
      PR(IIBC)=PL1*(SIGG(N,4)*SIN(PL2)-SIGG(N,2)*COS(PL2))
      PN=PN+PR(IIBC)
      IIBC=IIBC+1
      IF(IIBC-NUMPC)211,211,212
  212 JBC(IIBC)=NUMEL+1
  211 CONTINUE
C
      NREC1=N
      READ(NUM1'NREC1) HH,C,RRR(5),ZZZ(5),EE(2),S,VOL
      NREC1=NUMEL+1
      WRITE(NUM1'NREC1) HH,C,RRR(5),ZZZ(5),EE(2),S,VOL
C
C   CALCULATE PRINCIPAL STRESSES
C
      CC=(SIGG(N,1)+SIGG(N,2))/2.
      BB=(SIGG(N,1)-SIGG(N,2))/2.
      CR=SQRT(BB**2+SIGG(N,4)**2)
      SIG(5)=CC+CR
      SIG(6)=CC-CR
      SIG(7)=28.648*ATAN2(SIGG(N,4),BR)
      IF(IFH(N) .LE. 0) GO TO 300
C
C*************************************************************
C   CLASSIFY FAILED ELEMENTS & MODIFY MATERIAL PROPERTIES
C*************************************************************
C
      IFF(N)=0
      FFK=0.1
      UCO=0.
      DVOLP=0.
      SIG6P=0.
      IF(N-IUCO)216,215,216
  215 FK(N)=1.
      IF(IFH(N)-1) 254,254,270
C
  216 S1=-SIG(6)
      S3=-SIG(5)
```

```
      VOLL=0.
      IIX=IX(N,5)
      IX(N,5)=IX(N,1)
      DO 230 I=1,4
      R1=R(IX(N,I))+URR(IX(N,I))
      Z1=Z(IX(N,I))+UZZ(IX(N,I))
      R2=R(IX(N,I+1))+URR(IX(N,I+1))
      Z2=Z(IX(N,I+1))+UZZ(IX(N,I+1))
      COMM=.5*(R2*(ZZZ(5)-Z1)+R1*(Z2-ZZZ(5))+RRR(5)*(Z1-Z2))
      VOLL=VOLL+COMM
      IF(IX(N,3) .EQ. IX(N,4)) GO TO 231
  230 CONTINUE
  231 IX(N,5)=IIX
      DVOL(N)=VOLL-VOLM(N)
      IF(IFH(N)-3) 232,250,245
C
  232 ALFA2=(SIG(7)-BETA(N))/28.648
      SIG6P=CC-CR*COS(ALFA2)
      SIG1P=CC+CR*COS(ALFA2)
      S12P=CR*SIN(ALFA2)
      DVOLP=(1.-E(2,1))*(1.-2.*E(2,1))/E(1,1)*SIG6P*VOLM(N)
C
      IF(DVOL(N) .LT. DVOLP) GO TO 235
C
      IF(SIG6P .GT. -E(4,1)) GO TO 233
C
      IF(SIG6P .LT. -E(3,1)) GO TO 270
C
      IF(EE(2) .EQ. 0.10*E(2,1)) GO TO 234
      IFH(N)=1
      EE(2)=0.10*E(2,1)
      CALL QUAD(N,VOL,N)
      NREC1=N
      WRITE(NUM1'NREC1) HH,C,RRR(5),ZZZ(5),EE(2),S,VOL
C
  234 IF(SIG1P .GT. 50. .OR. S12P .GT. 50.) GO TO 290
      GO TO 290
C
  235 EMOD(N)=0.9*E(1,1)
      FK(N)=0.95
      CALL FRTF(S1,S3,FK(N),IKOD,UCO)
      IF(IKOD-1) 236,237,270
C
  236 EE(2)=E(2,1)
      IFH(N)=2
      CALL QUAD(N,VOL,N)
      NREC1=N
      WRITE(NUM1'NREC1) HH,C,RRR(5),ZZZ(5),EE(2),S,VOL
      IF(SIG(5) .GT. 50.) GO TO 260
      GO TO 290
C
  237 EMOD(N)=0.8*E(1,1)
      FK(N)=0.9
```

```
      IF(DVOL(N) .GT. 0.) GO TO 240
C
      IFH(N)=3
      EE(2)=.5-(.5-EE2P)*EMOD(N)/E(1,1)
      IF(EE(2) .GT. 0.49977)EE(2)=0.49977
      CALL QUAD(N,VOL,N)
      NREC1=N
      WRITE(NUM1'NREC1) HH,C,RRR(5),ZZZ(5),EE(2),S,VOL
      GO TO 260
  238 EMOD(N)=0.8*E(1,1)
      FK(N)=0.9
C
  240 IFH(N)=4
      BETA(N)=DVOL(N)
      IF(DVOL(N) .GT. 0.) BETA(N)=0.
      EE(2)=0.10*E(2,1)
      CALL QUAD(N,VOL,N)
      NREC1=N
      WRITE(NUM1'NREC1) HH,C,RRR(5),ZZZ(5),EE(2),S,VOL
  242 IF(ABS(SIG(5)) .GT. 50. .OR. ABS(SIG(6)) .GT. 50.)
     1GO TO 265
      GO TO 290
C
  245 IF(DVOL(N) .GT. BETA(N)) GO TO 242
      IFH(N)=3
      EE(2)=.5-(.5-EE2P)*EMOD(N)/E(1,1)
      IF(EE(2) .GT. 0.49977)EE(2)=0.49977
      CALL QUAD(N,VOL,N)
      NREC1=N
      WRITE(NUM1'NREC1) HH,C,RRR(5),ZZZ(5),EE(2),S,VOL
      GO TO 290
C
  250 IF((SIG(5)+SIG(6)) .GE. 0.) GO TO 240
      CALL FRTF(S1,S3,FK(N),IKOD,UCO)
      IF(IKOD .EQ. 3) GO TO 266
C
      IF(DVOL(N) .GT. 0. .AND. EE(2) .EQ. 0.1*E(2,1))
     1GO TO 253
      IF(DVOL(N) .LT. 0. .AND. EE(2) .NE. 0.1*E(2,1))
     1GO TO 253
      EE(2)=.5-(.5-EE2P)*EMOD(N)/E(1,1)
      IF(EE(2) .GT. 0.49977)EE(2)=0.49977
      IF(DVOL(N) .GT. 0.) EE(2)=0.1*E(2,1)
      CALL QUAD(N,VOL,N)
      NREC1=N
      WRITE(NUM1'NREC1) HH,C,RRR(5),ZZZ(5),EE(2),S,VOL
  253 IF(SIG(5) .GT. 50.) GO TO 260
      GO TO 290
C
  254 EE(2)=0.10*E(2,1)
      BETA(N)=SIG(7)
      CALL QUAD(N,VOL,N)
      NREC1=N
```

```
      WRITE(NUM1'NREC1) FH,C,RPR(5),ZZZ(5),FF(2),S,VOL
      GO TO 260
C
C*****************************************************************
C  TRANSFER EXCESSIVE STRESSES TO NODAL LOADS
C*****************************************************************
C
  255 IFF(N)=1
      BETA2=BETA(N)/28.648
      SRP=.5*SIG6P*(1.-COS(BETA2))
      SZP=.5*SIG6P*(1.+COS(BETA2))
      SRZP=-.5*SIG6P*(SIN(BETA2))
      GO TO 290
  260 IFF(N)=2
  261 IF(EE(2) .GE. E(2,1)) GO TO 262
      SIG72= SIG(7)/28.648
      SRP=.5*SIG(6)*(1.-COS(SIG72))
      SZP=.5*SIG(6)*(1.+COS(SIG72))
      SRZP=-.5*SIG(6)*SIN(SIG72)
      GO TO 290
  262 CCP=.5*(-SIG(5)+SIG(6))
      CRP=.5*(-SIG(5)-SIG(6))
      GO TO 279
  265 IFF(N)=4
      SRP=0.
      SZP=0.
      SRZP=0.
      GO TO 290
  266 IF(UCO .GT. 1.03) FFK=.1+.05*(UCO-1.03)/.06
      IF(UCO .GT. 1.09) FFK=.15
      GO TO 271
C
  270 IFH(N)=3
  271 IFF(N)=3
      TH=FK(N)*(E(5,1)-E(6,1))+E(6,1)
      DS1=2.*(1.+SIN(TH))/COS(TH)*(FK(N)*E(1,2)-TAN(TH)*
     1SIG(5))
      FK(N)=FK(N)-(.3+.7*FK(N))*(.5*FFK+.25*FFK*SIG(5)/
     110000.)
      IF(FK(N) .LT. 0.05) GO TO 288
      TH=FK(N)*(E(5,1)-E(6,1))+E(6,1)
      DS2=2.*(1.+SIN(TH))/COS(TH)*(FK(N)*E(1,2)-TAN(TH)*
     1SIG(5))
      DSP=(DS1-DS2)*E(7,1)
      IF(DSP .GT. DS1) DSP=DS1-50.
      EMOD(N)=E(1,1)*FK(N)**E(7,1)
      SIG6P=(SIG(6)-SIG(5))*(1.-DSP/DS1)+SIG(5)
      GO TO 289
  288 FK(N)=.05
      EMOD(N)=.001
      TH=.95*F(6,1)
      SIG6P=SIG(5)-2.*(1.+SIN(TH))/COS(TH)*(.04*E(1,2)-
     1TAN(TH)*SIG(5))
```

```
      IF(SIG(5) .GT. 0.) DSP=DS1
  289 IF(EMOD(N) .LT. 0.001*E(1,1)) EMOD(N)=0.001*E(1,1)
      EE(2)=.5-(.5-EE2P)*EMOD(N)/E(1,1)
      IF(EE(2) .GT. 0.49977)EE(2)=0.49977
      IF(DVOL(N) .GT. 0.) EE(2)=0.10*E(2,1)
      CALL QUAD(N,VOL,N)
      NREC1=N
      WRITE(NUM1'NREC1) HH,C,RRR(5),ZZZ(5),EE(2),S,VOL
  272 IF(SIG(5) .LE. 0.) GO TO 274
      SIG6P=SIG(6)*(1.-DSP/DS1)
      CCP=.5*SIG6P
      CRP=-.5*SIG6P
      GO TO 279
C
  274 CCP=.5*(SIG(5)+SIG6P)
      CRP=.5*(SIG(5)-SIG6P)
  279 ALFA2=SIG(7)/28.648
      SRP=CCP+CRP*COS(ALFA2)
      SZP=CCP-CRP*COS(ALFA2)
      SRZP=CRP*SIN(ALFA2)
C
  290 WRITE(ICUT,3002) N,IEE(N),IEH(N),UCO,EE(2),EE(5),
     1EMOD(N),DVOL(N),DVOLP,SIGG(N,1),SIGG(N,2),SIGG(N,4),
     2SIG(5),SIG(6),SIG(7),SIG6P
      IF(IEE(N)-1)700,710,710
  710 SRR=SIGG(N,1)-SRP
      SZZ=SIGG(N,2)-SZP
      SRZ=SIGG(N,4)-SRZP
  730 SIGG(N,1)=SRP
      SIGG(N,2)=SZP
      SIGG(N,4)=SRZP
  739 NREC1=NUMEL+1
      READ(NUM1'NREC1)HH,C,RRR(5),ZZZ(5),EE(2),S,VOL
      IF(IX(N,3) .EQ. IX(N,4)) GO TO 751
      DO 740 I=1,10
  740 ESS(I)=(HH(2,I)*SRR+HH(3,I)*SRZ+HH(5,I)*SRZ+HH(6,I)*
     1SZZ)*VOL
      ESR=.25*ESS(9)
      ESZ=.25*ESS(10)
C
      DO 750 I=1,4
      UR(IX(N,I))=ESS(I*2-1)+ESR+UR(IX(N,I))
  750 UZ(IX(N,I))=ESS(I*2)+ESZ+UZ(IX(N,I))
      GO TO 300
  751 DO 755 I=1,6
  755 ESS(I)=(HH(2,I)*SRR+HH(3,I)*SRZ+HH(5,I)*SRZ+HH(6,I)*
     1SZZ)*VOL
      DO 756 I=1,3
      UR(IX(N,I))=ESS(I*2-1)+UR(IX(N,I))
  756 UZ(IX(N,I))=ESS(I*2)  +UZ(IX(N,I))
  300 CONTINUE
  700 CONTINUE
      WRITE(ICUT,2003)(I,PR(I),I=1,NUMPC)
```

```
      TPEN=UZZ(1)+Z(1)
      WRITE(IOUT,2004)PN,TPEN
      GO TO 810
C
  800 DO 801 I=1,NUMNP
      URR(I)=B(2*I-1)+URR(I)
  801 UZZ(I)=B(2*I)+UZZ(I)
  810 CONTINUE
C
 2000 FORMAT(5H1E-NO,1X,'IKOD',3X,'PT1',3X,'PCC',5X,'MAX-S',
     15X,'MIN-S',5X,'ANGLE',2X,'DR-STRES',2X,'DZ-STRES',1X,
     2'DRZ-STRES',2X,'R-STRESS',2X,'Z-STRESS',1X,'RZ-STRESS'
     3)
 2001 FORMAT(2I5,2F6.2,1P9E10.2)
 2003 FORMAT(//5X,'PRESSURE BOUNDARY'//(5X,'PR(',I3,')=',
     1E16.0))
 2004 FORMAT(/5X,'TOTAL PRESSURE=',F16.0//5X,
     1'TOTAL PENETRATION=',F13.6)
 2008 FORMAT(I10,1P3E15.4)
 3000 FORMAT(/'  EL. NO.=',I5,5X,'IIKO=',I3,5X,'UCON=',
     1F10.3,5X,'UUCO=',F10.3,5X,'RATIO=',F10.3/)
 3002 FORMAT(I4,I2,I4,F6.2,F8.4,F6.2,1P10E10.2)
 3003 FORMAT(4H1NO.,' IFF IFH   UCO    EF2     FK    EMOD(N) ',
     1'  DVOL(N)  DVOLP(N)  R-STRESS  Z-STRESS RZ-STRESS  ',
     2'  MAX-ST    MIN-ST     ANGLE    SIG6P')
      RETURN
      END


      SUBROUTINE FRT(S1,S3,IKOD,UCO,PT1,PCC)
      COMMON E(7,10)
      PT1=0.
      PCC=0.
      UCO=0.
      IKOD=0
      IF(S3 .GT. 0.) GO TO 510
      PT1=S3/E(4,1)
      UCO=PT1
      IF(E(4,1) .LT. S3) GO TO 510
      IKOD=1
  510 PCC=(S1-S3)/(E(3,1)+E(3,2)*S3)
      IF(PCC .LT. UCO) GO TO 590
      UCO=PCC
      IF(PCC .GT. 1.) IKOD=3
  590 CONTINUE
      RETURN
      END


      SUBROUTINE FRTF(S1,S3,FK,IKOD,UCO)
      COMMON E(7,10)
```

```
      TH=FK*(E(5,1)-E(6,1))+E(6,1)
      UCO=0.
      IKOD=0
      IF(S3 .GT. 0.) GO TO 510
      UCO=S3/E(4,1)
      IF(UCO .GT. 1.) IKOD=1
      S3=0.
510   PCC=(S1-S3)/(2.*(1.+SIN(TH))/COS(TH)*(FK*E(1,2)+
     1TAN(TH)*S3))
      IF(PCC .LT. UCO) GO TO 580
      UCO=PCC
      IF(PCC .GT. 1.) IKOD=3
580   CONTINUE
      RETURN
      END
```